THE JOURNAL
OF
CHEMICAL PHYSICS

VOLUME 9 NOVEMBER, 1941 NUMBER 11

An Experimental Study of the Ultraviolet Absorption Spectrum of Pyrimidine

FRED M. UBER
Department of Physics, University of Missouri, Columbia, Missouri
(Received August 8, 1941)

The wave numbers of 112 absorption bands of pyrimidine vapor in the 2700–3300A region have been determined. The bands have been classified qualitatively into four categories as to their intensity. Assignments of individual bands into a number of series have been made and all prominent series were found to have spacings of approximately 1014 cm^{-1}. Other characteristic frequencies are 613, 669 and 680 cm^{-1}.

INTRODUCTION

PYRIMIDINE has a six-membered heterocyclic ring structure, with four carbon atoms and two nitrogen atoms in the ring. Its formula is $C_4H_4N_2$.

The absorption spectrum of pyrimidine in solution[1,2] indicates that it possesses at least three electronic absorption bands. One is below 2000A, another centers around 2400A, and the third lies in the region from 2700 to 3300A. The last one is relatively weak and does not show up particularly well in solution.

In the vapor state, the electronic band at 2400A has been shown to be diffuse so that only five broad peaks are clearly discernible.[2] These have separations of around 800–1000 cm^{-1}. The longer wave-length electronic band system at 2700–3300A has numerous sharp bands and seems to correspond to the well-known benzene system at 2600A and to the 2700–3100A band system of pyridine. In the benzene system, some 500 bands have been reported;[3] in pyridine, 255 bands;[4] and in pyrimidine, the clearly defined bands which are reported in this paper number only a few over 100, although higher dispersion would no doubt reveal more.

EXPERIMENTAL

Apparatus

A Wadsworth spectrograph mounting of the type described by Meggers and Burns[5] has been used. It was equipped with a 3-meter concave grating which gave a linear dispersion of about 7.4A per mm in the first order. The continuous source of ultraviolet radiation was furnished by a hydrogen discharge tube, and an iron arc operating at 4 amperes, direct current, was used to supply a comparison spectrum. The spectra were photographed on Eastman "40" plates and magnified tracings were made of them with a Leeds and Northrup recording microphotometer. The wave-length measurements were made from these tracings.

[1] F. Heyroth and J. H. Loofbourow, J. Am. Chem. Soc. **57**, 1728 (1935).
[2] F. M. Uber and R. Winters, J. Am. Chem. Soc. **63**, 137 (1941).
[3] W. F. Radle and C. A. Beck, J. Chem. Phys. **8**, 507 (1940).
[4] V. Henri and P. Angenot, J. chim. phys. **33**, 641 (1936).
[5] W. F. Meggers and K. Burns, Sci. Papers U. S. Bur. Stand. **18**, 185 (1922).

TABLE I. *Absorption bands of pyrimidine vapor.*

WAVE-LENGTH (A)	WAVE NUMBERS (cm^{-1})	SERIES ASSIGN-MENT	INTENSITY *s* = STRONG; *m* = MEDIUM; *w* = WEAK; *vw* = VERY WEAK
3289.6	30398	E_0	*w*
3250.6	30764	J_0	*w*
3245.7	30810		*vw*
3233.8	30923		*m*
3217.7	31078	A_0	*s*
3216.0	31095		*w*
3206.6	31186		*w*
3183.7	31410	E_1	*w*
3174.0	31506		*vw*
3172.3	31523		*vw*
3170.3	31543		*w*
3168.7	31559	*d*	*vw*
3166.3	31583		*vw*
3163.6	31610	F_0	*vw*
3160.8	31638		*vw*
3155.5	31691	B_0	*s*
3149.9	31747	C_0	*s*
3145.4	31792	J_1	*vw*
3143.8	31809		*vw*
3137.6	31871		*vw*
3123.6	32014	G_0	*m*
3116.0	32092	A_1	*s*
3106.8	32187	*a*	*m*
3095.4	32306		*vw*
3092.7	32334		*w*
3089.2	32371	D_0	*s*
3085.2	32413		*vw*
3083.9	32426	E_2	*vw*
3082.2	32444		*vw*
3077.2	32497		*w*
3075 0	32520		*vw*
3070.4	32569	*d*	*m*
3065.1	32625	F_1	*m*
3062.4	32654		*vw*
3059.6	32684		*vw*
3057.2	32710	B_1	*s*
3055.3	32730		*vw*
3052.6	32759	C_1	*s*
3048.6	32802	J_2	*m*
3046.1	32829		*m*
3041.3	32881		*w*
3039.8	32897		*vw*
3038.0	32916		*vw*
3035.5	32944		*w*
3031.5	32987	*b*	*m*
3027.5	33031	G_1	*m*
3026.3	33044		*vw*
3024.2	33067		*vw*
3020.9	33103	A_2	*m*
3019.2	33121		*vw*
3015.3	33164		*vw*
3011.9	33202	*a*	*m*
3006.1	33266		*w*
3002.5	33306		*w*
3000.7	33326		*vw*
2999.0	33344		*w*
2995.4	33385	D_1	*m*
2988.7	33459	E_3	*w*
2984.7	33504		*w*
2977.2	33589	*d*	*m*
2971.8	33650	F_2	*m*
2965.8	33718	B_2	*s*
2960.3	33780	C_2	*w*
2957.1	33817	J_3	*m*
2955.0	33840		*vw*
2948.2	33919		*m*
2945.5	33950		*w*
2941.5	33996	*b*	*m*
2937.3	34045	G_2	*m*
2930.8	34120	A_3	*m*
2925.7	34180		*w*
2922.6	34216	*a*	*w*
2921.1	34234		*vw*
2917.9	34271		*vw*
2915.1	34304		*vw*
2910.8	34355		*w*
2907.7	34391	D_2	*w*
2903.0	34447		*vw*
2902.1	34458	E_4	*w*+
2897.5	34513		*w*
2896.2	34528		*vw*
2889.3	34610	*d*	*vw*
2886.0	34650	F_3	*vw*
2882.5	34692		*vw*
2878.1	34745	B_3	*m*
2871.2	34829	J_4	*m*
2863.5	34922		*w*
2862.1	34939		*w*
2856.6	35007	*b*	*w*
2852.4	35058	G_3	*w*
2847.9	35114		*vw*
2845.7	35141	A_4	*w*
2842.4	35182		*w*
2833.7	35290		*vw*
2831.0	35323		*vw*
2829.0	35348		*vw*
2825.9	35387	D_3	*vw*
2821.1	35447		*vw*
2819.3	35470	E_5	*w*
2814.0	35537		*w*
2808.7	35604		*w*
2802.3	35685		*w*
2797.1	35751	B_4	*w*
2789.6	35847	J_5	*w*
2782.9	35934		*w*
2780.5	35965		*vw*
2776.5	36017	*b*	*vw*
2772.7	36066	G_4	*vw*
2770.1	36100		*vw*
2767.2	36138		*vw*
2765.6	36158	A_5	*vw*
2762.9	36194		*w*

Preparation of pyrimidine

The pyrimidine was made by reducing trichloropyrimidine with zinc dust and water, according to the method of Gabriel.[6] It was rendered anhydrous with metallic potassium and purified by distillation. The melting point of the purified pyrimidine was 21°C, which agrees with the value given by Gabriel.

The pyrimidine sample was sealed in a fused quartz absorption cell containing a side arm in which the liquid was maintained at a constant temperature of 28°C during the exposures. The cell had a length of 3 cm between the windows.

RESULTS

The wave-length measurements on 112 bands, together with their wave numbers, are given in Table I. The accuracy of the latter is probably somewhat better than 10 cm^{-1}. The intensity estimates were based on the appearance of the microphotometer tracings and are intended to give only the order of magnitude of the relative strengths of the bands. The assignment of many of the bands into series is indicated by the designations of column 3.

The arrangement of the bands into series or progressions has been graphed in Fig. 1. There are eight bands which have been classified as strong (*s*), all of which occur in either series *A*, *B*, *C*, or *D*. It seems probable that all of these arise in transitions from the lowest vibrational level of the ground state. In each of these series, as well as in all the others shown in Fig. 1, the bands are spaced about 1014 cm^{-1} apart. In this respect, the spectrum of pyrimidine is closely

[6] S. Gabriel, Ber. d. D. Chem. Ges. **33**, 3666 (1900).

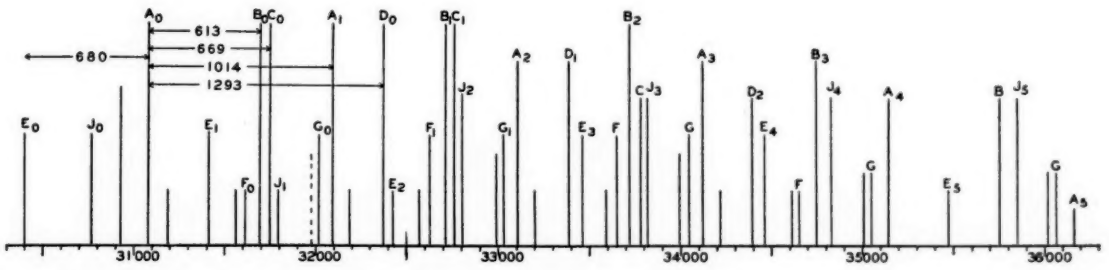

FIG. 1. Schematic absorption spectrum of pyrimidine. All series have spacings of approx. 1014 cm^{-1}. The lengths of lines are only *roughly* indicative of band intensities.

analogous to that of benzene analyzed by Sponer, Nordheim, Sklar, and Teller.[7] The benzene absorption bands have a characteristic spacing of 923 cm^{-1}, which these workers have interpreted as due to the totally symmetrical carbon vibration in the upper electronic state.

If the first member of the A series (A_0), be thought of as arising from the $0-0$ transition, then the first members of the B and C series could represent $0-1$ transitions with a displacement from A_0 of 613 and 669 cm^{-1}, respectively, these numbers corresponding to vibrational frequencies of the upper state. In line with this the origin of the E series, with its first member (E_0) 680 cm^{-1} lower than A_0, could be interpreted as a $1-0$ transition, where 680 cm^{-1} is regarded as a characteristic vibrational frequency of the ground state.

Any elaborate effort to construct a detailed energy level diagram on the limited data presented here would be premature. It must await additional evidence on the relative intensities of the bands as a function of temperature. However, it should be pointed out that the pyrimidine spectrum does not seem to resemble the absorption spectrum of pyridine which has been analyzed by Henri and Angenot.[4] They found all the bands in the pyridine series to be characterized by spacings of 600 or 542 cm^{-1}. On the other hand the pyrimidine spectrum appears to be quite similar, at least superficially, to the spectrum of benzene.

[7] H. Sponer, G. Nordheim, A. L. Sklar, and E. Teller, J. Chem. Phys. **7**, 207 (1939).

Infra-Red and Raman Spectra of Polyatomic Molecules

XV. Diborane*

FRED STITT†
Harvard University, Cambridge, Massachusetts,
and
Indiana University, Bloomington, Indiana
(Received September 9, 1941)

The infra-red spectrum of diborane has been studied on a prism spectrometer from 400 to 4000 cm^{-1}. Absorption occurs over much of the region investigated. A reliable and complete analysis of the infra-red and Raman spectra of diborane must await further work, but two alternative tentative analyses of the main features are presented which are in accord with the heat capacity of gaseous diborane from 100 to 300°K. One of these analyses is based on the assumed existence of a singlet electronic state at 412 cm^{-1} above the ground state and requires the potential barrier to internal rotation within the molecule to be of the order of 15,000 calories per mole. The alternative analysis assumes that no electronic state lies less than 1600 cm^{-1} above the ground state and requires a potential barrier of about 5000 calories per mole. Both analyses assume an ethane-like structure for the diborane molecule.

THE arrangement of the atoms in the diborane molecule has been shown by x-ray[1] and electron[2] diffraction studies to be very similar to that of ethane. The B−B and B−H distances are found to be about 1.86 and 1.27A, respectively, which are to be compared with corresponding C−C and C−H distances of 1.54 and 1.09A in ethane. Despite the larger interatomic distances in diborane, it has been found that internal rotation in the B_2H_6 molecule is restricted by a potential barrier somewhat higher than that found for C_2H_6.[3] The electronic structure of this boron hydride cannot be the same as that of ethane and has been the subject of considerable speculation.[4] The infra-red spectrum of diborane is found in this study to be considerably more complex than that of ethane. Although complete analysis of the diborane spectrum must await further work, it is shown here that the infra-red and Raman data available are compatible with an ethane-like structure and the existence of a rather high potential barrier to internal rotation.

EXPERIMENTAL

The author is especially indebted to Dr. A. B. Burg for supplying the diborane used in this investigation. Two different samples were studied, both of which were sent by air mail and maintained at dry ice temperature when not in use in order to prevent slow thermal decomposition. One sample was part of the same material of which portions were used to study the heat capacity of diborane.[3] This material was used for a preliminary survey of the infra-red spectrum and for studying the stronger bands. All of this work was repeated and extended to higher pressures using the second and larger sample. The original material showed a vapor pressure of 224.7 mm at −111.9°C (the melting point of CS_2) according to Dr. Burg. Since the decomposition and hydrolysis products of diborane are comparatively non-volatile with the exception of hydrogen, it is easy to purify a partially decomposed or hydrolyzed sample by simple distillation. Both samples were twice distilled from a trap maintained at −135°C before being introduced into the absorption cell, and both were similarly purified several times during the course of the work.

* This material was presented to the Division of Physical and Inorganic Chemistry of the American Chemical Society at St. Louis, April, 1941.

† The experimental work reported here was done at Harvard University during the tenure of a National Research Fellowship in Chemistry from 1937 to 1939.

[1] H. Mark and E. Pohland, Zeits. f. Krist. **62**, 103 (1925).
[2] S. H. Bauer, J. Am. Chem. Soc. **59**, 1096 (1937).
[3] F. Stitt, J. Chem. Phys. **8**, 981 (1940).
[4] See E. Wiberg, Berichte **69**, 2816 (1936).

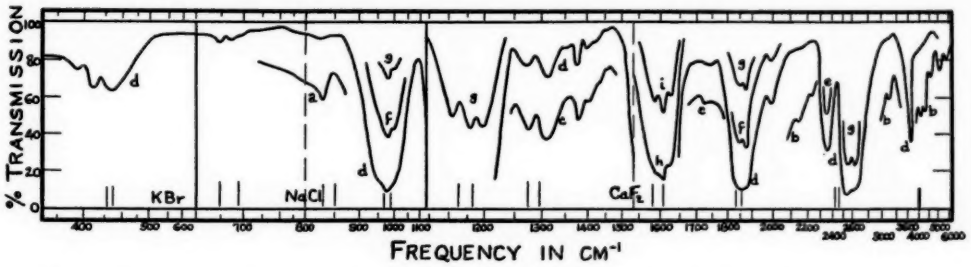

FIG. 1. Infra-red absorption spectrum of diborane. Length of absorption path: 30 cm. Gas pressure in mm Hg: a—705; b—575; c—255; d—100; e—40; f—35; g—11; h—4; i—2. Effective slit widths are shown at the bottom of the figure.

The automatic prism spectrometer described in I[5] of this series was used to study the absorption spectrum from approximately 400 to 4000 cm^{-1}. Fluorite, rocksalt, and potassium bromide prisms were used and the instrument was calibrated as in earlier work by observing the positions of bands of known wave-length. The gas was enclosed in 30-cm long cylindrical glass cells with either KBr or NaCl windows at pressures ranging from 2 to 705 mm mercury. Blanks were recorded over the entire region.

The first records obtained were with a gas pressure of 100 mm. The material was in the cell for three days. After the first 48 hours there was no visible indication of any reaction products in the cell, whereas at the end of 65 hours a fine white deposit in the shape of a spiral on the cell wall was noticed. The peculiar shape of the deposit, which was probably boric acid, suggested that reaction had taken place with some residue left on the wall in the cleaning of the cell, the last operation of which had been swabbing the cell with ether-soaked cotton. After more careful cleaning of the cells no such deposit was observed in some fifteen different cell fillings.

After the first experience just mentioned, the gas was allowed to remain in the cell only as long as was required to obtain the absorption records. In each case the vacuum-tight cell was filled to a known pressure of diborane, the cell was disconnected from the vacuum system, the records were obtained, the cell was again connected to the vacuum system, and the material was condensed by liquid air in a trap some distance from the cell. In every case except one, the gas condensed rapidly until the pressure was less than 2 mm, indicating that neither decomposition nor hydrolysis had been appreciable since hydrogen is formed in either case. At the highest pressure, 705 mm, the material did not condense well and the cell was found to be no longer vacuum-tight after the gas was removed. This leak was probably caused by slow reaction of the diborane with the Duco cement used to fasten the cell windows. Blank records were usually made just preceding and following each filling of the cell to detect any effect due to the possible deposition of any non-volatile product of reaction on the windows of the cell, but after the first experience mentioned above no such effect was ever detected. Since it is known that decomposition of the diborane is inappreciable in the space of a few hours[6] and since any reaction products in addition to hydrogen resulting from reaction of the diborane with the cell window cement are probably non-volatile in nature, it is believed that all of the absorption bands obtained are very probably due to B_2H_5.

Apiezon stopcock grease was used exclusively in handling diborane; no evidence of any reaction between the two was ever detected. Dr. Burg found in an experiment performed to test this point that the diborane is apparently unaffected by prolonged contact with Apiezon grease.

Figure 1 shows the transmission curves obtained. Curves at other pressures have been omitted from the figure in regions of strong absorption. The positions of the absorption maxima are tabulated in Table I. Braces in the table indicate those maxima which are assumed in the following discussion to be parts of the same band.

Stock[6] refers to a study of the infra-red spectrum of diborane made by Frl. G. Laski, but no details of this work have been published so far as the writer is aware.

DISCUSSION

It was hoped that the infra-red data reported here and the Raman data on liquid diborane obtained by Anderson and Burg[7] would together permit a reliable complete vibrational analysis of the diborane spectrum to be made. This object has not been achieved due primarily to the complexity of the infra-red spectrum. However a

[5] H. Gershinowitz and E. B. Wilson, Jr., J. Chem. Phys. **6**, 197 (1938).

[6] See *Hydrides of Boron and Silicon*, by Alfred Stock (Cornell University Press, 1933).

[7] T. F. Anderson and A. B. Burg, J. Chem. Phys. **6**, 586 (1938).

TABLE I. *Positions of infra-red absorption maxima of diborane.*

FREQUENCY cm^{-1}	UNCERTAINTY cm^{-1}	INTENSITY
393, 412, 431	±3	strong
673, 685	3	weak
831	3	weak
981	2	strong
1154, 1178, 1197	2	very strong
1274, 1311	2	medium
1377	3	medium
1405	5	medium
1587, 1608, 1626	3	very strong
1722	10	weak
1852, 1874	4	strong
1993	6	medium
2134	10	very weak
2217	10	very weak
2353	8	strong
2558	10	strong
2625	10	strong
3135	20	very weak
3670	40	strong
4040	50	weak
4250	50	weak
4550	75	weak
5150	75	weak
5800	100	weak

tentative analysis of the main features will be offered here. An ethane-like structure for diborane has been accepted as the correct one in the following discussion.

There are two factors which may be expected to result in a more complicated spectrum for diborane than that of ethane. The first of these is the occurrence of two abundant isotopes of boron, B^{10} and B^{11}, in the ratio of approximately 1 : 4. The relative numbers of $B^{11}-B^{11}$, $B^{10}-B^{11}$, and $B^{10}-B^{10}$ diborane molecules are therefore expected to be 16 : 8 : 1, respectively. Since less stringent selection rules apply to the molecules of lower symmetry, the presence of the $B^{10}-B^{11}$ molecules may be expected to give rise to other bands in the spectrum in addition to complicating the structure of bands arising from the $B^{11}-B^{11}$ molecules. A second complicating possibility is that low-lying electronic states may be involved in some of the transitions observed in the infra-red and Raman spectra. Mulliken[8] has shown that a number of low-lying electronic states are to be expected for the diborane molecule. He was unable to detect[9] any of these in the region from 8500 to 40,000 cm^{-1}. The diamagnetic character of diborane has been established[10] with the additional result that any paramagnetic states must lie at least 1050 cm^{-1} above the ground state. It seems very probable therefore that there are several electronic states which lie less than 8500 cm^{-1} above the ground state and some of which may lie in the infra-red spectral region investigated.

The vibrational selection rules applicable to the more symmetrical molecules of diborane are the same as for ethane and are summarized by Bartholomé and Karweil.[11] In this discussion the fundamental frequencies of diborane will be designated in the same manner as was used in discussing the ethane spectrum.[12] These labels and the selection rules applying to the fundamental vibrations are reproduced in Table II, where $\bar{D}_3$ refers to the point group used by Howard[13] (and called D'_{3h}) to describe the symmetry of the molecule for any value of the internal rotational angle, and D_{3d} and D_{3h} refer to the staggered and eclipsed configurations, respectively. The selection rules for the less symmetrical molecules are readily found from the correlation which exists between the classifications of the vibrations according to the point

TABLE II. *Designation of the fundamental frequencies of diborane.*

$\bar{D}_3$	FUNDAMENTAL FREQUENCIES	D_{3d}	D_{3h}	SELECTION RULES*	C_{3v}
A_1	$\nu(\pi)>\bar{\delta}(\pi)>\tau(\pi)$	A_{1g}	A_1'	$R(P)$	A_1
$\bar{A}_2$	$\bar{\nu}(\pi)>\bar{\delta}(\pi)$	A_{2u}	A_2''	$I(\|\|)$	
E	$\nu(\sigma)>\bar{\delta}(\sigma)>\tau(\sigma)$	E_u	E'	$I(\perp)$, $R(D)$†	E
$\bar{E}$	$\bar{\nu}(\sigma)>\bar{\delta}(\sigma)>\bar{\tau}(\sigma)$	E_g	E''	$R(D)$	
$\bar{A}_1$	ω_i (restricted internal rotation)	A_{1u}	A_1''		A_2

* Symbols: R—Raman active; I—Infra-red active; P—Polarized; D—Depolarized; $\|$, π—parallel; $\perp$, σ—perpendicular.
† For symmetry D_{3d} this type vibration is not permitted to be Raman active.

[8] R. S. Mulliken, J. Chem. Phys. **3**, 635 (1935).

[9] See J. Phys. Chem. **41**, 306 (1937).

[10] L. Farkas and H. Sachsse, Trans. Faraday Soc. **30**, 331 (1934). See also reference 5 of R. S. Mulliken, J. Chem. Phys. **3**, 635 (1935).

[11] E. Bartholomé and J. Karweil, Zeits. f. physik. Chemie **B39**, 1 (1938).

[12] F. Stitt, J. Chem. Phys. **7**, 297 (1939).

[13] J. B. Howard, J. Chem. Phys. **5**, 442 (1937).

groups mentioned above and according to the point group C_{3v}, as indicated in Table II.

If the potential function of the diborane molecule is not radically different from that of ethane, the fundamental vibrations are expected to fall into four groups as suggested by the designations of Table II. The ν or essentially B—H stretching frequencies are expected to be in the neighborhood of 2500 cm^{-1} as the Raman data of Anderson and Burg[7] and the work of Crawford and Edsall[14] on $B_3N_3H_6$ have already indicated. The δ or essentially B—H bending frequencies are likewise expected to be in the vicinity of 1200 cm^{-1}. The gaseous heat capacity of diborane at low temperatures[3] has led to the conclusion that the potential barrier hindering internal rotation is rather high, so that ω_i, the torsional oscillation, is at least as high as 300 cm^{-1}. The remaining vibrations, which have been labeled as τ vibrations here, are expected to be greater than ω_i and less than 1200 cm^{-1}. These predictions can be made somewhat less intuitive by assuming that a three constant potential function such as Howard[13] found fitted the ethane data fairly well also applies as a first approximation to diborane. The values thus calculated for the fundamental vibration frequencies of diborane are shown in Table III. In this table the figures in parentheses were assumed to be correct (see below) in order to find the constants of the potential function.

TABLE III. *Approximate fundamental frequencies (in cm^{-1}) calculated for diborane.*

A_1	2385	1315	(795)
A_2	2380	(1180)	
E	2485	1260	715
$\bar{E}$	(2490)	1240	860

The Raman data of Anderson and Burg for liquid diborane[15] as well as the infra-red frequencies for the gas are included in the first column of Table V. They are arranged approximately in order of decreasing intensities. Comparison of the infra-red and Raman spectra with predictions based on Table III and the selection rules immediately emphasizes several striking features of the experimental data. First, as Anderson and Burg pointed out, two strong sharp lines are observed in the Raman spectrum in the neighborhood of 2300 cm^{-1} whereas only one is expected. Their separation of 421 cm^{-1} seems too large to permit the assignment of them as a resonance degenerate pair such as occurs with ethane. Second, the very strong infra-red bands at 1608 and 1863 cm^{-1} are apparently not assignable as due to fundamental vibrations. Third, the only strong infra-red band below 980 cm^{-1} is found around 400 cm^{-1}, which is much lower than expected for the infra-red active $\tau(\sigma)$ vibration. It is the explanation of the origin of these features which presents the greatest difficulty in the analysis of the spectrum.

TABLE IV. *Suggested fundamental frequencies (in cm^{-1}) of diborane.*

A_1	2523	1180	793
A_2	2353	1178	
E	2590	1287	981
$\bar{E}$	2489	1377	831
$\bar{A}_1$	605 if El = 412; 350 if El = 1608		

It is only in the regions of comparatively high dispersion that the observed band contours may be interpreted as indicating band type. Parallel type bands are expected to show a separation of 35 cm^{-1} between the P and R branches and to have about one-fifth of their intensity in the Q branch, whereas the shape of the perpendicular type bands depends upon the magnitude of the interaction between vibration and rotation. The bands with centers at 1178 and 1608 cm^{-1} are therefore probably parallel type.[16]

A number of the observed frequencies may be readily identified as fundamentals on the basis of Tables II and III. Thus the Raman shifts of 793, 806, and 2489 cm^{-1} and the infra-red band at 1178 cm^{-1} are immediately assigned as shown in Table V and the values of the fundamentals $\nu(\pi)$, $\bar{\nu}(\pi)$, and $\nu(\sigma)$ are similarly determined with somewhat less certainty. The value of $\tau(\sigma)$, the low frequency infra-red active fundamental is taken as 981 cm^{-1} since 412 cm^{-1} is ruled out as a

[14] B. L. Crawford, Jr. and J. T. Edsall, J. Chem. Phys. 7, 223 (1939).

[15] In Table I of Anderson and Burg's paper, the shifts 2867.8e and 3119.7e are due to lines from the mercury arc and 1008.1e is a questionable line. (Communication from Dr. Anderson.)

[16] The band at 412 cm^{-1} is also apparently parallel type, but the shape of the long wave-length side of this band is rather uncertain due to the high percentage of stray radiation and the consequent low sensitivity in this extreme range of the KBr prism.

possibility by the heat capacity. The remaining five fundamental frequencies shown in Table IV have been chosen so as to lead to the simplest assignments in accordance with the selection rules and simultanously produce a calculated heat capacity in agreement with the observed. The choice of five frequencies of reasonable magnitude to satisfy these conditions is by no means as arbitrary as one might at first suppose, since the heat capacity agreement must extend over a considerable range of temperature (100 to 300°K). Two different values of ω_i are given in Table IV corresponding to different analyses of the spectrum as discussed below.

By far the strongest band in the infra-red spectrum of diborane is the parallel type band at 1608 cm^{-1}. Since this frequency probably is not a fundamental, and since overtone and combination vibrational transitions are expected to result in less intense absorption than the stronger fundamental bands, it seems very probable that another electronic state is involved here. The same may be said less forcefully with regard to the bands at 1863 and 412 cm^{-1}. Tentative analyses of the spectrum based on two different assumptions as to electronic levels are presented in Table V.[17] (The symmetry group symbol in parentheses following some of the assignments represents the highest symmetry group whose vibrational selection rules permit the assigned transition in case it is forbidden for D_{3d} symmetry.) In the first of these analyses, denoted by El=412, electronic states are assumed to exist at 412 cm^{-1} and at 1863 cm^{-1} above the ground state of the molecule. The 412 cm^{-1} electronic state would necessarily be singlet in view of the diamagnetic character and the observed heat capacity of diborane. On this basis the band at 412 cm^{-1} would be due to a pure electronic transition, that at 1608 cm^{-1} would be an electronic-vibrational (vibronic) transition, and the Raman line at 2102 cm^{-1} would also be due to a vibronic transition. The calculated heat capacity based on the fundamental frequencies shown in Table IV is included in Table VI. The electronic contribution to the heat capacity was calculated assuming the same vibrational frequencies for the upper electronic state as for the ground state. This assumption is probably approximately true and should cause little error in the calculated heat capacity. The potential barrier associated with $\omega_i=605$ cm^{-1} is about 15,000 calories per mole if the potential is assumed to be a sinusoidal function of the internal rotational angle.

In the other analysis, denoted by El=1608, electronic states are assumed to exist at 1608 cm^{-1} and 1863 cm^{-1} above the ground state and the band at 412 cm^{-1} is assigned as a vibronic difference band. Still a third electronic state in the neighborhood of 2100 cm^{-1} may be involved as suggested in Table V. This analysis is based on the same fundamental frequencies as the other except that $\omega_i=350$ cm^{-1} corresponding to a potential barrier of about 5000 calories per mole. The electronic state at 1608 cm^{-1} was assumed to be triply degenerate in calculating the heat capacity shown in Table VI.

TABLE V. *Alternative tentative analyses of the diborane spectrum.*

Frequency cm^{-1}	Assignment* El=412	El=1608
Raman		
2523	Fund $\nu(\pi)$	Fund $\nu(\pi)$ } Res.
2102	$\nu(\pi)'-412$	$2\bar{\delta}(\pi)$ or El }
793	Fund $\tau(\pi)$	
806	Fund $\tau(\pi)$ of $B^{10}-B^{11}$	
821	Fund $\tau(\pi)$ of $B^{10}-B^{10}$	
821	Fund $\bar{\tau}(\sigma)$	
2489	Fund $\bar{\nu}(\sigma)$	
1180	Fund $\bar{\delta}(\pi)$	
1008?	Fund $\tau(\sigma)$ (C_{3v})	
Infra-red		
1608	$412+\delta(\pi)'$	El
1178	Fund $\bar{\delta}(\pi)$	
2558	Fund $\nu(\sigma)$ } Res.	
2625	$2\delta(\sigma)$ }	
1863	El	
981	Fund $\tau(\sigma)$	
3670	$\bar{\nu}(\sigma)+\bar{\delta}(\pi)=3667$	
2353	Fund $\bar{\nu}(\pi)$	
412	El	$1608-\delta(\pi)=428$
		$\bar{\delta}(\sigma)-\tau(\sigma)=396$
1287	Fund $\delta(\sigma)$	
1377	Fund $\bar{\delta}(\sigma)$ (C_{3v})	
1993	$\bar{\delta}(\sigma)+\omega_i=1982$	$\bar{\delta}(\pi)+\bar{\tau}(\sigma)=2009$
680	$\bar{\delta}(\sigma)-\omega_i=682$ (C_{3v})	$2\omega_i$ (C_{3v})
831	Fund $\bar{\tau}(\sigma)$ (C_{3v})	
1722	$412+\delta(\sigma)'(?)$	$\bar{\delta}(\sigma)+\omega_i=1727$
2134	$\bar{\delta}(\sigma)+\bar{\tau}(\sigma)=2118$	
2217	$\bar{\delta}(\sigma)+\bar{\tau}(\sigma)=2208$ (D_{3h})	
3135	$\bar{\nu}(\pi)+\tau(\pi)=3146$	

* See Table II for designation of fundamental frequencies. Abbreviations: Fund—Fundamental; Res—Resonance; El—Electronic state. Primes refer to upper electronic state.

[17] Most of the assignments of the Raman lines in Table V agree with those of Anderson and Burg.

Many of the assignments shown in Table V must of course be regarded as tentative. Other sets of fundamental frequencies differing somewhat from those shown in Table IV may be found that satisfactorily reproduce the heat capacity, but those shown seem to allow the simplest assignments in analyzing the spectrum.

It is to be noted that the possibilities of assigning the band at 412 cm^{-1} are rather limited. This frequency is too small to be any fundamental except ω_i, but the selection rules eliminate its assignment as either ω_i or $2\omega_i$. Hence it must be either an electronic state or a difference band. The analyses of Table V correspond to these two possibilities. However the most attractive assignment as a difference band permitted by the selection rules and not involving another electronic state is $\tilde{\tau}(\sigma)-\omega_i$. A set of fundamental frequencies and an analysis in which this assignment is given this band is obtained by modifying the El=1608 analysis by assuming $\tilde{\tau}(\sigma)$ and ω_i to be 780 and 368 cm^{-1}, respectively. This also results in satisfactory agreement with the heat capacity and most of the observed bands receive simple assignments on this basis.

No reference was made above to the electronic or vibronic selection rules. Vibronic transitions involving totally symmetrical vibrations are expected to be most intense in accordance with the Franck-Condon principle provided the upper electronic state has the same equilibrium symmetry as the ground state.[18] The electronic levels assumed to exist in the above analyses are not readily correlated with the levels predicted by Mulliken.[8] This may indicate that neither of the above analyses is correct or it may be due to a breakdown in electronic selection rules, a different equilibrium configuration in other electronic states, or a different symmetry than $^1A_1$ for the ground state. Detailed discussion of these possibilities is perhaps better postponed until additional experimental data is at hand.[19]

All of the above discussion has been based on an ethane-like structure for the diborane molecule. The possibility that the complicated spectrum may be due to a different type structure should not be overlooked. Of the various alternative structures which have been suggested probably a "bridge" structure similar to that reported[20] for Al_2Cl_6 is the most likely one. Such a structure possesses the same point group symmetry as ethylene (V_h) and would have eighteen distinct fundamental vibrational frequencies, all non-degenerate, of which eight would be permitted to appear directly in the infra-red spectrum. The entire spectrum can be analyzed on this basis without assuming the existence of any low-lying electronic states and the existence of a high potential barrier is automatically explained with such a structure. However, this possibility will not be discussed here in detail in view of the evidence for an ethane-like structure for diborane.[21] Unfortunately the spectrum is apparently too complex for its interpretation to lead to a reliable determination of the structure of the molecule.

TABLE VI. *Comparison of calculated and observed heat capacities of gaseous diborane.*

TEMP. °K	$C_v°$ IN CALORIES/DEGREE-MOLE		
	OBSERVED*	CALCULATED El=412	CALCULATED El=1608
100	6.35±0.20	6.18	6.35
150	6.90 .15	6.93	7.02
200	8.15 .10	8.15	8.13
250	9.80 .10	9.76	9.76
300	11.60 .15	11.56	11.68

* Observed values were taken from the figure of reference 3.

I wish to thank Professor E. B. Wilson, Jr. for the use of the spectrometer and for his interest in this work. I am also indebted to Dr. S. H. Bauer and to Professor R. S. Mulliken for helpful discussions and suggestions concerning the interpretation of this data, and to Professors H. I. Schlesinger and A. B. Burg for providing the diborane and for interesting discussion.

[18] G. Herzberg and E. Teller, Zeits. f. physik. Chemie **B31**, 410 (1933).

[19] According to Mulliken's results only one electronic transition would be expected to appear with much intensity in absorption, namely $^1A_{1g}\rightarrow{}^1E_u$. This would result in a perpendicular type band if no simultaneous vibrational transition occurred. 1863 cm^{-1} may correspond to this ^1E_u state. 1608 cm^{-1} could correspond only to $^3A_{2u}$, but such a singlet-triplet transition should be very weak.

[20] K. J. Palmer and N. Elliott, J. Am. Chem. Soc. **60**, 1852 (1938).

[21] Bauer did not calculate curves for bridge structures in his first analysis of the electron diffraction photographs, but he has recently re-examined these data to determine whether or not this structure is definitely eliminated. He finds that curves calculated for bridge models are very sensitive to the values of the parameters of the model and in general do not agree with the experimental curves. However for certain values of the parameters the calculated curve resembles the observed one in most respects except for the absence of a small inner peak found on the photographs of both diborane and ethane. He believes therefore that a bridge structure is very probably incorrect, although perhaps not rigorously excluded by the electron diffraction photographs obtained. (Private communication.)

The Absorption Spectrum as a Quantitative Test for Mercury Vapor in Air

K. C. CLARK AND O. OLDENBERG
Research Laboratory of Physics, Harvard University, Cambridge, Massachusetts

(Received September 15, 1941)

In order to test the mercury vapor content of the air in a laboratory, the absorption spectrum of this vapor is compared with a set of calibration spectra. With a simple apparatus ("medium size" quartz one-prism spectrograph) vapor pressures far below the toxic limit can be determined.

I. PROBLEM AND PREVIOUS WORK

THE insidious, slow poisoning effect of breathing mercury vapor contained in the air of laboratories was first emphasized by Stock.[1] He worked out devices which should prevent the escape of any mercury vapor into the air. Goodman[2] reviewed recent work on this problem.

The practical problem of testing the mercury content of the air in a laboratory is not easily solved because of the very small concentrations involved. Mueller and Pringsheim[3] studied the mercury content of the air at the Physics Laboratory of the University of Berlin with the help of the resonance radiation of mercury which was partially absorbed when passing through the air; they measured the decreased intensity of this radiation with a photoelectric cell. Woodson,[4] working at the Research Laboratory of the General Electric Company, further developed this method; he applied a simpler source of light, an ultraviolet lamp (not described in detail), which emits about 90 percent resonance radiation. The only other technical device we know of is the mercury vapor detector built by the same company, which makes use of the property of selenium sulphide to turn dark when exposed to mercury vapor in the air.[5] Duffendack, Wolfe, and Lederer[6] mentioned, without giving details, that they determined the mercury vapor content in hydrogen discharge tubes by the absorption spectrum.

Recently, after we finished the experiments described below, an exhaustive study on the "Hazard of mercury vapor in scientific laboratories" was published jointly by the National Bureau of Standards and the Division of Industrial Hygiene, National Institute of Health.[7] The authors state that, for their purpose, the various *chemical* methods that have been proposed are distinctly unsatisfactory, and they apply the General Electric *optical* detector developed by Woodson. Their studies lead to a toxic limit of 0.1 mg/m³, that is, as low as 8/1000 of saturation at 20°C. It must be kept in mind, however, that some persons are oversensitive to mercury, as is known to be the case with other metal poisons. According to Stock, persons who once suffered from mercury poisoning may remain oversensitive to this poison. Stock[8] suggested a toxic limit as low as 0.015 mg/m³, that is, only 1/7 of the figure given above.

The techniques of measurement all involve special equipment. Because of the practical importance of the problem, we wish to call attention to a simple spectroscopic method which gives entirely satisfactory results with apparatus available in many laboratories of physics and chemistry.

II. METHOD AND APPARATUS

On a continuous background we study the absorption line 2537 of the mercury vapor contained in a long column of air to be tested, and calibrate the apparatus by photographing the same line with the same spectrograph and a

[1] A. Stock, Zeits. f. angew. Chemie **39**, 461 (1926) and **42**, 999 (1929).
[2] C. Goodman, Rev. Sci. Inst. **9**, 233 (1938).
[3] K. Mueller and P. Pringsheim, Naturwiss. **18**, 364 (1930); K. Mueller, Zeits. f. Physik **65**, 739 (1930).
[4] T. T. Woodson, Rev. Sci. Inst. **10**, 308 (1939).
[5] General Electric Company, pamphlet dated July 3, 1939.
[6] O. S. Duffendack, R. A. Wolfe, and F. Lederer, J. Opt. Soc. Am. **31**, 174 (1941).
[7] M. Shepherd, S. Schumann, R. H. Flinn, J. W. Hough, and P. A. Neal, J. Research Nat. Bur. Stand. **26**, 357 (1941). This paper gives more references.
[8] A. Stock and F. Cucuel, Ber. d. D. Chem. Ges. **67**, 122 (1934).

mercury vapor column of known length and partial pressure. At this laboratory a similar procedure has been applied to the quantitative determination of free hydroxyl radicals. The calibration is necessary even though the absorption coefficient of mercury vapor for the line 2537 is known in absolute units, for the reason that the spectrograph has a deteriorating effect on the appearance of the absorption line. Only if the spectrograph could resolve lines of considerably less width than the line 2537, would the spectrum give evidence of the true contour of this line,[9] and for the mercury line used this requirement is not even met by large grating spectrographs. All we can do with an imperfect spectrograph is to match absorption lines of equal intensity. For this purpose we photograph first the absorption spectrum of the air to be tested and next a set of calibration spectra, taken with various known concentrations of mercury vapor. Since we are dealing with pressures so low (0.0015 mm or less) that the vapor is strictly monatomic and no broadening effects occur among the mercury atoms, the intensity of the absorption line is determined only by the total amount of mercury vapor traversed, irrespective of its compression; and hence it is immaterial whether the calibration is carried out with a column of the same length as is used in the test of the air. In other words, Beer's law holds.[3] The average unknown concentration is immediately derived by matching the test absorption line to a calibration line of equal intensity[10] and by applying Beer's law. The calibration spectra are conveniently taken with a short column of saturated vapor, the pressure of which is regulated by the temperature. In any case, the mercury vapor is mixed with one atmosphere of air. For highest accuracy all spectra should be taken on the same plate. Care must be taken that the blackening of the continuous background is very nearly the same for all spectra to be compared. The sharp focus of the spectrograph and the narrow slit width must remain constant for both the test and calibration exposures, for they considerably influence the appearance of the absorption line photographed. Attention should be paid to the uniform temperature of the lenses and the prism by keeping the spectrograph in the same uniformly heated room for some length of time. Although the calibration described eliminates errors caused by the lack of resolving power of the spectrograph, still it must be found out whether the easily available spectrograph is an instrument sufficiently sensitive for the search of such small traces of mercury vapor as may be detrimental to health. An absorption line so weak that it would barely show up even in an ideal spectrograph would be entirely unobservable with an ordinary one-prism spectrograph. It is the purpose of the experiments described below to find out whether the method is practical, that is, whether concentrations as low as the toxic limit can be measured with a simple technique.

A "medium size" Hilger quartz spectrograph (one prism, $f=60$ cm, "all metal" instrument) was applied, which is easily transportable and available in many laboratories. Our instrument gives the highest resolution when used with full aperture; this indicates the highest quality of the prism and lenses. The slit width was 5/1000 mm. For the test of the room the air enclosed in the spectrograph had the same composition as the air of the room; for the calibration in which only a short column was used, the air enclosed was kept free of mercury vapor. Eastman lantern slide plates were used.

The continuous background was furnished by the positive crater of a carbon arc. The negative carbon was mounted to the side so that the light from the positive crater traversed as little as possible of the arc proper. The crater was focused by a large aluminum-plated concave mirror on the slit of the spectrograph. The path in air was about 8 m, the time of exposure 8 minutes.

Because of the high sensitivity with which the absorption spectrum shows up, the calibration has to be made with a very short absorption tube. The length of the tube used was 2.2 cm;

[9] See O. Oldenberg and F. F. Rieke, J. Chem. Phys. **7**, 486 (1939).

[10] A special instrument (J. Opt. Soc. Am. **27**, 147 (1937)) was described for the matching of absorption lines. In the same paper it was discussed how to compensate for a slight inequality of the backgrounds. For the present purpose, if the continuous backgrounds of all absorption spectra are equal, it is easy enough to match absorption lines, without a special instrument, under a low-power microscope, preferably a binocular microscope or an ordinary magnifying lens. Superposition of the plates permits a side-by-side comparison of the lines in question.

it was made of Pyrex with quartz windows and contained air of atmospheric pressure and a pool of liquid mercury. For the temperature control, it was surrounded by a water jacket.

III. Results

It is surprising how sensitive the apparatus is. The limit of observation for the absorption line is given by a saturated column 2.2 cm long, at a temperature as low as 2.5°C, that is, with a concentration of 2.7 mg/m³. Hence, for the air of the laboratory tested with a column 8 m long, the limit of observation would be a concentration of 0.0075 mg/m³. This is 1/13 of the toxic limit recently established[7] (0.1 mg/m³), or else ½ of the more conservative limit given by Stock.[1] The conclusion is that the simple apparatus described above is adequate for all practical purposes. Its range can be further lowered by using a longer optical path in the laboratory air. A plane mirror could well be added to localize this path.

This sensitivity improves on the estimate of that of the selenium sulphide method given by the National Bureau of Standards[7] as 0.150 mg/m³. This figure makes the selenium sulphide method too insensitive since the toxic limit is lower. With the optical apparatus constructed by Woodson, the physicists of the National Bureau of Standards achieved a sensitivity of 0.004 mg/m³.

The accuracy with which the simple spectrographic method described above may determine the mercury content is estimated as follows. The faintest calibration absorption lines observed, taken at temperatures of 2.5 and 6 degrees or concentrations of 2.7 and 3.8 mg/m³, differ so clearly that in the process of matching one may usually estimate one intermediate intensity. In this case, the accuracy of the result is about 20 percent. The accuracy is highest for the faintest absorption lines. For many spectra taken with somewhat stronger absorption lines, the accuracy was judged to be 50 percent. For the present purpose this is sufficient, as the mercury content of the air easily changes when doors or windows are opened.

The method here described will be useful in laboratories in which a good quartz spectrograph is available and only occasional tests are needed. It has an advantage over the method of Woodson[4] in that the continuous background permits us to distinguish between the absorptions by mercury or ozone or possible organic vapors. On the other hand, for technical purposes where many routine measurements are needed, the apparatus of Woodson has the advantage of an instantaneous response. This feature allowed the physicists of the National Bureau of Standards to find out the causes of certain sudden increases of the mercury content of the air.

With our spectrograph we tested various rooms with old wooden floors, in the numerous cracks of which presumably mercury droplets are hidden. Traces of mercury vapor, about 10 percent of toxicity (limit assumed as 0.1 mg/m³), could be found when doors and windows were kept closed for a day. Undoubtedly, it is easy to keep the concentration of mercury vapor far below toxicity. This result is in good agreement with the recent findings of the National Bureau of Standards.

The Spreading of Oils on Water

Part III. Spreading Pressures and the Gibbs Adsorption Relation

W. A. ZISMAN
Naval Research Laboratory, Anacostia Station, Washington, D. C.
(Received September 5, 1941)

The Gibbs adsorption relation between surface tension and concentration is applied to new data on the equilibrium pressure of spreading of oil drops containing long-chain alcohols. It is found that the graph of pressure against concentration is an hyperbola and an empirical formula is fitted to the measurements for each alcohol. There is derived an equation of state of the polar molecules adsorbed at the oil-water interface. It is then shown that the interfacial monolayer is a stable mixed film made up of polar and non-polar molecules, the latter being components originally of the oil. It is pointed out that these conclusions may be significant in the interpretation of film phenomena such as are involved in the stabilization of emulsions and the structure of cell membranes.

1. INTRODUCTION

IT has been shown that the spreading of non-volatile mineral oils on water is due to the presence of dissolved polar molecules[1,2] and that by measuring the maximum area of spreading A_0 the average interfacial area occupied by the adsorbed molecules can be computed. However, it is also possible to obtain A_0 by applying the Gibbs adsorption theorem to the measurements of the equilibrium spreading pressures of such oil drops. This was done by Langmuir[3] in his pioneer study of the spreading properties of stearic acid solutions in Nujol. His results using the two different methods disagreed by a factor of two which led him to conclude that the Gibbs relation gave the average area per molecule as it existed associated in pairs in the liquid phase.

The procedure adopted here was similar to that used by Langmuir[3] and Adams[4] to study the film pressures exerted by oil solutions. The cleaned water surface of a Cenco hydrophil balance was covered with a "piston film" of an insoluble substance such as eicosyl alcohol, eicosanoic acid, or octadecanoic acid. Initially, when the oil drop to be studied was placed on the water, the piston film was placed under sufficient compression to prevent the spreading of the oil disk. If the piston film pressure was then decreased until the disk commenced to spread, the movable barrier of the balance could be slid back and forth causing the disk to expand and contract, and as long as the disk was thin and flat, the pressure on the mica float remained constant. The equilibrium pressure so determined was the equilibrium spreading pressure F due to the reversible adsorption of the polar molecules at the oil-water interface. When an acid was used for the piston film, the water in the Cenco balance was maintained at pH 2 with sulphuric or hydrochloric acid.

It was found that F was independent (to within the experimental error of 0.2 percent) of the type of insoluble film used for the piston film. This was to be expected so long as the molecules of the piston film were highly insoluble in oil. The temperature of the apparatus and the air surrounding it being maintained constant to within 0.2°C of 25°C, the experimental procedure consisted in measuring F for a series of accurately prepared solutions of the alcohol in oil.

If there are no electrically charged molecules present in the interfacial film, and if the solution of the alcohol in oil behaves like an ideal solution, Gibbs adsorption theorem leads to the well-known relation

$$\Gamma = -(\partial\gamma/\partial w)w/R\theta, \qquad (1)$$

where Γ is the surface excess in gram moles of adsorbed polar molecules per square cm of interface, R is the gas constant (8.314×10^7),

[1] W. A. Zisman, J. Chem. Phys. **9**, 534 (1941).
[2] W. A. Zisman, J. Chem. Phys. **9**, 729 (1941).
[3] I. Langmuir, J. Frank. Inst. **218**, 143 (1934).
[4] N. K. Adam, Proc. Roy. Soc. **B122**, 134 (1937).

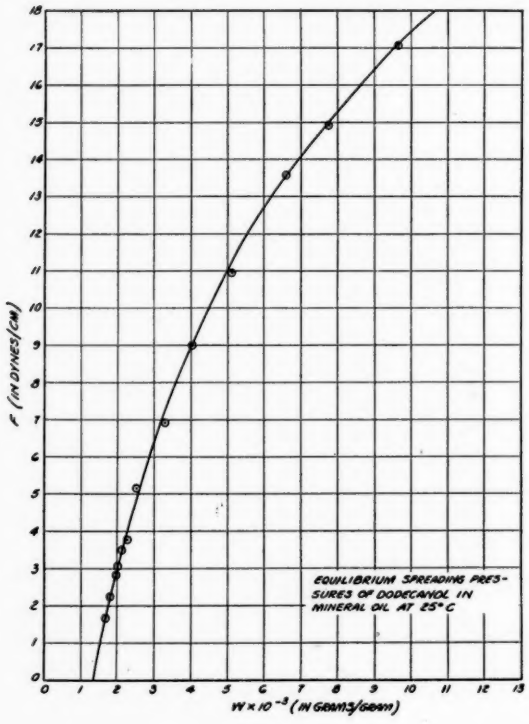

FIG. 1.

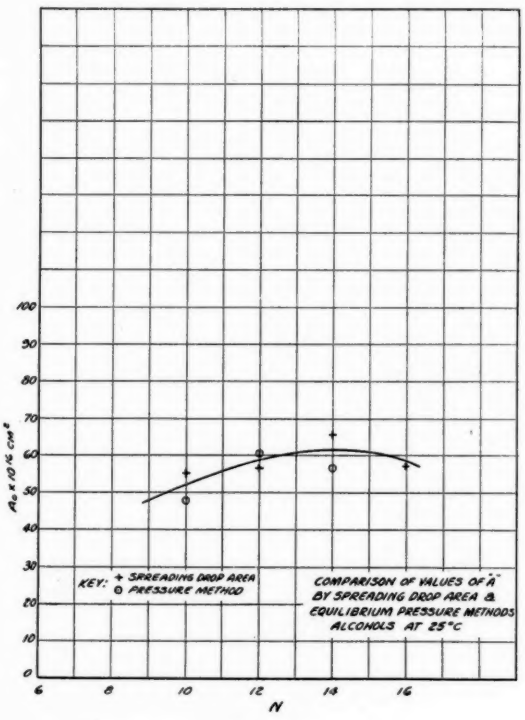
KEY: + SPREADING DROP AREA
⊙ PRESSURE METHOD
COMPARISON OF VALUES OF Ā BY SPREADING DROP AREA & EQUILIBRIUM PRESSURE METHODS ALCOHOLS AT 25°C
N

FIG. 2.

γ is the surface tension at the oil-water interface, and θ is the absolute temperature.

The spreading pressure F is related to the surface tensions γ and γ_0 of the interface with and without the presence of adsorbed molecules by

$$F=\gamma-\gamma_0. \tag{2}$$

Therefore $\partial\gamma/\partial w=\partial F/\partial w$ and (1) can be written

$$\Gamma=-(\partial F/\partial w)w/R\theta. \tag{3}$$

The total number of adsorbed molecules expressed in moles per cm² is necessarily $1/A(6.06\times10^{23})$. If the adsorbed molecules occupy an interfacial layer δ cm thick, the volume of 1 square centimeter of this layer is δ cm³, and if the density of the layer is ρ and the molecular weight of the adsorbed molecules is M, then the number of polar molecules normally present in that layer without adsorption will be $\rho\delta w/M$ moles per cm² of interface.

The surface excess, Γ, is therefore given by

$$\Gamma=\frac{1}{A(6.06\times10^{23})}-\delta\rho w/M. \tag{4}$$

It is a simple matter to show that the term $\delta\rho w/M$, for the substances and concentrations employed here, amounts to only 0.4 percent of the first term of (4) at the lowest concentration and 4 percent at the highest concentration. In the case of dodecanol δ is the length of the molecule or 18×10^{-8} cm, $\rho=0.840$, $M=200$, and w varies from 1.3×10^{-3} to 13×10^{-3} g/g.

Applying (3) and (4) to the experimentally determined relation between F and w permits a calculation of A as a function of w. As the external pressure should approach zero when w approaches w_0, the intercept of the experimental curve relating F and w should give a value of w_0 for each alcohol in agreement with that found by an independent method in Part II. Finally, for the particular value of A corresponding to the concentration w_0, the Gibbs relation should give a result in agreement with the value of A_0 found in Part III.

2. Experimental Results on Film Pressures

Solutions in mineral oil of decanol, dodecanol, and tetradecanol were used since these com-

pounds do not ionize at the oil-water interface, have low solubilities in water and satisfactory solubilities in oil, and are sufficiently non-volatile to prevent experimental difficulties in measuring w. The mineral oil used was identical with that employed throughout Parts I and II, while the alcohols were all Eastman preparations which had been shown in Part II to be of high purity. Measurements were also made on solutions of octanol, but the volatility of the octanol was too great to permit reliable results at low film pressures.

The measurements on dodecanol are given in Fig. 1 to illustrate the general character of the results. Each graph was free from any signs of hysteresis as would be expected from the reversibility of the adsorption of molecules having brief lifetimes of orientation at the oil-water interface. The curves all fitted the hyperbola

$$F=w/(a+bw)+k \qquad (5)$$

within the limits of precision of the apparatus (from 0.2 percent at the highest pressures to 0.5 percent at the lowest pressures). Using this empirical formula the intercept on the w axis w_0 and the initial slope $(\partial F/\partial w)_0$ were calculated, and with them and relations (3) and (4) A_0 was obtained. The resulting values of a, b, k, w_0, and A_0 for the three alcohols are presented in Table I.

Upon comparing the above values of w_0 with those given in Table I of Part II, it will be seen that there is agreement within 3 percent or better for each alcohol. The values of A_0 are in fair accord with those presented in Table I of Part II, and this is made more evident by the graph of Fig. 2. Since A_0 is computed from the measurement of a slope and an intercept, the agreement is quite satisfactory for the precision of the apparatus used.

The total pressure acting on the polar molecules adsorbed at the oil-water interface is the sum of the external pressure F exerted by the piston film, and the resultant of the tensions acting at the periphery of a disk of the pure oil. Since the latter was shown in Part I to be -11.3 dynes/cm, it follows that the intercept of Eq. (5) on the F axis should be the same, i.e., k should also be -11.3 dynes cm. It will be noted that although the individual values of k in Table I are not quite correct, the mean of the three determinations is -11.0. This is in a good agreement as could be expected, for k is the intercept on the F axis obtained by extrapolation from a curve fitted to the experimental data for values of w greater than w_0, and this is made difficult because the slope changes appreciably in the vicinity of w_0.

The following conclusions can now be made: first, to the order of accuracy of these measurements the Gibbs adsorption relation (1) holds for dilute solutions of alcohols in oil; and second, the measured values of A_0 and w_0 obtained by the two independent methods described here and in Part II agree sufficiently well to eliminate the possibility that edge diffusion loss is a serious source of error for molecules having 10 or more carbon atoms.

The agreement found here between the two methods and the disagreement by a factor of two found by Langmuir in the case of stearic acid,[3] may mean that the Gibbs relation holds only for non-ionizable molecules, or as Langmuir pointed out (3), it may mean that the acids are associated in pairs in oil solution. If the latter reason is correct, it follows that the alcohols are not associated in pairs in oil solution.

3. Theoretical Considerations Relative to the Equation of State

From the above discussion it is seen that if f is the total film pressure acting on the polar molecules in the oil-water interface, then it is related to the externally applied film pressure F by

$$f=11.3+F. \qquad (6)$$

Hence the empirical formula (5) can be rewritten

$$f=w/(a+bw). \qquad (7)$$

Although f is not accessible for measurement with the technique described here unless it exceeds 11.3 dynes/cm, it is the theoretically

Table I. *Calculated constants for alcohols in oil. Temp.* = 25°C.

N	a	b	k	w_0	A_0
14	0.0102	0.0303	−10.7	1.63×10^{-3}	56.3×10^{-16} cm²
12	0.0113	0.0272	− 9.0	1.34	60.2
10	0.0056	0.0264	−13.3	1.15	47.5

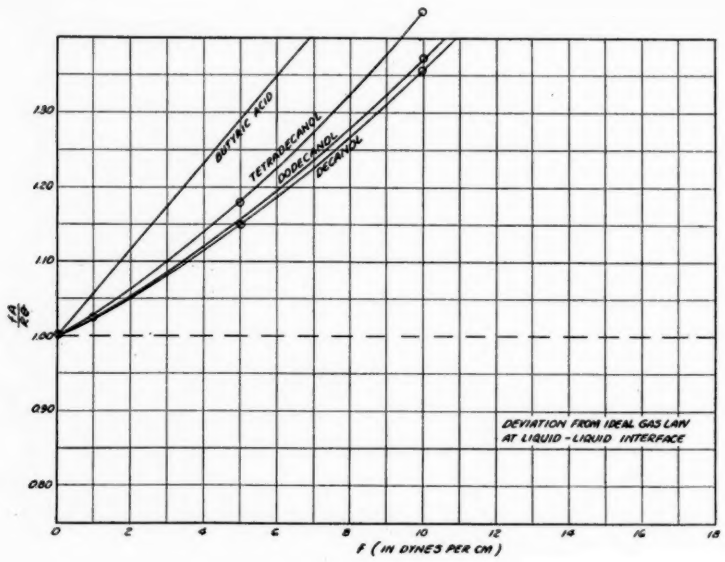

FIG. 3.

significant variable for use in discussing the equation of state of the adsorbed molecules.

Applying relation (3) to (7) one obtains

$$\Gamma=\frac{w}{R\theta}\left[\frac{1}{a+bw}-\frac{wb}{(a+bw)^2}\right]. \tag{8}$$

Substituting (4) in (8) and neglecting the small correction term $\delta\rho w/M$ there results the convenient relation

$$f(1-bf)A=R_1\theta, \tag{9}$$

where

$$R_1=R/6.06\times10^{23}=1.37\times10^{-16}. \tag{10}$$

Evidently, the ideal gas law in two dimensions ($fA=R_1\theta$) is not obeyed by these interfacial films except in the limiting case of small pressures. A plot of $fA/R_1\theta$ against f is given in Fig. 3 for each alcohol. These curves are similar to the results of the analysis by Schofield and Rideal[5] using the data of Harkins and King[6] on the adsorption of butyric acid at the benzene-water interface. Their results are also given in Fig. 3 for comparison.

Equation (9) can be written

$$fA/R_1\theta=1+b(1+bf+b^2f^2+b^3f^3+\cdots)f. \tag{11}$$

Following Schofield and Rideal[5] this can be arranged in a two-dimensional form of the Amagat equation of state, i.e., $f(A-B)=xR_1\theta$, or

$$fA/R_1\theta=x+Bf/R_1\theta. \tag{12}$$

From (11) and (12) $x=1.00$, and B, the second virial coefficient, is given by

$$B/R_1\theta=b(1+bf+b^2f^2+b^3f^3+\cdots). \tag{13}$$

Schofield and Rideal showed that x was between 0.95 and 1.00 while B was between 24×10^{-16} and 25×10^{-16} cm^2 for butyric acid at the benzene-water interface. A calculation of B with (13) when $f=15$ for the three alcohols studied here resulted in values between 19×10^{-16} and 24×10^{-16} cm^2. Use was made of $f=15$ because Eq. (7) is most accurately fitted to the data in the range $f=11.3$ to $f=20$ dynes/cm.

Schofield and Rideal demonstrated by their analyses of surface tension data at the air-water interface that x decreased from unity as the cohesive forces between the polar molecules of the aliphatic fatty acids became more powerful. If this is true at the oil-water interface, the result already given for the value of x indicates the absence of cohesive forces between the adsorbed alcohol molecules. They also demonstrated in the case of the long-chain molecules that at the air-water interface $fA/R_1\theta$ did not exceed unity until f was large enough to cause a close packing of the monolayer. But from Fig. 3 it is seen that this condition exists at the oil-water

[5] R. Schofield and E. Rideal, Proc. Roy. Soc. **A109**, 69 (1925).

[6] W. D. Harkins and R. King, J. Am. Chem. Soc. **41**, 983 (1919).

interface for all values of f, however small. From the results in Table I it is seen that A_0 ranges from 50×10^{-16} to 60×10^{-16} cm^2. Since the actual cross-sectional area of these alcohols is well known to be between 20×10^{-16} and 22×10^{-16} cm^2, it is difficult to understand how such a condition of packing could exist for all film pressures studied unless there were non-polar hydrocarbon molecules of the oil packed in between the adsorbed alcohol molecules thus forming a mixed interfacial film or a two-dimensional solution. If such is the case, B appears to be the average cross-sectional area of all the molecules forming the mixed film.

Another method of analyzing these data is more illuminating. For example, if the values of w and $\partial F/\partial w$ obtained from the graph of the observed spreading pressures as a function of decanol concentration are applied to relations (3) and (4), the resulting values of A are given in Table II.

Evidently the highest film pressures used caused A to approach a limiting value of approximately 43×10^{-16} cm^2. This is nearly twice the cross-sectional area of the decanol molecule. It may therefore be true that as w increases the mixed film of decanol and hydrocarbon molecules approaches a 1 : 1 proportion of the components.

A similar analysis of the data obtained with the dodecanol solutions resulted in a limiting value of A of 46×10^{-16} cm^2. A like analysis of solutions of tetradecanol could not be made due to the fact that it became insoluble in the oil as the concentrations increased in the necessary range.

TABLE II. *Area per molecule of decanol as a function of pressure.*

f(DYNES/CM)	$w\times10^3$	$\left(\frac{\partial F}{\partial w}\right)\times10^2$	$w\times\left(\frac{\partial F}{\partial w}\right)$	$A\times10^{16}$ CM^2
11.3	1.10	65.4	7.12	57.2
17.8	2.42	35.7	8.63	46.4
24.6	5.15	18.1	9.33	42.5
27.5	7.06	13.0	9.16	42.9

It is possible that the non-polar components of these mixed films can be squeezed out at high film pressures, but the necessary pressures must be in excess of 30 dynes/cm.

The qualitative conclusions reached in Parts I and II are therefore found to be correct, and hence this simple conception as to the nature of the mixed interfacial film permits the explanation of a considerable number of experimental observations.

Several conclusions can also be drawn that may prove of some interest in connection with other studies of phenomena at the liquid-liquid interface. It is obviously no longer safe to assume that results of film studies at the air-water interface can be carried over to interpret phenomena at the liquid-liquid interface. The fact that stable films exist made up of considerable proportions of non-polar hydrocarbons, and that they automatically are created at certain liquid-liquid interfaces may have some bearing on the interpretation of film phenomena such as in the study of emulsions and cells. It indicates interesting possibilities since it is now understandable how a non-polar and normally non-reactive hydrocarbon can have great influence on the physical state and stability of an interfacial film.

It is a pleasure to acknowledge the assistance of Mr. D. L. Pickett in carrying out these experiments.

Freezings and Compressions to 50,000 kg/cm²

P. W. BRIDGMAN
The Physics Laboratories, Harvard University, Cambridge, Massachusetts
(Received September 3, 1941)

THE object of this note is to present in accessible form the more important results of recent measurements, at pressures higher than those previously reached, of the freezing and compression of substances ordinarily liquid. The previous range of pressure for data of this sort has been, except for water, 12,000 kg/cm². In this paper the compressions are measured to 50,000, and the melting determinations are carried as near to this limit as is possible in the temperature range of this work, which in no case exceeded 225° and more usually was restricted to 175°, and under the limitations imposed by the very considerable subcoolings which occur at high pressures. A particular point of the investigation was to measure the compressions of both liquid and solid phases of the same substance over their accessible regions of stability; this sort of measurement has not previously been made to any adequate extent. All of the compressions have been measured at two temperatures, 25° and 75°, and a number at 125° and 175° in addition. In the more detailed presentation, which will probably be published in the *Proceedings of the American Academy*, compressions are given as a function of temperature. The results given here are for a single temperature, 50°, and were obtained by linear interpolation between the results for 25° and 75°.

The method was a simple modification of the method by which compressions of solid substances have been measured[1] in the range up to 50,000. The liquid is sealed into a lead capsule, and the over-all compression of the capsule and its contents is then determined by the previous method. The freezing parameters are determined in the same way. The detailed paper must be consulted for data from which the probable accuracy for each substance can be estimated. At each temperature at least two independent set-ups with different pressure vessels were made for every substance, so that the results given here for the compression are the average of at least four runs. In general, the compressions are probably accurate to better than 2 percent. The melting determinations were made at 25° intervals, and, in general, only two temperatures were investigated with the same filling of the apparatus.

The freezing temperatures as a function of pressure are given in Table I to the nearest degree. All temperatures listed below room temperature were obtained by a graphical interpolation between the points at higher temperatures and the recorded freezing point at atmospheric pressure. In the more detailed paper fuller tables will be given in which the volume change on freezing, the slope of the freezing curve, the latent heat, the change of internal energy, and the difference of entropy between solid and liquid are tabulated in addition to temperature. As a partial substitute, three diagrams of the freezing parameters are given here, from which all the essential information may be extracted. In Fig. 1, the melting temperature is shown as a

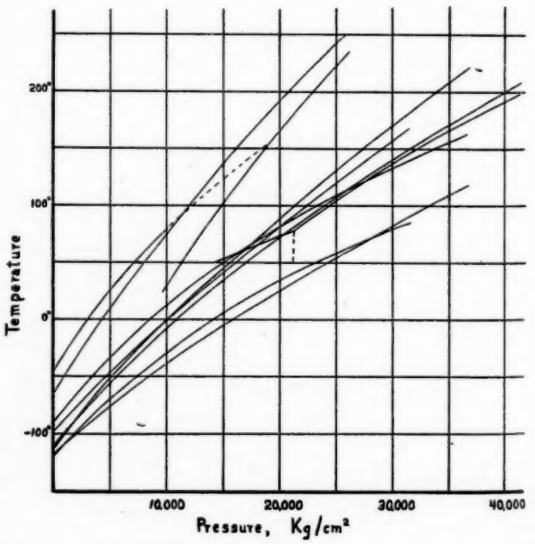

FIG. 1. Melting temperature against pressure. At 15,000 kg/cm² the order of substances, reading from top to bottom, is: chloroform, chlorobenzene, chlorobenzene (second modification), water (ice VI), *n*-butyl alcohol, carbon bisulfide, methylene chloride, *n*-propyl bromide, ethyl bromide, ethyl alcohol.

[1] P. W. Bridgman, Proc. Am. Acad. **74**, 21–51 (1940).

TABLE I. *Melting temperatures as function of pressure.*

PRESSURE KG/CM²	ETHYL ALCOHOL	*n*-BUTYL ALCOHOL	ETHYL BROMIDE	*n*-PROPYL BROMIDE	CHLORO-FORM	CARBON BISULFIDE	CHLORO-BENZENE	METHYLENE CHLORIDE	WATER
0	−117°.3	−89°.8	−119°	−110°	−63°.5	−111°.6	−45°.2	−96°.7	
5,000	−76	−33	−70	−56	+10	−51	+25	−46	
10,000	−39	+12	−29	−8	76	0	80 30*	0	
15,000	−5	49	+5	+34	137	+46	103	+42	52.5
20,000	+25	80	34	71	192	89	166	82	73.8
25,000	54	108	58	105	243	130	222	120	102.8†
30,000	82	132	80	138		170		157	137.1
35,000	109	155		169		209			166.6
40,000				197					192.3

* Second modification of the solid.
† Melting of ice VI above this, of ice VII below.

function of pressure, that is, the melting curve. In Fig. 2 the fractional change of volume on freezing is shown as a function of pressure, that is, the volume decrement in cm³ when freezing occurs of that quantity of the substance which occupies 1 cm³ at atmospheric pressure at 20°C. In Fig. 3 the latent heat is shown as a function of pressure along the melting curve, in units of kg cm/g, the natural mechanical units which result from a direct application of Clapeyron's equation to the data.

The compressions at 50°C are given in Table II as a function of pressure, from 5000 kg/cm² as zero. These compressions are the volume decrements in cm³ of that quantity of the substance which occupies 1 cm³ at atmospheric pressure at 20°C. In a number of instances figures are given in parentheses in the 5000 row. These are the absolute volumes in cm³ of those substances for which the volume has been previously measured at 5000. For these substances the absolute volume at any pressure of the table may be obtained by subtracting the volume decrement from the first figure. Thus, the volume at 50,000 kg/cm² and 50°C of that quantity of methyl alcohol which occupies 1 cm³ at atmospheric pressure at 20° is 0.620 cm³ (0.620=0.828−0.208). A knowledge of the absolute volumes as a function of pressure of those substances which have not been previously measured up to 5000 must wait for further measurements. In addition to the substances listed in the table, in the detailed paper the compressions of chlorobenzene are also given; this substance has two solid modifications with too complicated stability relations to reproduce here. The columns of compressions for the

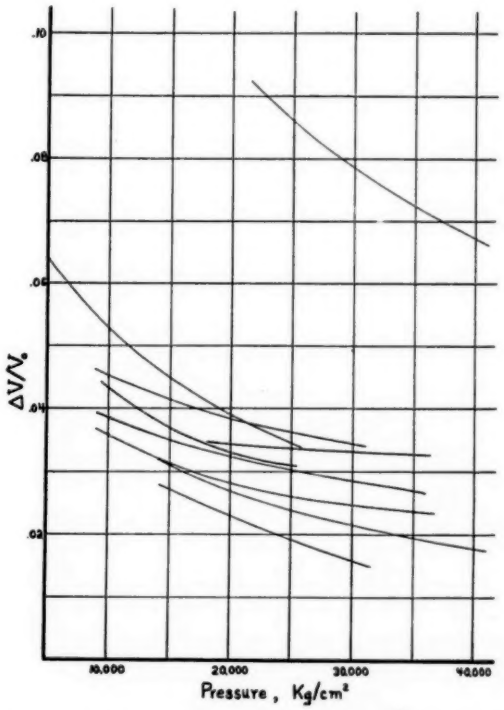

FIG. 2. The change of volume on freezing in terms of the volume of the liquid at atmospheric pressure and room temperature as unity as a function of pressure on the melting curve. At 25,000 kg/cm² the order of substances, reading from top to bottom, is: water (ice VII), methylene chloride, chloroform, ethyl alcohol, chlorobenzene (second modification), *n*-butyl alcohol, carbon bisulfide, *n*-propyl bromide, ethyl bromide.

majority of substances are broken by the occurrence of freezing; the freezing pressures and volume discontinuities are indicated in footnotes.

The melting parameters are of interest over this wider pressure range in view of recent activity in theories of the liquid state and of melting and the revival of the opinion in some

quarters that a critical point between liquid and solid may be a possibility. This new work only fortifies the conclusions which I had drawn from previous work[2] in the lower pressure range. In the first place, the melting curves of all substances are similar in qualitative aspects, so that it is appropriate to speak of "the" melting curve. The melting curve rises to indefinitely high temperatures as pressure increases indefinitely, but concave toward the pressure axis and with continually more slowly turning tangent, and without those features of behavior which would be demanded by either an approaching critical point, maximum, or temperature asymptote. If one plots as a function of either pressure or temperature along the melting curve either volume discontinuity or slope, curves will be obtained convex toward the pressure or temperature axis, and with no indication that the axis will ever be reached. The three possibilities just mentioned demand the opposite curvature, and when the plot is made against temperature, plunging of the curve vertically into the temperature axis at a finite temperature. Furthermore, if there is a critical point, the three parameters, latent heat, energy difference, and entropy difference, should all vanish at a finite temperature or pressure, the same for all. A plot of these quantities indicates no such tendency, but they either remain approximately constant or rise.

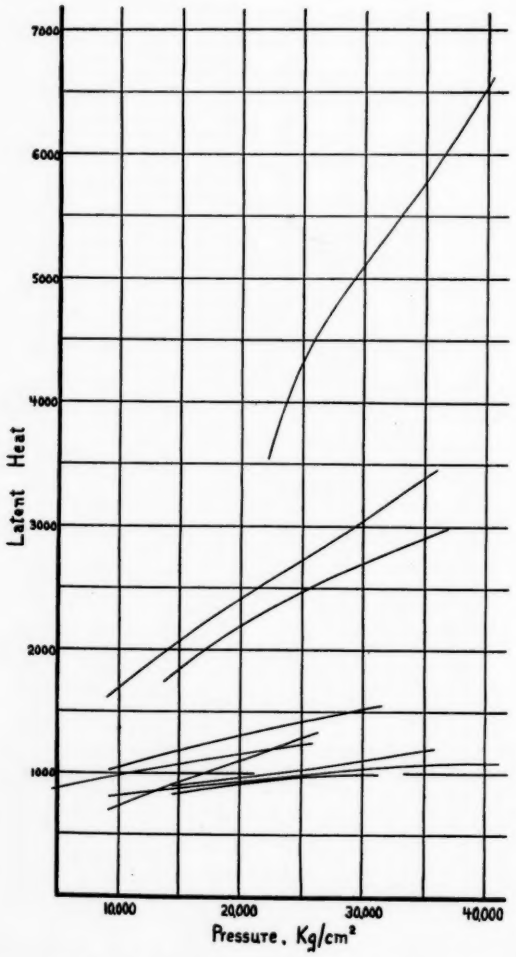

FIG. 3. Latent heat of melting, in units of kg cm per g of substance, against pressure along the melting curve. At 25,000 kg/cm² the order of substances, reading from top to bottom, is: water (ice VII), *n*-butyl alcohol, ethyl alcohol, methylene chloride, chlorobenzene (second modification), chloroform, carbon bisulfide, *n*-propyl bromide, ethyl bromide.

In one respect these new results show an alteration of behavior in the new pressure range. In the lower pressure range the latent heat either remained approximately constant, or if it increased, in all cases the increase was slower than the increase of absolute temperature, so that in all cases the entropy difference between solid and liquid decreased along the curve. But among the nine substances studied here the entropy increases for five, and for three, water, ethyl and *n*-butyl alcohol, the increase is very considerable. One consequence of this is that the tendency of the specific heat of the liquid to be greater than that of the solid is strengthened as pressure and temperature increase along the melting curve.

Another effect which becomes more prominent in the higher pressure range is the subcooling of the liquid. As pressure increases along the melting curve, and in spite of the increasing temperature, pressure has to be pushed in general further beyond the pressure of thermodynamic equilibrium in order to compel freezing to begin. This constituted a serious experimental difficulty and prevented the exploration of the melting curves of several substances over as wide a range as would otherwise have been possible. Along with the difficulty of compelling the nucleus of the solid to form, there is also a very greatly increased sluggishness of the growth of the solid phase into the liquid. With ethyl cyclohexane, for example, solid and liquid were maintained in contact in the region of stability

[2] P. W. Bridgman, Rev. Mod. Phys. **7**, 13 (1935).

TABLE II. *Volume decrements at 50°C from 5000 kg/cm² as zero.*

Pressure kg/cm²	Methyl Alcohol	Ethyl Alcohol	n-Propyl Alcohol	i-Propyl Alcohol	n-Butyl Alcohol	n-Amyl Alcohol	Ethyl Bromide	n-Propyl Bromide	n-Butyl Bromide	Ethyl Acetate	n-Amyl Oxide	Chloroform	Carbon Bisulfide	Benzene	Methylene Chloride	Ethylene Bromide	Cyclohexane	Methyl Cyclohexane	p-Xylene	Water
5,000	(.828)	(.827)	(.848)	(.841)	(.853)	(.851)	(.818)	(.833)	(.835)	.000	.000	.000	(.836)	.000	.000	.000	.000	.000	.000	(.883)
10,000	.064	.066	.056	.062	.060	.058	.063	.066	.064	.062	.057	.111[g]	.064	.041	.065	.042	.091[k]	.059	.032	.062
15,000	.102	.104	.092	.100	.095	.096	.101	.103	.101	.100	.124[f]	.139	.104	.074[c]	.103	.071	.119	.094	.054	
20,000	.130	.132	.117	.126	.151[b]	.123	.128	.131	.129	.154[e]	.146	.159	.160[h]	.094	.170[j]	.093	.140	.145[i]	.071	[m]
25,000	.151	.189[a]	.138	.146	.169	.144	.171[e]	.177[d]	.151	.172	.164	.177	.179	.111	.190	.111	.157	.160	.085	.240
30,000	.167	.203	.155	.164	.182	.162	.188	.190	.169	.187	.178	.191	.196	.125	.204	.125	.171	.174	.097	.253
35,000	.180	.216	.170	.179	.194	.177	.202	.200	.185	.199	.191	.203	.209	.137	.216	.138	.183	.186	.108	.263
40,000	.190	.226	.183	.191	.204	.190	.213	.209	.198	.208	.202	.213	.221	.147	.225	.148	.193	.196	.116	.272
45,000	.199	.236	.195	.202	.214	.200	.222	.216	.210	.216	.212	.221	.231	.156	.233	.158	.202	.205	.125	.280
50,000	.208	.244	.205	.212	.222	.210	.230	.222	.221	.224	.222	.229	.239	.164	.239	.167	.210	.213	.132	.289

[a] Freezes at 24,400; $\Delta v = .034$.
[b] Freezes at 15,400; $\Delta v = .035$.
[c] Freezes at 23,500; $\Delta v = .020$.
[d] Freezes at 20,300; $\Delta v = .029$.
[e] Freezes at 17,800; $\Delta v = .030$.
[f] Freezes at 11,300; $\Delta v = .038$.
[g] Freezes at 8,100; $\Delta v = .056$.
[h] Freezes at 15,500; $\Delta v = .031$.
[i] Transition at 12,500; $\Delta v = .009$.
[j] Freezes at 16,000; $\Delta v = .041$.
[k] Freezes at 8,100; $\Delta v = .031$.
[l] Freezes at 16,300; $\Delta v = .028$.
[m] Liquid freezes to ice VI, and ice VI transforms to ice VII in this range.

of the solid for more than one hour while pressure was varied from 12,500 to 50,000 and back, during which only one-tenth of a volume of 0.2 cm³ solidified. For other substances, it was possible because of this effect to make extensive measurements of the compression of both the solid and the subcooled liquid in the region of stability of the solid up to the maximum pressure. This effect may well result in a suppression of the solid phase altogether. Of the 21 substances investigated here, four were not brought to freeze at all. In spite, then, of our conclusions about the universal character of the melting curve, the conclusion must not be drawn that any liquid whatever can be made to crystallize at any temperature by the exercise of sufficient pressure. However, such a substance without doubt becomes glassy and therefore solid as far as ordinary mechanical properties are concerned.

Contrasted with the increased subcooling of the liquid, in every case melting began immediately on carrying the solid back across the melting line into the domain of thermodynamic stability of the liquid. It remains then a rule, for which the only known apparent exception is certain complex silicates, that the crystalline solid cannot be superheated.

One of the striking features of the figures for compression is the small range of numerical values of the compressions at 50,000. The volume of all the substances measured here at 50,000 is about six-tenths of its initial value, whether or not it freezes; this includes water. For a wider range of substances, however, a much wider range of compression may be exhibited; thus caesium at 50,000 is compressed to 0.48 of its initial volume, and iron to 0.98.

With regard to the relative behavior of liquid and solid phases, the relations are what would be expected. In no case is the compressibility of the solid phase greater than that of the liquid at the same pressure. In most cases it is definitely less, but by not more than 25 percent. In one or two cases there is no measurable difference, but even for them there is a distinct discontinuity in the second pressure derivative of volume at the freezing point. In those cases where the liquid can be carried far into the region of stability of the solid, the compressibility of the liquid remains greater than that of the solid over the entire range, so that the volumes of liquid and solid approach each other with increasing pressure along the isothermals in the metastable region.

Along the melting curve not only does the difference of volume between liquid and solid become smaller with increasing pressure, but also the absolute volumes of liquid and solid separately appear to become smaller, the effect of increasing pressure being dominant over that of increasing temperature. On the other hand, the internal energy of both pure phases appears in general to increase along the melting curve.

I am indebted to my assistant Mr. L. H. Abbot for making the readings and for financial assistance to the Milton Fund of Harvard University and the Rumford Fund of the American Academy of Arts and Sciences.

The Effect of Electrostatic Forces on Electrokinetic Potentials

W. G. EVERSOLE AND W. W. BOARDMAN
Division of Physical Chemistry, State University of Iowa, Iowa City, Iowa

(Received August 11, 1941)

Assuming that the ions in solution near a charged wall are subjected only to electrostatic and kinetic forces, it is shown that the potential gradient normal to the wall is determined principally by the valence and concentration of the ion of opposite charge to the wall. Assuming that the valence and concentration of this ion determine the effect of the salt on the electrokinetic potential of the wall, the surface potential of the wall and the thickness of the immobilized liquid layer are calculated from electrokinetic potential data. Salts of "normal" ions (NaCl, $BaCl_2$, etc.) cause relatively small changes in the surface potential and thickness of the immobilized layer at a glass surface and these changes occur only at very low salt concentrations. Salts containing "abnormal" ions (H^+, OH^-, La^{+++}, etc.) produce larger changes and the change continues over a much wider concentration range. The extreme effectiveness of salts like $AlCl_3$ and $ThCl_4$ in lowering negative electrokinetic potentials cannot be accounted for by the higher valence of the ions.

IF a charged wall is in contact with a dilute solution of a single salt in which the ions are subject only to thermal agitation and electrostatic forces, the density of the space charge in the solution near the wall, Π, is given by Eq. (1).

$$\Pi = n\nu Z\epsilon \exp(-Z\epsilon\psi/KT) - n\nu' Z'\epsilon \exp(Z'\epsilon\psi/KT). \quad (1)$$

n = No. of salt molecules/cc of solution.
Z and ν = the valence, and number of ions per salt molecule, of the ions having the same sign of charge as the wall (peptizing ions).
Z' and ν' = the valence, and number of ions per salt molecule, of ions having the opposite sign of charge to the wall (precipitating ions).
$\epsilon = 4.80\times10^{-10}$ e.s.u.
$K = 1.38\times10^{-16}$ erg/°K
T = Absolute temperature, °K
ψ = Magnitude of the potential in the solution, e.s.u.

Since $\nu Z = \nu' Z'$, Eq. (1) may be written,

$$\Pi = -n\nu' Z'\epsilon[\exp(Z'\epsilon\psi/KT) - \exp(-Z\epsilon\psi/KT)]. \quad (2)$$

Combining Eq. (2) with Poisson's equation for a flat surface,

$$\frac{d^2\psi}{dX^2} = \frac{4\pi}{D} n\nu' Z'\epsilon[\exp(Z'\epsilon\psi/kT) - \exp(-Z\epsilon\psi/KT)], \quad (3)$$

where X is the distance from the wall measured normal to the surface.

Multiplying Eq. (3) by $2d\psi/dX$ and integrating,

$$\left(\frac{d\psi}{dX}\right)^2 = \left[\frac{8\pi\nu' nKT}{D}\right]\frac{1}{Z}[Z\exp(Z'\epsilon\psi/KT) + Z'\exp(-Z\epsilon\psi/KT) - (Z+Z')], \quad (4)$$

the integration constant, $-(Z+Z')$, being evaluated by setting $\psi=0$ and $d\psi/dX=0$ at $X=\infty$.

Equation (4) permits the numerical calculation of $d\psi/dX$ for any selected values of n and ψ. In Table I are tabulated the ratios of $d\psi/dX$ for salts of different valence types to $d\psi/dX$ for a uni-univalent salt at the same concentration of precipitating ion, $(\nu' n)$, and for $\psi = 50$ millivolts which is of the usual order of magnitude of electrokinetic potentials. The values of these ratios reveal very clearly the much greater dependence of the potential gradient on Z' than on Z. This is entirely consistent with the empirical valence rule that the effect of a "normal" salt on electrokinetic potential (and stability of

TABLE I. *The effect of the valence type of the salt on the potential gradient in the solution at $\psi = 50$ millivolts.*

Z'	Z	$\left(\frac{d\psi}{dX}\right)_{Z'-Z} \div \left(\frac{d\psi}{dX}\right)_{1-1}$
1	1	1.00
1	2	1.03
1	3	1.05
2	1	3.06
2	2	3.08
2	3	3.10
3	1	8.5
3	3	8.5

slightly hydrated sols) is determined principally by the valence and concentration of the precipitating ion.

A "normal" salt may perhaps be defined as a salt whose ions are largely influenced only by thermal agitation and electrostatic forces. "Abnormal" ions, usually listed for water solutions as hydrogen, hydroxide, heavy metal and organic ions, may be subject to large specific adsorptive forces in addition.

The fact that the ratios in Table I are roughly equal to Z'^2 is not significant as other ratios are obtained for other values of ψ.

Integration of the general form of Eq. (4) to give ψ as a useful function of X does not seem possible. However, in a recent paper[1] this equation has been integrated for the special case of a binary salt, $(Z'=Z)$, and the electrokinetic potential (ζ) has been expressed by the function

$$\ln\frac{\cosh(Z\epsilon\zeta/2KT)-1}{\cosh(Z\epsilon\zeta/2KT)+1}$$

$$=\ln\frac{\cosh(Z\epsilon\psi^0/2KT)-1}{\cosh(Z\epsilon\psi^0/2KT)+1}-2\kappa t. \quad (5)$$

ψ^0 = the surface potential of the solid wall.

t = the thickness of the immobilized liquid layer at the wall.

ζ, the electrokinetic potential, was taken as the value of ψ at a distance, t, from the ψ^0 plane. $\kappa=(8\pi n\epsilon^2Z^2/DKT)^{\frac{1}{2}}$, where D is the dielectric constant of the solvent.

TABLE II. *ψ^0 and t for a glass wall in contact with solutions of "normal" salts.*

SALT	K IN FIG. 1	Z'	ν'	ψ^0 MILLIVOLTS	$t\times10^8$ CM
LiCl	—	1	1	80	24
NaCl	—	1	1	76	25
KCl	0.45	1	1	77	30
RbCl	—	1	1	74	32
CsCl	—	1	1	66	36
K_2SO_4	0.40	1	2	77	30
$K_3Fe(CN)_6$	0.38	1	3	74	36
$K_4Fe(CN)_6$	0.50	1	4	77	30
$MgCl_2$	0.45	2	1	68	32
$BaCl_2$	0.50	2	1	63	31
$ThCl_4$	0.50	4	1	(?)	>1000
$ThCl_4+$	0.65	1	4	+98	32

[1] W. G. Eversole and P. H. Lahr, J. Chem. Phys. **9**, 530 (1941).

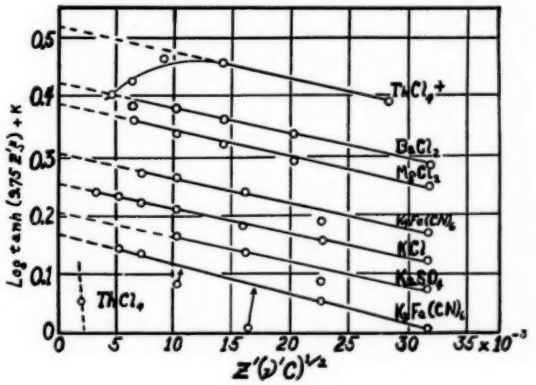

FIG. 1.

Equation (5) may be written more compactly,

$$\ln\tanh(Z\epsilon\zeta/4KT)=\ln\tanh(Z\epsilon\psi^0/4KT)-\kappa t. \quad (6)$$

Introducing numerical values into Eq. (6) for water solutions at 25°C ($D=78.8$), expressing concentration in mols per liter, $C(=1000n/6.06\times10^{23})$, and changing to common logarithms,

$$\log\tanh(9.75Z\zeta)=\log\tanh(9.75Z\psi^0)-0.142tZC^{\frac{1}{2}} \quad (7)$$

for ζ and ψ^0 in volts, and t in cm$\times10^{-8}$.

This equation is valid only for binary salts. However, since it has been shown that the electrical effect of a salt is determined principally by the valence and concentration of the precipitating ion, Eq. (7) may be used as an approximation for salts of other valence types if the valence, Z', and concentration, $\nu'C$, of the precipitating ion are used in the calculations.

If ψ^0 and t are independent of concentration, a plot of log tanh $(9.75Z'\zeta)$ against $Z'(\nu'C)^{\frac{1}{2}}$ should be a straight line with a slope $-0.142t$, and with an intercept on the axis of ordinates from which ψ^0 can be calculated.

In Fig. 1 some of the excellent electrokinetic potential data of Kruyt and van der Willigen[2] are plotted in this way for several salts which are usually considered "normal." The data were obtained by streaming potential measurements with a glass wall which was negative with the exception of the curve marked $ThCl_4^+$, where the wall was positive. In plotting Fig. 1, different

[2] H. R. Kruyt and P. C. van der Willigen, Kolloid Zeits. **45**, 307 (1929).

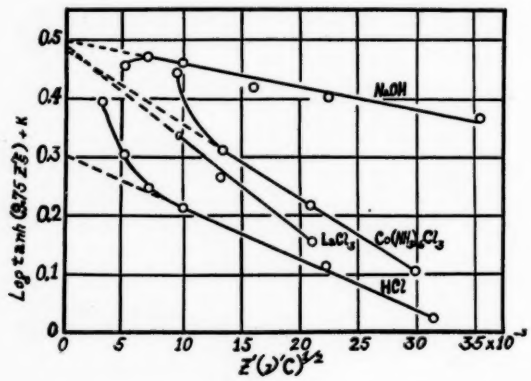

FIG. 2.

values (Table II) were added to log tanh $(9.75Z'\zeta)$ for the different salts in order to separate the curves. Otherwise the curves for all salts with the same value of Z' so nearly coincide that it is impossible to distinguish the experimental points. Table II contains values of ψ^0 and t obtained from Fig. 1 for the different salts together with the values for the other 4 alkali chlorides which were omitted from the figure to avoid crowding. If the $ThCl_4$ is disregarded for the moment, it can be seen from Table II that, for the ten remaining salts of 5 different valence types, the maximum deviation from the median value is only 12 percent for ψ^0 and 20 percent for t. This is probably approaching the precision of the measurement of much ζ potential data. However, the measurements of Kruyt and van der Willigen appear to be much more accurate, and these relatively small variations are probably significant. It will be noted that for the alkali halides ψ^0 decreases and t increases with increasing molecular weight. Also three of the four potassium salts give the same value of ψ^0 and t. Data for the fourth, $K_3Fe(CN)_6$, were less consistent than for the other three, as can be seen from Fig. 1.

It can be concluded, at least tentatively, that even for normal salts a certain minimum concentration of salt is necessary to stabilize ψ^0, and that different salts stabilize it at somewhat different values, depending on the nature of the precipitating ion. This may account for the extreme difficulty if not the impossibility of measuring ζ potentials in pure water.

Returning to the case of $ThCl_4$, it can be noted from Fig. 1 that this salt decreases the ζ potential very rapidly. In fact no curve can be drawn because there is only one experimental point before the sign of the ζ potential is reversed. Assuming a ψ^0 value of the same order of magnitude as for the other salts, a value of $t \leqq 1400$A or a value of $Z' \leqq 110$ would be required to account for the effect of this salt on the negative glass surface. It seems evident that this salt (and $AlCl_3$ which exhibits a similar behavior) should not be considered normal salts even though their ions do possess a "rare gas" structure. It seems probable that the mechanism of their effect is entirely different. Probably these salts hydrolyze to form a positive complex, possibly colloidal oxide, which coats the negative glass surface and sets up a new ψ^0 plane at which the potential is positive. When the new positive ψ^0 has been stabilized, further addition of salt should affect ζ differently, since the chloride ion is now the precipitating ion. This situation is represented in Fig. 1 by the curve, $ThCl_4^+$. ψ^0 for this surface is somewhat higher numerically than for the glass surface, whereas t is about the same. Behavior would appear normal in this case because the positive complex would have little effect on the positive wall, since it would represent a peptizing "ion."

In Fig. 2 and Table III, similar data from the same source[2] are given for a few salts of "abnormal" ions. The curves do not become linear until the concentration becomes fairly large and the ψ^0 values, obtained by extrapolating the linear portions of the curves, show much more variation than for normal salts. This effect probably results from the fact that the abnormal ion tends to be adsorbed at the surface and to produce a change in ψ^0 which depends on the sign of the charge on the adsorbed ion. Strongly adsorbed precipitating ions may easily reverse the sign of the potential. The curves for $LaCl_3$ and $Co(NH_3)_6Cl_3$ show that a high valence alone is not sufficient to account for the reversal of the

TABLE III. *ψ^0 and t for a glass wall in contact with solutions of "abnormal" ions.*

SALT	K IN FIG. 2	Z'	ν'	ψ^0 MILLIVOLTS	$t \times 10^8$ CM
NaOH	0.60	1	1	111	27
HCl	0.60	1	1	56	61
$LaCl_3$	0.60	3	1	36	110
$Co(NH_3)_6Cl_3$	0.80	3	1	18	88

sign of the charge on the wall at the extreme dilutions at which this phenomenon occurs with $ThCl_4$ and $AlCl_3$.

Conclusion

Many electrokinetic phenomena can be accounted for on the basis of the thermal and electrical energy of the ions in a solution near a charged wall, and the classical assumption of an immobilized liquid layer attached to the solid wall.

Values of the surface potential of the solid and the thickness of the immobilized layer can be calculated from electrokinetic potentials.

NOVEMBER, 1941 JOURNAL OF CHEMICAL PHYSICS VOLUME 9

Thermodynamic Properties of Binary Solid Solutions. Phase Separation

Edwin N. Lassettre, *Laboratory of Chemistry, The Ohio State University, Columbus, Ohio*

and

John P. Howe, *Metcalf Research Laboratory, Brown University, Providence, Rhode Island*

(Received September 5, 1941)

A previously developed method of calculating the thermodynamic functions of a mixture is further examined. For a lattice which is large in at least two dimensions it is shown that the largest eigenvalue of the fundamental matrix is doubly degenerate over a finite temperature range, and within this range a separation into phases takes place. An approximation to the phase boundary which is valid at low temperatures is obtained.

In an earlier[1a] paper (hereafter designated by I), the occurrence of phase transitions is related to degeneracy of the largest eigenvalue of a certain matrix. In the present paper we shall examine in more detail the degeneracy which leads to a separation into phases.

In general, if a binary mixture separates into phases at all, there will be a temperature T_c and a mole fraction X_c such that when $X=X_c$ and $T=T_c$ the mixture separates into two phases. In the present problem, therefore, we have to investigate whether the largest eigenvalue is degenerate over a *temperature range*.

The question of separation into phases has been considered by Rushbrooke[1] using the method of Bethe.[2] Rushbrooke predicted a phase separation in this case and calculated the critical solution temperature. Later Kirkwood[3] considered the problem further using the moment method. He finds a phase separation also, and the predicted critical solution temperature is in good agreement with that of Rushbrooke. In both cases these investigators obtained an expression for the activity which corresponds to a metastable phase at low temperatures. The phase separation is introduced by showing that the free energy of a system consisting of two phases is lower than the free energy of the metastable phase. Kirkwood's approximation is most accurate at high temperatures while the region of applicability of Rushbrooke's method is less clear.

As shown in I the present treatment, which makes use of the grand ensemble, gives only the solution corresponding to the stable phase. This being the case, it is convenient to begin the perturbation approximation from a low temperature at which the system already consists of two phases. In so doing, the dependence of a phase transition on the size of lattice is clearly brought out and the difficulty with the three-filament lattice, treated in the preceding paper, is completely resolved.

I. Properties of the Unperturbed Solutions

We have previously treated the problem of calculating the thermodynamic functions for a

[1a] E. N. Lassettre and J. P. Howe, J. Chem. Phys. **9**, 747 (1941).
[1] Rushbrooke, Proc. Roy. Soc. **A166**, 296 (1938).
[2] H. A. Bethe, Proc. Roy. Soc. **A150**, 552 (1935).
[3] J. G. Kirkwood, J. Phys. Chem. **43**, 97 (1939).

mixture in which the molecules are distributed at the lattice points of a crystal lattice and for which only the interaction between nearest neighbors is considered. The crystal is supposed to be made up of N parallel lattice planes each containing m lattice points. An arrangement of molecules in the crystal is called a *configuration* while an arrangement of molecules in a given lattice plane is called a *distribution*. There are 2^m possible distributions of molecules on a given lattice plane. Let p_l be the number of molecules of type 1 in the lth such distribution, let i_l be the number of contacts between unlike molecules in the distribution, and let ν_{lk} be the number of contacts between unlike molecules of the lth and kth distributions (assumed to be on adjacent planes). The problem of computing the thermodynamic properties is then reduced to solving the set of homogeneous equations:

$$\mu\phi_l=\lambda^{p_l}z^{i_l}\sum_k z^{\nu_{lk}}\phi_k. \tag{1a}$$

In these equations λ is a number which may be varied arbitrarily from 0 to ∞, and $z=\exp(-V_{12}/kT)$, where $2V_{12}$ is the change in energy attending the transformation of a contact between two molecules of type 1 and a contact between two molecules of type 2 into two contacts between a molecule of type 1 and a molecule of type 2. ϕ_l is the probability of finding the lth distribution in the Nth lattice plane, which forms one surface of the crystal.

The change in work content on mixing $\bar{n}$ molecules of component 1 with $mN-\bar{n}$ molecules of component 2 is

$$A=\bar{n}\log\alpha_1+(mN-\bar{n})\log\alpha_2, \tag{2a}$$

where $\mu=\alpha_2^{-m}$, $\lambda=\alpha_1/\alpha_2$. It has been shown that $\phi_l^2/z^{i_l}\lambda^{p_l}$ is the probability of distribution l on a plane far in the interior of the lattice. Hence the mean composition is given by

$$\bar{n}=N\sum_l p_l\phi_l^2/z^{i_l}\lambda^{p_l}. \tag{3a}$$

The appropriate eigenvalue of (1a) is the largest one and ϕ_l denotes the corresponding eigenfunction. Equation (3a) implies that ϕ_l is normalized in such a way that

$$\sum_l \phi_l^2/z^{i_l}\lambda^{p_l}=1. \tag{4a}$$

These relations suffice to determine the work content as a function of composition and temperature if V_{12} is known. In what follows we shall confine our attention to the case of a simple cubic lattice.

Investigation of the problem outlined in Section I involves obtaining a solution to Eq. (1a). Since this equation has not been solved exactly, we are reduced to approximate methods at the outset. The method selected is a perturbation method of the standard sort which is most easily explained by rewriting Eq. (1a) in matrix form as follows:

$$\mu\boldsymbol{\phi}=\boldsymbol{\Lambda}\mathbf{A}\mathbf{Z}\boldsymbol{\phi}. \tag{1}$$

In this equation $\boldsymbol{\phi}$ is a vector

$$\boldsymbol{\phi}=\begin{pmatrix}\phi_1\\ \phi_2\\ \cdot\\ \cdot\\ \cdot\end{pmatrix} \tag{2}$$

and $\mathbf{A}$ is a diagonal matrix the general element of which is $\lambda^{p_l}\delta(l-k)$ where

$$\delta(l-k)=\begin{cases}0 \text{ if } l\neq k\\ 1 \text{ if } l=k\end{cases}.$$

$\mathbf{A}$ is a diagonal matrix whose general element is $z^{i_l}\delta(l-k)$ and $\mathbf{Z}$ is a matrix whose general element is $z^{\nu_{lk}}$. Also by $\boldsymbol{\phi}'$ we designate a row matrix:

$$\boldsymbol{\phi}'=\overbrace{\phi_1\phi_2\cdots}.$$

The scalar product of $\boldsymbol{\phi}$ by itself is then:

$$\boldsymbol{\phi}'\boldsymbol{\phi}=\sum_l \phi_l^2.$$

For the purpose of labeling the variable we shall replace z by y in the matrix $\mathbf{Z}$. On expanding $\mathbf{Z}$ in powers of y we obtain:

$$\mathbf{Z}=\mathbf{Z}_0+y\mathbf{Z}_1+y^2\mathbf{Z}_2+y^3\mathbf{Z}_3+\cdots. \tag{3}$$

In this expansion the general coefficient of y^n is a matrix whose elements are $\delta(n-\nu_{lk})$, the δ function being defined as before. $\mathbf{Z}_0$ is therefore the unit matrix in 2^m dimensions. By setting y equal to zero we obtain the unperturbed equation:

$$\mu_0\boldsymbol{\phi}_0=\boldsymbol{\Lambda}\mathbf{A}\boldsymbol{\phi}_0. \tag{4}$$

Since $\boldsymbol{\Lambda}\mathbf{A}$ is a diagonal matrix, the eigenvalues are merely the diagonal terms, i.e., $\mu_{0r}=z^{i_r}\lambda^{p_r}$. When $0<\lambda<1$ and $0<z<1$ the largest eigenvalue

is 1. When $\lambda>1$ and $0<z<1$ the largest eigenvalue is λ^m. These two eigenvalues cross when $\lambda=1$ and hence a transition is indicated. Since the transition occurs at the point $\lambda=1$ we confine our attention to the case in which $\mathbf{\Lambda}=\mathbf{I}$ where $\mathbf{I}$ is the unit matrix.

A complete set of eigenvectors is the set of unit vectors $\mathbf{e}_r$ for which all components vanish except the rth which is equal to unity. Since these vectors satisfy (4),

$$\mathbf{A}\mathbf{e}_r=z^{i_r}\mathbf{e}_r. \tag{5}$$

It is convenient to designate the vectors $\mathbf{e}_r$ by giving the number of molecules in the distribution r and their positions. Thus, let $\mathbf{f}_0$ be the unit vector for which the rth distribution contains no molecule of type 1, and let $\mathbf{f}_1(q_1)$ be the unit vector for which the rth distribution contains one molecule of type 1 at the position q_1, etc. It is also convenient to have a corresponding designation in terms of molecules of type 2. Thus, let $\mathbf{g}_0$ be the unit vector for which the rth distribution contains no molecule of type 2, and let $\mathbf{g}_1(q_1)$ be the unit vector for which there is one molecule of type 2 at the point q_1, etc. These symbols constitute merely different ways of denoting the same set of vectors. Thus, for every $\mathbf{f}$ there is a $\mathbf{g}$ which is identically equal to it and vice versa.

We need finally a formula for $\mathbf{Z}_n\mathbf{e}_r$. To obtain it, we expand the vector in a series of unit vectors

$$\mathbf{Z}_n\mathbf{e}_r=\sum_s a_s\mathbf{e}_s.$$

Because of orthogonality of the unit vectors we find

$$a_s=\mathbf{e}'_s\mathbf{Z}_n\mathbf{e}_s=\delta(n-\nu_{rs})$$

and hence

$$\mathbf{Z}_n\mathbf{e}_r=\sum_s \delta(n-\nu_{rs})\mathbf{e}_s. \tag{6}$$

According to (6) the only units $\mathbf{e}_s$ which occur are those for which $\nu_{rs}=n$. As an example, let $\mathbf{e}_r=\mathbf{f}_0$, $n=1$; then $\mathbf{e}_s=\mathbf{f}_1(q_1)$, and we obtain

$$\mathbf{Z}_1\mathbf{f}_0=\sum_{q_1}\mathbf{f}_1(q_1). \tag{7}$$

In a similar way we also find

$$\mathbf{Z}_1\mathbf{g}_0=\sum_{q_1}\mathbf{g}_1(q_1). \tag{8}$$

The sum extends over all possible lattice points in the first plane.

II. Expansion of μ in the Powers of y

To investigate the behavior of the largest eigenvalue in the neighborhood of $y=0$ we expand as follows:

$$\mu=\mu_0+y\mu_1+y^2\mu_2+\cdots, \tag{9}$$

$$\boldsymbol{\phi}=\boldsymbol{\phi}_0+y\boldsymbol{\phi}_1+y^2\boldsymbol{\phi}_2+\cdots. \tag{10}$$

Substituting these series and series (3) into (1) we obtain on equating coefficients the general formula:

$$\sum_{s=0}^{n}\mu_s\boldsymbol{\phi}_{n-s}=\mathbf{A}\sum_{s=0}^{n}Z_s\boldsymbol{\phi}_{n-s}. \tag{11}$$

The various order perturbations are obtained by setting n equal to 0, 1, 2, $\cdots$ and solving the resulting equations successively.

(a) Zero order

When $n=0$ (11) becomes

$$\mu_0\boldsymbol{\phi}_0=\mathbf{A}\boldsymbol{\phi}_0. \tag{12}$$

This equation was treated in the preceding section. The largest eigenvalue is $\mu_0=1$ and is doubly degenerate. The corresponding eigenvector is

$$\boldsymbol{\phi}_0=a\mathbf{f}_0+b\mathbf{g}_0, \tag{13}$$

where a and b are constants.

(b) First order

When $n=1$ we get from (11)

$$\mu_0\boldsymbol{\phi}_1+\mu_1\boldsymbol{\phi}_0=\mathbf{A}\boldsymbol{\phi}_1+\mathbf{A}\mathbf{Z}_1\boldsymbol{\phi}_0. \tag{14}$$

Multiply (14) by $\mathbf{f}_0'$ and $\mathbf{g}_0'$, respectively, using (13) and we obtain the simultaneous equations:

$$\begin{aligned} a\mu_1&=0\\ b\mu_1&=0. \end{aligned} \tag{15}$$

These have non-vanishing solutions only when $\mu_1=0$; the degeneracy is not removed. To obtain $\boldsymbol{\phi}_1$ we use (7), (8), and (14)

$$(\mathbf{I}-\mathbf{A})\boldsymbol{\phi}_1=a\mathbf{A}\sum_{q_1}\mathbf{f}_1(q_1)+b\mathbf{A}\sum_{q_1}\mathbf{g}_1(q_1), \tag{16}$$

but $\mathbf{A}\mathbf{f}_1=z^4\mathbf{f}_1$ and $\mathbf{A}\mathbf{g}_1=z^4\mathbf{g}_1$, hence

$$\boldsymbol{\phi}_1=\frac{z^4}{1-z^4}\sum_{q_1}[a\mathbf{f}_1(q_1)+b\mathbf{g}_1(q_1)]. \tag{17}$$

We may add to (17) any multiples of $\mathbf{f}_0$ and $\mathbf{g}_0$ and still satisfy (14). Since this step affects

only the normalization of ϕ and does not influence the value of μ it is omitted in this and all subsequent steps.

(c) **Second order**

In this case (11) becomes

$$\mu_0\phi_2+\mu_1\phi_1+\mu_2\phi_0=\mathbf{A}(\phi_2+\mathbf{Z}_1\phi_1+\mathbf{Z}_2\phi_0). \quad (18)$$

To determine μ_2 multiply by $\mathbf{f}_0'$ and $\mathbf{g}_0'$ as before. Using the results of the zero and first order perturbations we obtain

$$a\mu_2=\frac{mz^4}{1-z^4}a, \quad b\mu_2=\frac{mz^4}{1-z^4}b. \quad (19)$$

These equations have non-vanishing solutions when

$$\mu_2=mz^4/(1-z^4). \quad (20)$$

The degeneracy is still not removed. Using (b) and the definitions of $\mathbf{f}$ and $\mathbf{g}$

$$\mathbf{Z}_2\phi_0=a\sum_{q_1,q_2}{}''\mathbf{f}_2(q_1,q_2)+b\sum_{q_1q_2}{}''\mathbf{g}_2(q_1,q_2), \quad (21)$$

$$\mathbf{Z}_1\phi_1=\frac{z^4}{1-z^4}[am\mathbf{f}_0+bm\mathbf{g}_0+2a\sum_{q_1,q_2}\mathbf{f}_2(q_1,q_2)+2b\sum_{q_1,q_2}\mathbf{g}_2(q_1,q_2)]. \quad (22)$$

In these summations, the double prime indicates that we omit terms in which the positions of q_1 and q_2 are interchanged. This arises since the two molecules are identical and exchanging them does not give a new configuration. The point $q_1=q_2$ is also omitted, since two molecules cannot occupy the same lattice point. If we expand ϕ_2 as a series of unit vectors and determine the expansion coefficients from (18), (21), and (22) we obtain

$$\phi_2=\frac{1+z^4}{1-z^4}\sum_{q_1,q_2}[aC_{q_1q_2}\mathbf{f}_2(q_1,q_2)+bC_{q_1q_2}\mathbf{g}_2(q_1,q_2)], \quad (23)$$

where

$$C_{q_1q_2}=\begin{cases}z^6/(1-z^6) \text{ if } q_1 \text{ and } q_2 \text{ are neighboring positions.}\\ z^8/(1-z^8) \text{ otherwise.}\end{cases} \quad (24)$$

The degeneracy has not yet been removed, and it is clear that if m, the number of lattice points in the first plane, is sufficiently large the third-order perturbation will not remove the degeneracy.

The degeneracy is finally removed by a perturbation of the mth order (m being the number of lattice points in the first plane). The outline of a proof of this statement is provided in the following section.

III. Degeneracy of the Largest Eigenvalue

(*A*) *ϕ_n has the form $a\alpha_n+b\beta_n$ where α_n and β_n are linear combinations of the unit vectors $\mathbf{f}_s$ and the unit vectors $\mathbf{g}_s$, respectively, and $s\leqslant n$.*

Note that the statement is true when $n=0$, 1, 2. Assume that it is also true when n is equal to 0, 1, 2, $\cdots n-1$, respectively. Then from (11)

$$(\mathbf{I}-\mathbf{A})\phi_n=a\sum_{s=1}^{n}(\mathbf{A}\mathbf{Z}_s-\mathbf{I}\mu_s)\alpha_{n-s}+b\sum_{s=1}^{n}(\mathbf{A}\mathbf{Z}_s-\mathbf{I}\mu_s)\beta_{n-s}. \quad (25)$$

Now consider the effect of operating with $\mathbf{Z}_s$ on α_{n-s}. By hypothesis α_{n-s} contains terms $\mathbf{f}_t$, $t\leqslant n-s$, but from (6) $\mathbf{Z}_s\mathbf{f}_t$ can be expanded in a series of unit vectors and the unit vectors in the expansion must be such that the number of contacts between distributions is s. It follows immediately that $\mathbf{Z}_s\mathbf{f}_t$ can be expanded in a series of unit vectors $\mathbf{f}_u$ such that $u\leqslant s+t$ and hence $u\leqslant n$. In the same way it follows that $\mathbf{Z}_s\mathbf{g}_t$ can be expanded in a series of unit vectors $\mathbf{g}_u$ such that $u\leqslant s+t$ and hence $u\leqslant n$. Therefore, using the above equation we see that $(\mathbf{I}-\mathbf{A})\phi_n$ has the prescribed form and hence ϕ_n has also. Since the proposition is true when $n=0$, 1, 2, it is true for all n by induction.

(*B*) *In (A) β_n can be obtained from α_n by replacing every $\mathbf{f}$ by the corresponding $\mathbf{g}$.*

Note that the proposition is true when $n=0$, 1, and 2. Corresponding to anyone of the unit vectors $\mathbf{f}_s$ there is a unit vector $\mathbf{g}_s$ for which the non-vanishing component represents a distribution with molecules of type 1 replaced by those of type 2 and vice versa. ν_{rs} of (6) is unchanged under this transformation (provided the transformation is applied to both distributions r and s) and hence the expansion of $\mathbf{Z}_s\mathbf{g}_t$ can be obtained from $\mathbf{Z}_s\mathbf{f}_t$ by replacing every $\mathbf{f}$ by the corresponding $\mathbf{g}$. Furthermore, the unperturbed eigenvalue associated with $\mathbf{f}_s$ is the same as that

associated with the corresponding vector $\mathbf{g}_s$. With these facts the proposition is easy to prove by induction.

(*C*) *If the number of lattice points in the first plane is m, the degeneracy is not removed by any perturbation up to and including the m−1th.*

In order to obtain the second-order secular determinant which must be solved for μ_n we multiply (11) by $\mathbf{f}_0'$ and $\mathbf{g}_0'$, respectively. If we use (*A*) some simplifications are possible. Consider first the term $\mathbf{f}_0'\boldsymbol{\phi}_{n-s}$. Because of the fact that we have omitted the *arbitrary* multiples of $\mathbf{f}_0$ and $\mathbf{g}_0$ at each order perturbation $\mathbf{f}_0$ must be orthogonal to $\boldsymbol{\phi}_{n-s}$ if $n-s \geqslant 1$. Also $\mathbf{f}_0'\boldsymbol{\phi}_0=a$. But $\mu_0\mathbf{f}_0'\boldsymbol{\phi}_n=\mathbf{f}_0'\mathbf{A}\boldsymbol{\phi}_n$ as we readily see on expanding $\boldsymbol{\phi}_n$ as a series of unit vectors. Hence, using (*A*),

$$a\mu_n=a\sum_{s=1}^{n}\mathbf{f}_0'\mathbf{A}\mathbf{Z}_s\boldsymbol{\alpha}_{n-s}+b\sum_{s=1}^{n}\mathbf{f}_0'\mathbf{A}\mathbf{Z}_s\boldsymbol{\beta}_{n-s},$$

$$b\mu_n=a\sum_{s=1}^{n}\mathbf{g}_0'\mathbf{A}\mathbf{Z}_s\boldsymbol{\alpha}_{n-s}+b\sum_{s=1}^{n}\mathbf{g}_0'\mathbf{A}\mathbf{Z}_s\boldsymbol{\beta}_{n-s}. \tag{26}$$

But by (*A*) $\boldsymbol{\beta}_{n-s}$ cannot contain a unit $\mathbf{g}_u$ for which u exceeds $n-s$ and hence $\mathbf{Z}_s\boldsymbol{\beta}_{n-s}$ cannot contain a unit $\mathbf{g}_t$ for which t exceeds n. Operation with $\mathbf{A}$ does not change this since $\mathbf{g}_t$ is an eigenvector of $\mathbf{A}$. Hence $\mathbf{A}\mathbf{Z}_s\boldsymbol{\beta}_{n-s}$ cannot contain the vector $\mathbf{f}_0$ (which is equal to $\mathbf{g}_m$) unless $n \geqslant m$. If $n<m$,

$$\sum_{s=1}^{n}\mathbf{f}_0'\mathbf{A}\mathbf{Z}_s\boldsymbol{\beta}_{n-s}=0.$$

In a similar way

$$\sum_{s=1}^{n}\mathbf{f}_0'\mathbf{A}\mathbf{Z}_s\boldsymbol{\alpha}_{n-s}=0 \quad \text{if} \quad n<m.$$

By (*B*), however, we see that

$$\sum_{s=1}^{n}\mathbf{f}_0'\mathbf{A}\mathbf{Z}_s\boldsymbol{\alpha}_{n-s}=\sum_{s=1}^{n}\mathbf{g}_0'\mathbf{A}\mathbf{Z}_s\boldsymbol{\beta}_{n-s}.$$

It follows at once that the two roots μ_n of the secular determinant of (26) are equal if $n<m$. When $n=m$, $\mathbf{Z}_s\boldsymbol{\beta}_{n-s}$ may contain $\mathbf{g}_m=\mathbf{f}_0$ and hence the non-diagonal terms will not vanish. Under these circumstances the roots of the secular determinant are unequal and degeneracy is removed.

According to this last proposition the first m terms of the power series expansion of one eigenvalue are equal to the first m terms in the expansion of the other. If z is sufficiently small for the remaining terms to be negligible the two roots are effectively degenerate. The situation is expressed more precisely as follows. Compute α_2 (i.e., $\alpha_2=\mu^{-1/m}$) from each of the two eigenvalues by expansion in powers of y. In the limit as $m\to\infty$ the two series will be identical and the largest eigenvalue is degenerate over a *temperature interval* corresponding to the radius of convergence of the power series.

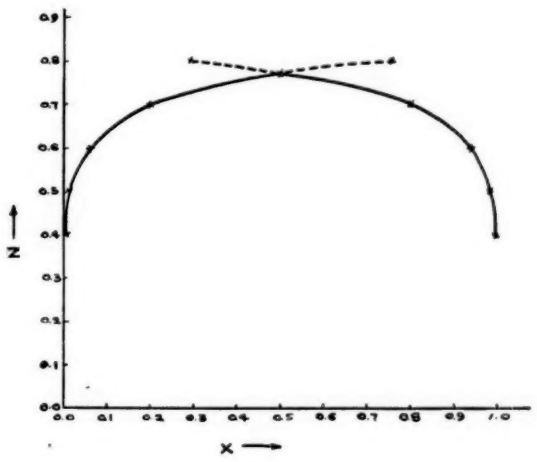

FIG. 1.

It is now clear that when m is sufficiently large and y is sufficiently small the largest eigenvalue is degenerate provided the perturbation theory gives a convergent series. Concerning the question of convergence a definite answer cannot as yet be given because of the difficulty of obtaining the general term of the series. However, one of the most obvious possibilities is that the series could diverge because $y=0$ is a branch point. This is quite conceivable since $y=0$ is a point at which two roots of an algebraic equation become equal. This possibility can be eliminated at once, however, because when $\lambda=1$ the general secular determinant can be factored by means of rational operations into two factors each of order 2^{m-1}; each of these factors contains one root which approaches to unity as y approaches zero. It follows immediately that $y=0$ is not a branch point for either root. This result is true for all *finite* values of m and is connected with the fact that the energy of interaction for a configuration is invariant under the operation which replaces a molecule of type 1 by a molecule

of type 2 and vice versa. In what follows, convergence is explicitly assumed.

To investigate the composition we use the formula

$$X=\boldsymbol{\phi}'\mathbf{A}^{-1}\mathbf{P}\boldsymbol{\phi}/\boldsymbol{\phi}'A^{-1}\boldsymbol{\phi},$$

where $\mathbf{P}$ is a diagonal matrix whose general element is $p_l\delta(l-k)$, and X is the mole fraction of component 1. This equation is the matrix form of Eq. (3a). With the first- and second-order corrections to μ and $\boldsymbol{\phi}$ it is possible to compute the first and second derivatives of X with respect to y at $y=0$ and hence get the first three terms in the Taylor series expansion of X. The result is

$$X=\frac{b^2}{a^2+b^2}+\frac{a^2-b^2}{a^2+b^2}y^2+OCy^4. \qquad (27)$$

The mole fraction thus depends on the constants a and b which are arbitrary, and takes on its minimum value when $b=0$, and its maximum value when $a=0$. These two points must be opposite points on the phase boundary curve since the activity is constant for all intermediate compositions. In order to make calculations for a cubic lattice we set $y=z$. When z is sufficiently large the maximum and minimum values of X become equal (at $X=\frac{1}{2}$). The corresponding value of T must be the critical solution temperature. The phase boundary curve to this order of approximation is shown in Fig. 1. The dotted portions of Fig. 1 come by extending Eq. (27) beyond $X=\frac{1}{2}$. It is to be expected that these portions have no real significance. They arise because of errors due to the approximations involved and would no doubt be absent if an exact calculation could be made.

From the derivation it is clear that the approximation is valid only when z is small and hence the predicted critical solution point cannot be accurate. Moreover, from Fig. 1 we see that the tangent to the approximate phase boundary curve is not continuous at $X=\frac{1}{2}$. This is no doubt due to error in the approximation for large values of z. The value of z for which $X=\frac{1}{2}$ is $z_c=0.77$. From Kirkwood's treatment we obtain $z_c=0.72$ on neglecting terms of order $1/T^2$ and higher (regular solution approximation). If the terms of order $1/T^2$ are retained the critical point is lowered to $z_c=0.66$. Rushbrooke finds $z_c=0.67$, in good agreement with Kirkwood. Inclusion of higher order terms would no doubt lead to improved agreement.

A rather crude but illuminating physical interpretation of the various orders of approximation is possible. The zero-order approximation corresponds to a system which consists of phases of the pure components, the first-order perturbation introduces a correction in which the phase contains *isolated* molecules of the second component, while the second-order perturbation permits the interaction of like particles two at a time. The approximation to the phase boundary curve which we have obtained involves the introduction of *isolated* molecules into the pure phase and hence suggests that an approximation of the Henry law type is valid at very low temperatures where the phase is dilute with respect to one component. This latter point is of interest because it indicates that the effect of dilution overcomes the tendency of like molecules to cluster together as the temperature decreases and affords some justification for the use of Henry's law for partially miscible components at low temperatures.

On the basis of the treatment of this paper we conclude that the model provides for a separation into phases when the lattice considered is large in at least two dimensions. The three-row filament, treated in the I, exhibits no phase separation because it is large in only one dimension.

The Partition Functions of Molecules with Internal Torsion

I. Single Asymmetric Top Attached to Rigid Framework

DONNA PRICE*
Mallinckrodt Chemical Laboratory, Harvard University, Cambridge, Massachusetts
(Received August 8, 1941)

Crawford's method of treating "pseudo-rigid" molecules is extended to the case involving an asymmetric top. The exact classical kinetic energy for a molecule consisting of a rigid framework to which asymmetric tops are attached is given. From this the quantum-mechanical operator is derived for the case of one top of small moment of inertia and of small asymmetry. The energy matrix for the molecule is obtained from the operator; and by use of a perturbation method, the partition function for translation, over-all rotation and internal rotation, correct to the second order, is obtained from the matrix. This includes effects due to translational and angular momentum couplings.

CRAWFORD[1] has given an essentially rigorous treatment of molecules consisting of a rigid framework to which symmetric tops are attached. However, the applications of his results are restricted not only by the requirement of geometrically symmetric tops, but also by the additional limitation of constant over-all moments of inertia for the molecule.

It is the purpose of this work to extend the treatment to molecules containing asymmetric tops. This paper deals with the case of a single asymmetric top such that the moment of inertia is small, and the asymmetry is small, i.e., the center of gravity of the top is near its axis of rotation, attached to a rigid framework. Molecules which satisfy these conditions are those in which the top is a group such as $-NH_2$, $-ND_2$, $-OH$, $-OD$, or $-CHD_2$.

KINETIC ENERGY

The classical kinetic energy for a molecule consisting of a rigid framework to which asymmetric tops are attached is most conveniently expressed in vector form. In order to do this, let the vector $\mathbf{R}$ describe the position, in a space-fixed system, of a point O within the molecule, and let O be the origin of a moving coordinate system associated with the molecule. This moving system will be referred to as the "primary system." In addition, there is a moving "secondary system" associated with each top. Then the position of the mth particle in the ith top is:

$$\mathbf{R}_{im}=\mathbf{R}+\mathbf{r}_i+\boldsymbol{\varrho}_{im},$$

where $\mathbf{r}_i$ is the vector from O to the origin of the secondary system i, and $\boldsymbol{\varrho}_{im}$ is the vector in the secondary ststem from the origin to particle m. The velocity of the same particle is

$$\dot{\mathbf{R}}_{im}=\dot{\mathbf{R}}+\boldsymbol{\omega}\times\mathbf{r}_i+\mathbf{v}_i+\boldsymbol{\omega}\times\boldsymbol{\varrho}_{im}+\boldsymbol{\omega}_i\times\boldsymbol{\varrho}_{im}+\boldsymbol{\mu}_{im},$$

where $\boldsymbol{\omega}$ is the angular velocity of the primary system; $\mathbf{v}_i$, the apparent velocity, in the primary system, of the origin of the secondary system i; $\boldsymbol{\omega}_i$, the apparent angular velocity, in the primary system, of the secondary system i;[2] and $\boldsymbol{\mu}_i$, the apparent velocity, in the secondary system i, of the particle. Hence the kinetic energy of the molecule is given by:

$$2T=\sum_{i,m} m_{im}\dot{R}_{im}^2.$$

It is found most convenient to take $\mathbf{R}$ to the center of gravity of the synthetic molecule made

* Sarah Berliner Research Fellow of the American Association of University Women (1940–41); Research Fellow of Radcliffe College (1940–41).

[1] Bryce L. Crawford, Jr., J. Chem. Phys. **8**, 273 (1940). To facilitate cross reference to Crawford's paper, see table in Appendix I.

[2] $\omega_0=0$, otherwise $i=0$ refers to the framework. It is a matter of choice as to whether the lower atom of the top, e.g., O of $-OH$ or N of $-NH_2$, be included in the framework or in the top. In several cases considered, there seemed no practical difference, i.e., the decrease in m_1 effected by placing this atom in the framework was offset by a corresponding increase in r_1 and in the distance of the center of gravity of the top from its axis. Therefore in the examples given below, the tops include all the atoms of the chemical unit. However, the formulas are completely general, and either grouping can be used.

up of the framework atoms and of masses $m_i=\sum_m m_{im}$ placed at the corresponding origins of the secondary systems i. The origin for top i is taken on the axis of rotation, i.e., the Z axis of the secondary system i, so that the Z component of the vector from the origin to the center of gravity of the top is zero. For these conditions, $\mathbf{v}_i=0$ and

$$\sum_{i,m} m_{im}\mathbf{r}_i+\sum_m m_{0m}\boldsymbol{\varrho}_{0m}=0. \tag{1}$$

Furthermore, in the case of rigid rotation, $\boldsymbol{\mu}_{im}=0$. With these simplifications, the kinetic energy becomes

$$\begin{aligned}2T=\dot{R}^2M&+\sum_{im} m_{im}\{\boldsymbol{\omega}\times(\mathbf{r}_i+\boldsymbol{\varrho}_{im})\}^2\\&+\sum m_{im}(\boldsymbol{\omega}_i\times\boldsymbol{\varrho}_{im})^2+2\dot{\mathbf{R}}\cdot\boldsymbol{\omega}\times\sum_{i=1}\boldsymbol{p}_i\\&+2\dot{\mathbf{R}}\cdot\sum\boldsymbol{\omega}_i\times\boldsymbol{p}_i+2\boldsymbol{\omega}\cdot\sum\mathbf{r}_i\times(\boldsymbol{\omega}_i\times\boldsymbol{p}_i)\\&+2\boldsymbol{\omega}\cdot\sum m_{im}\boldsymbol{\varrho}_{im}\times(\boldsymbol{\omega}_i\times\boldsymbol{\varrho}_{im}),\end{aligned} \tag{2}$$

where $M=\sum_{im} m_{im}$ and $\boldsymbol{p}_i=\sum_m m_{im}\boldsymbol{\varrho}_{im}$. The last four terms of this expression correspond to interactions and exclude the terms for $i=0$ because of (1) and the definition of $\boldsymbol{\omega}_0$. Hence if $\boldsymbol{p}_i$ and the moments of inertia of the tops are small, a perturbation treatment of these terms will be most likely to succeed. These conditions lead to a choice of tops such as $-$OH, $-$OD, $-NH_2$, $-ND_2$, $-CHD_2$. Relation (2) may be reduced by either standard vector methods or by matrix technique to a quadratic form in the velocities.

For the case of a single top, the quadratic form in the seven velocities $\dot{R}_\alpha$, ω_α, and ω_1 has the symmetric matrix

$$Q=\left[\begin{array}{ccccccc}M&0&0&0&p_z&-p_y&\lambda_1\\&M&0&-p_z&0&p_x&\lambda_2\\&&M&p_y&-p_x&0&\lambda_3\\&&&A_{11}&A_{12}&A_{13}&\gamma_1\\&&&&A_{22}&A_{23}&\gamma_2\\&&&&&A_{33}&\gamma_3\\\hline&&&&&&C\end{array}\right] \tag{3}$$

where $\boldsymbol{p}=\boldsymbol{p}_1$, (A_{kl}) is the inertia matrix for the whole molecule, and $\dot{R}_\alpha$, ω_α, p_α are components of $\dot{\mathbf{R}}$, $\boldsymbol{\omega}$, $\boldsymbol{p}$ taken in the primary system.[3] If the matrix (a_{kl}) is the orthogonal matrix made up of the direction cosines for the primary and secondary systems,

$$\lambda_k=a_{3,k+1}p_{k+2}-a_{3,k+2}p_{k+1}=a_{2k}p^{(x)}-a_{1k}p^{(y)}, \tag{4}$$

(indices cyclic)

$$\gamma_k=[\mathbf{r}\times\boldsymbol{\lambda}]_k+\eta_k, \tag{5}$$

$$\eta_k=a_{3k}C-a_{2k}\mathrm{E}-a_{1k}\mathrm{F}, \tag{6}$$

where C is the moment of inertia of the top about its axis, and E and F are respectively the yz and xz products of inertia of the top. It is important to note that, because of the manner in which the components of the vectors were chosen, all the elements of the matrix in (3) are either constants or functions of the top angle θ_1 only. Moreover, this matrix suggests the type of association between the primary system and the framework which will be most useful. In order to obtain A_{kk} large relative to A_{kl}, $k\neq l$, the principal axes of the synthetic molecule are chosen as the axes in the primary system.

The Hamiltonian form of the kinetic energy is a quadratic form in the momenta

$$P_\alpha=\left(\frac{\partial T}{\partial R_\alpha}\right),\quad \mathrm{P}_\alpha=\left(\frac{\partial T}{\partial\omega_\alpha}\right),\quad \mathrm{p}_1=\left(\frac{\partial T}{\partial\omega_1}\right),$$

for which the matrix is Q^{-1}. The inversion of Q is most easily effected by the method of submatrices.[4] In the partitioning, the leading submatrix chosen is the 6×6 one marked off in (3). If this submatrix is T_1, then the first approximation for the inverse is

$$(T_1^{-1})_{ij}=\delta_{ij}\Delta_i, \tag{7}$$

---

[3] $$\begin{aligned}A_{kl}&=\sum_{i=0}^{1}\sum_{m=1}^{}m_{im}(\delta_{kl}r_{im}^2-r_{imk}r_{iml})\\&=\delta_{kl}\{m_1r^2+\sum_m m_{0m}\rho_{0m}^2+\sum_m m_{1m}\rho_{1m}^2+2\sum_{\alpha=1}^{3}r_{1\alpha}p_\alpha\}\\&\quad-m_1r_kr_l-r_kp_l-r_lp_k-\sum_m m_{0m}\rho_{0mk}\rho_{0ml}\\&\quad-\sum_m m_{1m}\rho_{1mk}\rho_{1ml},\end{aligned}$$

where $r=r_1$, and δ is the Kronecker symbol.

The notation $p_i^{(\alpha)}$ will be used to denote components in the ith secondary system.

[4] See R. A. Frazer, W. J. Duncan, and A. R. Collar, *Elementary Matrices* (Cambridge University Press, 1938), particularly pp. 113, 120, and 102.

where

$$\Delta_i=\begin{cases}M^{-1} & i\leqq 3\\ [\text{constant part of } A_{i'i'}]^{-1} & i>3\end{cases}\qquad i'=i-3.$$

It may be seen, by comparing this with the second approximation given by (8), that (7) is itself an excellent approximation if the principal axes of the synthetic molecule are the axes for the primary system, the ratio m_1M^{-1} is about $\frac{1}{3}$ or less, and the top satisfies the conditions that $\boldsymbol{p}_1$ and its moment are small.

$$(T_1^{-1})_{ij}=\Delta_i[2\delta_{ij}-\Delta_j(T_1)_{ij}].^5 \qquad (8)$$

Hence (7) is the value of T_1^{-1} used to obtain Q^{-1}. In a similar manner, certain elements of Q^{-1} may be neglected, so that a good approximation is the symmetrical matrix.

$$Q^{-1}=\begin{pmatrix}\square_1 & 0 & 0 & 0 & 0 & 0 & -\lambda_1\Delta_1\Omega^{-1}\\ & \square_2 & 0 & 0 & 0 & 0 & -\lambda_2\Delta_2\Omega^{-1}\\ & & \square_3 & 0 & 0 & 0 & -\lambda_3\Delta_3\Omega^{-1}\\ & & & \square_4 & 0 & 0 & -\gamma_1\Delta_4\Omega^{-1}\\ & & & & \square_5 & 0 & -\gamma_2\Delta_5\Omega^{-1}\\ & & & & & \square_6 & -\gamma_3\Delta_6\Omega^{-1}\\ & & & & & & \Omega^{-1}\end{pmatrix} \qquad (9)$$

where

$$\square_i=\text{Constant part of}\begin{cases}\Delta_i(1+\Delta_i\lambda_i^2\Omega^{-1}) & i\leqq 3\\ \Delta_i(1+\Delta_i\gamma_{i'}^2\Omega^{-1}) & i>3\end{cases} \qquad (10)$$

and is nearly equal to Δ_i (the equality is more closely approached if all diagonal elements of T_1 are of the same order), and

$$\Omega=C-\frac{\lambda^2}{M}-\sum_{\alpha=1}^{3}\Delta_{\alpha+3}\gamma_\alpha^2 \quad \text{where} \quad \lambda^2=\sum_{\alpha=1}^{3}\lambda_\alpha^2. \qquad (11)$$

Here and whenever it appears below, the index α has a range 1–3 only. Of the same order as the previous approximations is the neglect of all but the largest terms in the expressions for the elements of the seventh row and column of (9) except in the case of (11) which must be exact.

Therefore the Hamiltonian form of the kinetic energy is

$$\begin{aligned}2T=&\textstyle\sum_\alpha \square_\alpha P_\alpha^2+\sum_\alpha \square_{\alpha+3}P_\alpha^2+p_1^2\Omega^{-1}\\ &-2\textstyle\sum_\alpha \lambda_\alpha\Delta_\alpha\Omega^{-1}p_1P_\alpha\\ &-2\textstyle\sum_\alpha \gamma_\alpha\Delta_\alpha\Omega^{-1}p_1P_\alpha,\end{aligned} \qquad (12)$$

where the first three terms are the translational, over-all rotational, and internal rotational energies of the molecule, and the last two terms are the coupling between internal rotation and translation, and internal rotation and over-all rotation, respectively. In other words, the coupling between over-all rotation and translation is negligible in this particular case. The coefficients $\square_\alpha$ are constants and have the dimensions of reciprocal mass; $\square_{\alpha+3}$ are constants and have dimensions of reciprocal moments of inertia; Ω^{-1} is a function of the top angle θ_1 and analogous to a corrected moment of inertia for the top; $\lambda_\alpha\Delta_\alpha\Omega^{-1}$ and $\gamma_\alpha\Delta_{\alpha+3}\Omega^{-1}$ are functions of θ_1 with the dimensions of reciprocal mass times reciprocal length, and reciprocal mass times length^{-2}, respectively.

Quantum-Mechanical Hamiltonian

The correct wave-mechanical Hamiltonian[6] is then

$$\begin{aligned}\mathbf{H}_{op}=&\tfrac{1}{2}\textstyle\sum_\alpha \square_\alpha\boldsymbol{P}_\alpha^2+\tfrac{1}{2}\sum_\alpha \square_{\alpha+3}\mathbf{P}_\alpha^2\\ &+\tfrac{1}{2}|Q^{-1}|^{\frac{1}{3}}\mathbf{p}_1\Omega^{-1}|Q^{-1}|^{-\frac{1}{3}}\mathbf{p}_1\\ &-\tfrac{1}{2}|Q^{-1}|^{\frac{1}{3}}\textstyle\sum_\alpha \mathbf{p}_1\lambda_\alpha\Delta_\alpha\Omega^{-1}|Q^{-1}|^{-\frac{1}{3}}\boldsymbol{P}_\alpha\\ &-\tfrac{1}{2}\textstyle\sum_\alpha \Delta_\alpha\lambda_\alpha\Omega^{-1}\mathbf{p}_1\boldsymbol{P}_\alpha\\ &-\tfrac{1}{2}|Q^{-1}|^{\frac{1}{3}}\textstyle\sum_\alpha \mathbf{p}_1\gamma_\alpha\Delta_{\alpha+3}\Omega^{-1}|Q^{-1}|^{-\frac{1}{3}}\mathbf{P}_\alpha\\ &-\tfrac{1}{2}\textstyle\sum_\alpha \gamma_\alpha\Delta_{\alpha+3}\Omega^{-1}\mathbf{p}_1\mathbf{P}_\alpha+V,\end{aligned} \qquad (13)$$

where V is the potential energy, $|Q^{-1}|$ is the determinant of Q^{-1},

$$\mathbf{p}_1=\frac{h}{2\pi i}\frac{\partial}{\partial\theta_1},\qquad \boldsymbol{P}_\alpha=\frac{h}{2\pi i}\frac{\partial}{\partial R_\alpha}$$

and the $\mathbf{P}_\alpha$ are the Klein operators[6,7] involving

[5] If the diagonal elements of T_1 are all of an order of 70–100 (when atomic weight and angstrom units are used), (8) gives diagonal elements of T_1^{-1} to an accuracy of 0.1 percent. If one diagonal element is of order 10; others, of 100, (8) gives the corresponding diagonal element of T_1^{-1} to 1 percent. The off-diagonal elements of T_1^{-1} are neglected since they are of the order of 1 percent or less than corresponding diagonal elements, and (7) introduces about that error in the diagonal elements. The fact that the quantities neglected in (7) and (9) are functions of θ_1 of small absolute value, and enter the final result as quantum-mechanical averages improves this approximation.

[6] E. Bright Wilson, Jr. and J. B. Howard, J. Chem. Phys. **4**, 260 (1936).

[7] O. Klein, Zeits. f. Physik **58**, 730 (1929).

functions of the Eulerian angles, i.e., coordinates of the primary system. It is possible to write (13) in this way since the $\boldsymbol{P}_\alpha$ transform as vectors, and any operator of one set commutes with any operator of the other two sets though the $\mathbf{P}_\alpha$ do not commute among themselves. Moreover (13) may be simplified by using the fact that $|Q^{-1}|$ is practically constant. This may be shown in the following manner.

This argument will be presented for the $-$OH group. An analogous procedure may be used for any top to be considered. Numerical values are for angstrom and atomic mass units, and previous equations needed are (4), (5), (6), and (11).

Let

$$\Delta_k = \max.\ (\Delta_{\alpha+3}),$$

then

$$\Sigma_\alpha\, \Delta_{\alpha+3}\gamma_\alpha^2 \leqq \Delta_k^2,$$

$$\gamma_\alpha = [\mathbf{r}\times\boldsymbol{\lambda}]_\alpha + \eta_\alpha; \quad \boldsymbol{\gamma} = \mathbf{r}\times\boldsymbol{\lambda} + \mathbf{n},$$

$$\gamma^2 = [\mathbf{r}\times\boldsymbol{\lambda}]^2 + \eta^2 + 2\,\Sigma_\alpha \eta_\alpha (\mathbf{r}\times\boldsymbol{\lambda})_\alpha,$$

$$\eta_\alpha = a_{3\alpha}C - a_{2\alpha}\mathrm{E},$$

$$\eta^2 = C^2 + \mathrm{E}^2 - 2\,\Sigma_\alpha\, a_{2\alpha}a_{3\alpha}, \quad \mathrm{E}C = C^2 + \mathrm{E}^2,$$

since (a_{kl}) is orthogonal.

$$\therefore\ \gamma^2 = r^2\lambda^2 - (\mathbf{r}\cdot\boldsymbol{\lambda})^2 + C^2 + \mathrm{E}^2 + 2\,\Sigma_\alpha\, \eta_\alpha (\mathbf{r}\times\boldsymbol{\lambda})_\alpha$$

$$\leqq r^2\lambda^2 + 2|r|\,|\lambda|\,(C^2+\mathrm{E}^2)^{\frac{1}{2}} + (C^2+\mathrm{E}^2)$$

or

$$\Sigma_\alpha\, \Delta_{\alpha+3}\gamma_\alpha^2 \leqq \Delta_k\gamma^2 \leqq \Delta_k[|r|\,|\lambda| + (C^2+\mathrm{E}^2)^{\frac{1}{2}}]^2.$$

For $-$OH,

$$(C^2+\mathrm{E}^2)^{\frac{1}{2}} = 0.884, \quad |\lambda| = 0.925, \quad \mathrm{F} = 0.$$

The values of $|r|$ will, of course, depend on the molecule; but the larger $|r|$ is, the smaller will be Δ_k (reciprocal moment). Typical values are the set: $M\sim 70$, $|r|\sim 1.65$ and $\Delta_k \sim 0.01$. For this case

$$\Sigma_\alpha\, \Delta_{\alpha+3}\gamma_\alpha^2 \leqq 0.058\,\lambda^2 M^{-1} = 0.013.$$

Hence from (11)

$$\Omega^{-1} = C^{-1}[1 + (\lambda^2/CM) + C^{-1}\,\Sigma_\alpha\, \Delta_{\alpha+3}\gamma_\alpha^2] \qquad (14)$$

is exact to 0.7 percent. In a specific case, the exact expression for Ω^{-1} is easily obtained, but it is necessary to show that (14) is fairly exact for the proof given below.

By the method of triangulation,[4]

$$|Q^{-1}| = \prod_{i=1}^{6} \square_i \Omega^{-1}\left\{1 - \Omega^{-1}\,\Sigma_\alpha\left(\frac{\lambda_\alpha^2\Delta_\alpha^2}{\square_\alpha} + \frac{\gamma_\alpha^2\Delta_{\alpha+3}^2}{\square_{\alpha+3}}\right)\right\}. \qquad (15)$$

The $\square_i$ are constants, so only the last factor need be considered. The second term of this factor is certainly small compared to 1 (see above), hence only a small error will be introduced by the approximation $\square_i \leqq \Delta_i$. With this simplification, the variable factor becomes

$$\Omega^{-1}\{1 - \Omega^{-1}(\lambda^2 M^{-1} + \Sigma_\alpha\, \Delta_{\alpha+3}\gamma_\alpha^2)\}. \qquad (16)$$

The value of Ω^{-1} given by (14) is used in the second term in the bracket of (16). This term becomes, with the neglect of squares of small quantities,

$$(\lambda^2/CM) + C^{-1}\,\dot{\Sigma}_\alpha\, \Delta_{\alpha+3}\gamma_\alpha^2 = \Omega C^{-1} - 1.$$

Hence (16) becomes

$$\Omega^{-1}\Omega/C = C^{-1}, \text{ a constant.}$$

Consequently $|Q^{-1}|$ is also constant.

With this simplification, (14) becomes

$$\mathbf{H}_{op} = \tfrac{1}{2}\,\Sigma_\alpha\, \square_\alpha \boldsymbol{P}_\alpha^2 + \tfrac{1}{2}\,\Sigma_\alpha\, \square_{\alpha+3}\mathbf{P}_\alpha^2 + \tfrac{1}{2}\mathbf{p}_1\Omega^{-1}\mathbf{p}_1$$

$$- \tfrac{1}{2}\,\Sigma_\alpha\, \Delta_\alpha(\mathbf{p}_1\lambda_\alpha\Omega^{-1} + \lambda_\alpha\Omega^{-1}\mathbf{p}_1)\boldsymbol{P}_\alpha$$

$$- \tfrac{1}{2}\,\Sigma_\alpha\, \Delta_{\alpha+3}(\mathbf{p}_1\gamma_\alpha\Omega^{-1} + \gamma_\alpha\Omega^{-1}\mathbf{p}_1)\mathbf{P}_\alpha + V. \qquad (17)$$

Wave Functions and Energy Levels for Top

If

$$2V = V_1(1 - \cos\nu\theta_1),$$

where ν is the number of minima encountered in one complete revolution of the top, and V_1 is the height of the potential barrier, then

$$\mathbf{H}_{1_{op}} = \tfrac{1}{2}\mathbf{p}_1\Omega^{-1}\mathbf{p}_1 + \tfrac{1}{2}V_1(1 - \cos\nu\theta_1) \qquad (18)$$

is the portion of (17) corresponding to the rotation of the top. For the type of molecule considered here, Ω^{-1} has the form

$$\Omega^{-1} = A + B(\theta_1),$$

where A is a constant, and

$$B(\theta_1) = a\cos\theta_1 + b\cos 2\theta_1 + c\sin\theta_1 + d\sin 2\theta_1.$$

Moreover, the coefficients in B are only a few percent of A. Hence let

$$\mathbf{H}_{1op} = \mathbf{H}_1^{\,0} + \mathbf{H}_1',$$

where

$$\mathbf{H}_1^{\,0} = \tfrac{1}{2}A\mathbf{p}_1^2 + \tfrac{1}{2}V_1(1 - \cos\nu\theta_1)$$

and

$$\mathbf{H}_1' = \tfrac{1}{2}\mathbf{p}_1 B(\theta_1)\mathbf{p}_1.$$

The wave equation obtained in the usual manner from $\mathbf{H}_1^{(0)}$ is

$$\frac{d^2\psi_r^{(0)}}{d\theta_1^2} + \frac{8\pi^2}{Ah^2}[w_r^{(0)} + \tfrac{1}{2}V_1\cos\nu\theta_1 - \tfrac{1}{2}V_1]\psi_r^{(0)} = 0$$

$$r = 0, 1, 2, \cdots, \qquad (19)$$

from which the Mathieu equation is derived by making the substitution $2x = \nu\theta_1$. For large values of V_1, the energy levels are vibrational in nature, and ν-fold degenerate; their limiting value is

$$w_t^{(0)} = \tfrac{1}{8}h^2 A\pi^{-2}\beta(2t+1), \qquad (20)$$

where t is the vibrational quantum number $t = 0, 1, 2, \cdots$, h is Planck's constant, and

$$\beta = \pi\nu(2V_1/Ah^2)^{\frac{1}{2}}.$$

For very small values of V_1, the energy levels are rotational in nature, and except for $m = 0$,

doubly degenerate. Their limiting values are

$$w_m^{(0)} = (h^2A/8\pi^2)m^2, \quad m=0, \pm1, \pm2, \cdots. \quad (21)$$

In the standard manner, it is found that the correct zeroth-order wave functions for these two limiting cases are

$$\psi_m^{(0)} = e^{im\theta_1}/(2\pi)^{\frac{1}{2}} \; m \neq \pm 1;$$

$$\psi_1^{(0)} = \psi_{-1}^{(0)*} = [e^{-i\theta_1} + (b-id)(b^2+d^2)^{-\frac{1}{2}}e^{i\theta_1}]/2\pi^{\frac{1}{2}}$$

and the orthonormal Hermite functions

$$\psi_t^{(0)} = N_t \exp(-\tfrac{1}{2}\beta\theta_1^2) H_t(\beta^{\frac{1}{2}}\theta_1) \quad t=0, 1, 2, \cdots,$$

respectively. Moreover, the first-order corrections to the energies, arising from the perturbation $\mathbf{H}_1'$, are

$$w_m' = \begin{cases} \pm\dfrac{h^2}{8\pi^2}(b^2+d^2)^{\frac{1}{2}} & m=\pm1, \\ 0 & \text{otherwise} \end{cases} \quad (22)$$

$$w_t' = \tfrac{1}{16}h^2\beta\pi^{-2}\{(2t+1)(a+b) - (\tfrac{1}{2}a+2b)\tfrac{1}{2}\beta^{-1}(2t^2+2t+3)\}, \quad (23)$$

respectively. Both w_m'' and w_t'' are proportional to the squares of the coefficients occurring in $B(\theta_1)$, and are therefore negligible.

In general, the actual Mathieu levels $w_r^{(0)}$ [8] fall in neither of the above extreme cases. However, they approximate the harmonic oscillator levels for low r, free rotation levels for larger r, and the transition at a limiting value r_0 is reasonably sharp.

[8] See E. L. Ince, Proc. Roy. Soc. Edinburgh **52**, 355 (1931) for form of $\psi_r^{(0)}$. Note that Ince gives solutions periodic in π and in 2π for x where $2x=\nu\theta_1$. In order that these solutions satisfy the requirement that $\psi(\theta_1)$ have the period 2π in θ_1, they must have the period $\nu\pi$ in x. Consequently Ince's levels a_n and b_n, n odd, must be omitted for ν odd. Moreover, for $\nu>2$ Ince does not give all the solutions of period $\nu\pi$ required by this problem, e.g., for $\nu=3$, Ince's levels a_n and b_n, n even, are derived from solutions of a period π in x while the requirements of this problem call not only for these solutions, but also for an equal number with the period 3π in x. In such cases, it has been the practice to sum over the levels for which Ince's solutions are also solutions for the problem, and multiply the result by a factor determined by the number of solutions omitted. In the case of $\nu=3$, the procedure would be to sum over Ince's values a_n and b_n, n even, and multiply that result by 3 since Ince omits half the solutions required by the problem, and those omitted are doubly degenerate. This treatment infers that the sum over the levels arising from solutions of period π in x is exactly equal to the sum of those from solutions of period 3π (but not of π). Where this treatment has been tested by actual computation, it has been found entirely adequate.

. Since the perturbation $\mathbf{H}_1'$ is quite small, it is assumed below that $\psi_r \cong \psi_r^0$ is an adequate approximation for the top wave function.

Energy Matrix

Let the basis functions be $\psi_r\psi_R\psi_T$, where ψ_R is a function of the Eulerian angles only and is the orthonormal wave function for the rigid asymmetric top molecule, and ψ_T is a function of x, y, z only and the orthonormal wave function for a particle in a box. Since Q^{-1} contains elements which are functions of θ_1 only, the energy matrix, obtained from (17), divided into submatrices designated by the top quantum numbers is

$$\mathbf{H}_{rr} = w_r\mathbf{E} + \tfrac{1}{2}\sum_\alpha \square_\alpha \boldsymbol{P}_\alpha^2 + \tfrac{1}{2}\sum_\alpha \square_{\alpha+3}\mathbf{P}_\alpha^2 - \tfrac{1}{2}A\sum_\alpha(\mathbf{p}_1\gamma_\alpha+\gamma_\alpha\mathbf{p}_1)_{rr}\Delta_{\alpha+3}\mathbf{P}_\alpha, \quad (24)$$

$$\mathbf{H}_{rr'} = -\tfrac{1}{2}AM^{-1}\sum_\alpha(\mathbf{p}_1\lambda_\alpha+\lambda_\alpha\mathbf{p}_1)_{rr'}\boldsymbol{P}_\alpha - \tfrac{1}{2}A\sum_\alpha\Delta_{\alpha+3}(\mathbf{p}_1\gamma_\alpha+\gamma_\alpha\mathbf{p}_1)_{rr'}\mathbf{P}_\alpha, \quad (25)$$

where $\mathbf{E}$ is the identity matrix; and $\boldsymbol{P}_\alpha$ and $\mathbf{P}_\alpha$ are quantum-mechanical matrices and functions of the translational quantum numbers n_x, n_y, n_z, and the rotational quantum numbers J, K, M. Also, in accord with the approximations made in obtaining Q^{-1}, only the largest terms of $\gamma_\alpha\Omega^{-1}$ and $\lambda_\alpha\Omega^{-1}$ are retained. The general forms of λ_α and γ_α are

$$\lambda_\alpha = f_\alpha \sin\theta_1 + g_\alpha\cos\theta_1, \quad (26)$$

$$\gamma_\alpha = a_{3\alpha}C + l_\alpha\sin\theta_1 + q_\alpha\cos\theta_1. \quad (27)$$

The first term of (27) is constant since the $a_{3\alpha}$ are direction cosines for the rotation axis of the top. The limiting values of the coefficients appearing in (24) and (25) are, in condensed notation,

$$(\mathbf{p}_1\lambda_\alpha+\lambda_\alpha\mathbf{p}_1)_{rr'}$$

$$(t, t+3) = -(t+3, t) = \tfrac{1}{4}hi\pi^{-1}g_\alpha \times[(t+1)(t+2)(t+3)]^{\frac{1}{2}}/\sqrt{2}\beta^{\frac{1}{2}},$$

$$(t, t+2) = -(t+2, t) = -\tfrac{1}{2}hi\pi^{-1}f_\alpha[(t+1)(t+2)]^{\frac{1}{2}},$$

$$(t, t+1) = -(t+1, t) = -\tfrac{1}{2}hi\pi^{-1}g_\alpha \times[1-\tfrac{1}{4}(t+1)\beta^{-1}](t+1)^{\frac{1}{2}}\sqrt{2}\beta^{\frac{1}{2}},$$

$$(m, m+1)=(m+1, m)^*=\tfrac{1}{2}h\pi^{-1}(m+\tfrac{1}{2})(g_\alpha+if_\alpha), \quad |m|>2$$

$$(1, 2)=(-2, -1)=(2, 1)^*=(-1, -2)^*$$
$$=\tfrac{1}{4}\sqrt{2}\pi^{-1}(b+id)(b^2+d^2)^{-\frac{1}{2}}(g_\alpha+if_\alpha),$$
$$(2, -1)=(-1, 2)^*=-(1, -2)=-(-2, 1)^*$$
$$=\tfrac{1}{4}\sqrt{2}\pi^{-1}(g_\alpha+if_\alpha),$$

others zero.

$$(\mathbf{p}_1\gamma_\alpha+\gamma_\alpha\mathbf{p}_1)_{rr'}$$

Exactly the same as above, with q_α and l_α replacing g_α and f_α, respectively, except

$$(t, t+1)=-(t+1, t)=-\tfrac{1}{2}hi\pi^{-1}q_\alpha \times[1+a_{3\alpha}C-\tfrac{1}{4}(t+1)\beta^{-1}](t+1)^{\frac{1}{2}}\sqrt{2}\beta^{\frac{1}{2}},$$

$$(m, m)=\begin{cases}0 & m=\pm 1\\ mha_{3\alpha}C\pi^{-1} & \text{otherwise.}\end{cases}$$

If the matrices $\mathbf{H}_{rr'}$ of (25) are considered as perturbations, the energy matrix diagonal in r and correct to the third order in elements of $\mathbf{H}_{rr}$ is given by the perturbation treatment[6] as

$$\bar{\mathbf{H}}_{rr}=\mathbf{H}_{rr}+\Delta\mathbf{H}_r, \tag{28}$$

$$\Delta\mathbf{H}_t=-\tfrac{1}{2}A\{\mathrm{R}^2+(\mathbf{RS}+\mathbf{SR})+\mathrm{S}^2 -\tfrac{1}{2}(2t+1)\beta^{-1}[\mathrm{R}^2+\tfrac{1}{2}(\mathbf{RS}+\mathbf{SR})+\mathrm{I}^2] +\tfrac{1}{16}(6t^2+6t+5)\beta^{-2}\mathrm{R}^2\}, \tag{29}$$

$$\Delta\mathbf{H}_m=\begin{cases}-\tfrac{1}{4}(\mathrm{R}^2+\mathrm{I}^2)A & |m|>2\\ -11A(\mathrm{R}^2+\mathrm{I}^2)/24 & m=\pm 2\\ -\tfrac{1}{6}(\mathrm{R}^2+\mathrm{I}^2)A & m=\pm 1\\ 0 & m=0\end{cases} \tag{30}$$

$$\mathbf{R}=\textstyle\sum_\alpha(\Delta_\alpha g_\alpha\mathbf{P}_\alpha+\Delta_{\alpha+3}q_\alpha\mathbf{P}_\alpha),$$
$$\mathbf{I}=\textstyle\sum_\alpha(\Delta_\alpha f_\alpha\mathbf{P}_\alpha+\Delta_{\alpha+3}l_\alpha\mathbf{P}_\alpha),$$
$$\mathbf{S}=C\textstyle\sum_\alpha\Delta_{\alpha+3}a_{3\alpha}q_\alpha\mathbf{P}_\alpha.$$

Partition Function

The partition function is obtained from the energy matrix by a method based on perturbation theory.[9] The symmetry number of the type of molecule discussed here, with frozen internal rotation, is one. Moreover, the symmetry number for an attached asymmetric top is also one. Hence these quantities enter the expression for the partition function only as a factor of unity.

Zeroth order expression

For this approximation, the energy matrix is considered as

$$\mathbf{H}_{rr}=w_r\mathbf{E}+\tfrac{1}{2}\textstyle\sum_\alpha\square_\alpha\boldsymbol{P}_\alpha^2+\tfrac{1}{2}\sum_\alpha\square_{\alpha+3}\mathbf{P}_\alpha^2.$$

This gives for the partition function

$$Q=Q_TQ_RQ_M{}^{(0)}$$

where

$$Q_T=v(2kT\pi)^{\frac{3}{2}}h^{-3}(\square_1\square_2\square_3)^{-\frac{1}{2}}$$

is the translational factor;

$$Q_R=8\pi^2(2kT\pi)^{\frac{3}{2}}h^{-3}(\square_4\square_5\square_6)^{-\frac{1}{2}}$$

is the rotational factor; v is the volume of the container; k, Boltzmann's constant; T, absolute temperature, and

$$Q_M{}^{(0)}=\sum_{r=0}^{\infty}\exp(-w_r/kT). \tag{31}$$

Since

$$w_r=w_r{}^{(0)}+w_r'$$

and w_r' is only a few percent of $w_r{}^{(0)}$, a good approximation for (31) is

$$Q_M{}^{(0)}=\sum_{r=0}^{\infty}\exp(-w_r{}^{(0)}/kT) -\frac{1}{kT}\sum_r w_r'\exp(-w_r{}^{(0)}/kT). \tag{32}$$

If the correction term is broken into a sum over vibrational and rotational levels, and the limiting values of $w_r{}^{(0)}$ and w_r' [Eqs. (20)–(23)] used, (32) becomes

$$Q_M{}^{(0)}=(1-D_1/kT)\sum_{r<r_0}\exp(-w_r{}^{(0)}/kT) +\sum_{r\geq r_0}\exp(-w_r{}^{(0)}/kT) -(2D_1\nu/kT)\sum_{t=0}^{t_0}t\exp(-w_t{}^{(0)}/kT) +(D_2\nu/kT)\sum_{t=0}^{t_0}t^2\exp(-w_t{}^{(0)}/kT), \tag{33}$$

where

$$D_1=\tfrac{1}{16}h^2\pi^{-2}\{(\beta-\tfrac{1}{4})a+(\beta-1)b\};$$
$$D_2=\tfrac{1}{32}h^2\pi^{-2}(a+4b).$$

[9] E. B. Wilson, Jr., J. Chem. Phys. 7, 948 (1939).

Since at room temperature for $V_1=2000$ cal./mole and $(a+b)=5$ percent A, D_1/kT is about 0.004, (33) may be further simplified to

$$Q_M^{(0)}=\sum_r \exp(-w_r^{(0)}/kT) - (2D_1\nu/kT)\sum_{t=0}^{t_0} t\exp(-w_t^{(0)}/kT) + (D_2\nu/kT)\sum_{t=0}^{t_0} t^2\exp(-w_t^{(0)}/kT). \quad (34)$$

General formulae for the sums occurring in the correction terms of (34) can, of course, be given, but generally t_0 is so small that it is just as convenient to sum the terms directly. The first term of (34) is an ordinary Mathieu sum.

First-order correction

In this case, the energy matrix is given by (24) which may be written

$$\mathbf{H}_{rr}=w_r\mathbf{E}+\tfrac{1}{2}\sum_\alpha \square_\alpha \mathbf{P}_\alpha^2+\tfrac{1}{2}\sum_\alpha \square_{\alpha+3}\mathbf{P}_\alpha^2 + \sum_\alpha (s_\alpha)_r\mathbf{P}_\alpha, \quad (35)$$

where the last sum is zero for vibrational levels,[10] and the limiting values of its coefficients are

$$s_\alpha=\begin{cases} 0 & r<r_0 \\ 0 \quad m=0,\pm1 & r\geq r_0 \\ -\tfrac{1}{2}\Delta_{\alpha+3}mha_{3\alpha}CA\pi^{-1} \quad |m|>1 & r\geq r_0. \end{cases} \quad (36)$$

Then the linear transformation

$$\mathbf{P}_\alpha=\mathbf{P}_\alpha'-(s_\alpha)_r/\square_{\alpha+3} \quad (37)$$

converts (35) to

$$\mathbf{H}_{rr}=\tfrac{1}{2}\sum_\alpha \square_\alpha \mathbf{P}_\alpha^2+\tfrac{1}{2}\sum_\alpha \square_{\alpha+3}\mathbf{P}'_\alpha + (w_r-\tfrac{1}{2}\sum_\alpha{}'(s_\alpha)_r^2/\square_{\alpha+3})\mathbf{E}. \quad (38)$$

Since the Jacobian of (37) is one, the partition function from (38) is

$$Q=Q_TQ_RQ_M^{(1)},$$

where Q_T and Q_R have the values given above, and

$$Q_M^{(1)}=\sum_r \exp-(w_r-\tfrac{1}{2}\sum_\alpha(s_\alpha)_r^2/\square_{\alpha+3})/kT = \sum_r \exp-w_r(1-\Gamma_r/w_r)/kT, \quad (39)$$

[10] This is true since the Hermite functions are real; the operators $\mathbf{P}_\alpha$, pure imaginary; see reference 6.

where the limiting values are

$$\frac{\Gamma_r}{w_r}=\begin{cases} 0 & r<r_0 \\ \sigma=C^2\sum_\alpha \Delta_{\alpha+3}a_{3\alpha}{}^2 & r\geq r_0 \quad (|m|>1). \end{cases}$$

For a treatment completely analogous to Crawford's,[1] let

$$\kappa_r=1-\epsilon_r=\sigma^{-1}\Gamma_r w_r^{-1}.$$

Then $\kappa_r\leqq 0$ for vibrational levels, $\epsilon_r\leqq 0$ for rotational levels ($|m|>1$). These parameters in (39) give

$$Q_M^{(1)}=\sum_r \exp[-(w_r/kT)(1-\sigma\kappa_r)] = \sum_r \exp\left[-(w_r/kT)(1-\sigma)\left(1+\frac{\sigma}{1-\sigma}\epsilon_r\right)\right] \quad r_0>2. \quad (40)$$

Hence, if the sum is split into rotational and vibrational levels,

$$Q_M^{(1)}=\sum_{r<r_0}\exp(-w_r/kT) + \sum_{r\geq r_0}\exp[-(1-\sigma)w_r^{(0)}/kT] \quad r_0>2.^{11} \quad (41)$$

This expression differs from $Q_M^{(0)}$ only by the fact that

$$\sum_{r\geq r_0}\exp(-w_r^{(0)}/kT)$$

in the former is here replaced by

$$\sum_{r\geq r_0}\exp[-(1-\sigma)w_r^{(0)}/kT].$$

Second-order correction

Here the energy matrix is given by (28). For this correction, it is assumed immediately that the levels $r<r_0$ are vibrational; $r\geq r_0$, rotational. After evaluating (29) and rearranging, (28) becomes

$$\mathbf{H}_{tt}=\tfrac{1}{2}\widetilde{\mathbf{P}'}N\mathbf{P}'+w_t\mathbf{E}+\tfrac{1}{2}t\widetilde{\mathbf{P}'}E\mathbf{P}'+\tfrac{1}{2}t^2\widetilde{\mathbf{P}'}F\mathbf{P}' \quad r<r_0, \quad (42)$$

where the column matrix

$$\mathbf{P}'=\{\mathbf{P}_x\mathbf{P}_y\mathbf{P}_z\ \mathbf{P}_x\mathbf{P}_y\mathbf{P}_z\}$$

[11] If $r_0\leqq 2$, substitution of (36) in (39) shows that (41) becomes

$$Q_M^{(1)}=\sum_{r\leq 2}\exp(-w_r/kT)+\sum_{r>2}\exp[-(1-\sigma)w_r^{(0)}/kT].$$

Since Ω/C is always near unity for this type of molecule, (41) is sufficiently accurate in any case satisfying the initial restrictions.

and N, E, F are 6×6 symmetrical matrices.[12] The first term of (42) may be diagonalized by an orthogonal transformation (of which the Jacobian is one). After this has been done, the integration can be carried out. Similarly, for $r\geq r_0$

$$\mathbf{H}_{mm}=\tfrac{1}{2}\widetilde{\boldsymbol{P}}'\mathrm{M}_m\boldsymbol{P}'+w_m\mathbf{E}+\sum_\alpha(\mathrm{s}_\alpha)_m\mathbf{P}_\alpha, \quad (43)$$

where M_m is a 6×6 matrix,[12] and

$$\mathrm{M}_m=\mathrm{M} \quad |m|>2; \quad \mathrm{M}_{+1}=\mathrm{M}_{-1}; \quad \mathrm{M}_{+2}=\mathrm{M}_{-2};$$
$$(\mathrm{M}_0)_{ij}=\delta_{ij}\square_i.$$

Here it is necessary to diagonalize the quadratic form, and then make a linear transformation to remove linear terms before integrating. Fortunately the results after integration may be expressed in terms of the original matrices. As a result of these operations, the partition function is found to be

$$Q=\frac{8\pi^2}{h^6}v(2\pi kT)^3\Big\{|N|^{-\frac{1}{2}}\Big(\sum_{r<r_0}\exp(-w_r^{(0)}/kT)$$
$$-\nu\Big[\frac{2D_1}{kT}+\tfrac{1}{2}\chi(N^{-1}E)\Big]\sum_{t=0}^{t_0}t\exp(-w_t^{(0)}/kT)$$
$$+\nu\Big[\frac{D_2}{kT}-\tfrac{1}{2}\chi(N^{-1}F)\Big]\sum_{t=0}^{t_0}t^2\exp[-w_t^{(0)}/kT]\Big)$$
$$+\sum_{r\geq r_0}|\mathrm{M}_r|^{-\frac{1}{2}}\exp[-(1-\sigma)w_r^{(0)}/kT]\Big\} \quad (44)$$
$$r_0>2,$$

where, as before, the limiting energies have been used instead of w_r in the correction terms, $\chi(N^{-1}E)$ and $\chi(N^{-1}F)$ are the characters of the product matrices indicated, and σ has the same value as in the first-order expression.[13] If $r_0\leqq2$, the last term in the bracket of (44) becomes

$$\sum_{r_0\leq r<3}|\mathrm{M}_r|^{-\frac{1}{2}}\exp(-w_r/kT)$$
$$\sum_{r\geq3}|\mathrm{M}_r|^{-\frac{1}{2}}\exp[-(1-\sigma)w_r^{(0)}/kT],$$

while if $r_0>4$, it is

$$|\mathrm{M}|^{-\frac{1}{2}}\sum_{r\geq r_0}\exp[-(1-\sigma)w_r^{(0)}/kT]$$

and for the limiting case of free rotation ($r_0=0$), (44) becomes

$$Q=\frac{8\pi^2}{h^6}v(2\pi kT)^3\Big\{\sum_{r\leq2}|\mathrm{M}_r|^{-\frac{1}{2}}\exp(-w_r/kT)$$
$$+\sum_{r>2}|\mathrm{M}_r|^{-\frac{1}{2}}\exp[-w_r^{(0)}(1-\sigma)/kT]\Big\}$$
$$\leqq\frac{8\pi^2}{h^2}v(2\pi kT)^3\Big\{\sum_{r\leq2}|\mathrm{M}_r|^{-\frac{1}{2}}\exp(-w_r^{(0)}/kT)$$
$$+\sum_{r>2}|\mathrm{M}_r|^{-\frac{1}{2}}\exp[-w_r^{(0)}(1-\sigma)/kT\Big\}. \quad (45)$$

To evaluate the sums occurring in (44) and (45), use the value for $w_t^{(0)}$ given in (20), and

$$w_r^{(0)}=[a_r^{(0)}+(16\pi^2/\nu^2h^2A)V_1](\tfrac{1}{32}h^2\nu^2A\pi^{-2})$$
$$=(a_r^{(0)}+2\eta)(\tfrac{1}{4}V_1\eta^{-1}),$$

so that

$$\sum_r\exp(-w_r^{(0)}/kT)$$
$$=\exp(-\mu)\sum_r\exp(-a_r^{(0)}\mu/2\eta), \quad (46)$$

where

$$\mu=V_1/2kT \quad \text{and} \quad \eta=(8\pi^2/\nu^2h^2A)V_1.$$

At present, the only tables available are those for $a_r^{(0)}$ [8,14] and thermodynamic contributions arising from $\sum_r\exp(-w_r^{(0)}/kT)$.[15] However, tables for the sums over the rotational and

---

[12] $(\mathrm{M})_{ij}=\delta_{ij}\square_i-\frac{1}{2}A\Delta_i\Delta_jW_{ij}$,

$$W_{ij}=\begin{cases}(g_ig_j+f_if_j) & i,\ j\leq3\\ (q_{i'}q_{j'}+l_{i'}l_{j'}) & i,\ j>3\\ (g_iq_{j'}+f_il_{j'}) & i\leq3,\ j>3\end{cases} \qquad i'=i-3.$$

$\mathrm{M}_{\pm1}$ and $\mathrm{M}_{\pm2}$ are the same as above except for the factor of $\frac{1}{3}$ and $\frac{1}{2}\frac{1}{4}$, respectively, instead of $\frac{1}{2}$.

$(N)_{ij}=\delta_{ij}\square_i-A\Delta_i\Delta_jY_{ij}$,

$$Y_{ij}=\begin{cases}g_ig_j(1-\frac{1}{2}\beta^{-1}+\frac{5}{16}\beta^{-2})+\frac{1}{2}\beta^{-1}f_if_j & i,\ j\leq3\\ q_{i'}q_{j'}\{1+C^2a_{3i'}a_{3j'}-\frac{1}{2}\beta^{-1}+\frac{5}{16}\beta^{-2}\\ \quad+C(1-\frac{1}{4}\beta^{-1})(a_{3i'}+a_{3j'})\}+\frac{1}{2}\beta^{-1}l_{i'}l_{j'} & i,\ j>3\\ g_iq_{j'}\{1-\frac{1}{2}\beta^{-1}+\frac{5}{16}\beta^{-2}+\frac{1}{2}C(1-\frac{1}{4}\beta^{-1})(a_{3i}+a_{3j'})\}\\ \quad+\frac{1}{2}\beta^{-1}f_il_{j'} & i\leq3,\ j>3\end{cases}$$

$$E_{ij}=\begin{cases}-\Delta_i\Delta_j[g_ig_j(\frac{3}{8}\beta^{-2}-\beta^{-1})+\beta^{-1}f_if_j] & i,\ j\leq3\\ -\Delta_i\Delta_j[q_{i'}q_{j'}\{\frac{3}{8}\beta^{-2}-\beta^{-1}-\frac{1}{2}C(a_{3i'}+a_{3j'})\beta^{-1}\}\\ \quad+\beta^{-1}l_{i'}l_{j'}] & i,\ j>3\\ -\Delta_i\Delta_j[g_iq_{j'}\{\frac{3}{8}\beta^{-2}-\beta^{-1}-\frac{1}{4}C(a_{3i}+a_{3j'})\beta^{-1}\}\\ \quad+\beta^{-1}f_il_{j'}] & i\leq3;\ j>3\end{cases}$$

$$F_{ij}=-\tfrac{3}{8}\beta^{-2}\Delta_i\Delta_j\begin{cases}g_ig_j & i,\ j\leq3\\ q_{i'}q_{j'} & i,\ j>3\\ g_iq_{j'} & i\leq3,\ j>3.\end{cases}$$

[13] σ is here an approximation for the quantity $C^2A\sum_{\alpha\beta}a_{3\alpha}a_{3\beta}\Delta_{\alpha+3}\Delta_{\beta+3}m_{\alpha\beta}$ where $m_{\alpha\beta}$ represents the elements in the submatrix $i,\ j>3$ of M^{-1}, and consequently varies with r if $r_0\leq4$. However, the variation is so slight, and the quantity itself so small that σ is a good approximation.

[14] E. Bright Wilson, Jr., Chem. Rev. **27**, 17 (1940).

[15] K. S. Pitzer, J. Chem. Phys. **5**, 469 (1937).

vibrational levels are now being prepared by Crawford, and should be available shortly.

There is good reason to believe that the case of the top $-NO_2$, and that of more than one top can be treated by a modification of the above procedure. These will be presented in a later paper.

In conclusion, I should like to express my appreciation to Professor E. Bright Wilson, Jr. for suggesting this problem and directing the investigation; to Professor B. L. Crawford, Jr. for reading the manuscript; and to the American Association of University Women whose grant made this work possible.

Appendix I

The following table was prepared to facilitate cross-reference between Crawford's paper and this one. The quantities are analogous, but not necessarily equal, e.g., those in the second column may vary slightly with θ_1 (indicated by $^+$) while those in the first column are constant.

Physical Significance	Crawford's Symbol ($m=1$)	This Paper
Moments of inertia of top	A_m	C
Principal moments of inertia of molecule	I_i	A_{ii}
Direction cosines, top axis	λ_{mi}	$a_{3\alpha}$
Top angle	α_m	θ_1
Angular velocity of top	$\dot{\alpha}_m$	ω_1
Angular velocity of molecule	$\boldsymbol{\omega}$	$\boldsymbol{\omega}$
Angular momentum of top	$\mathbf{P}_m$	$\mathbf{p}_1$
Angular momentum of molecule	$\mathbf{P}$	$\mathbf{P}$
Geometrical parameter	$\Omega_m=1-\sum_{i=1}^{3}(A_m/I_i)\lambda_{mi}^2$	$\Omega/C=1-(\lambda^2/CM)$ $-C^{-1}\sum_\alpha \Delta_{\alpha+3}\gamma_\alpha^2$ $^+$
Corrected moments of inertia for top	$F_m=A_m\Omega_m$	Ω
Reciprocal of corrected moments	$1/F_m$	$\Omega^{-1}=A+B(\theta_1)$ $^+$
Reciprocal moments for molecule	$1/I_i$	$\Delta_{\alpha+3}$
Elements of matrix of Hamiltonian form of kinetic energy corresponding to reciprocal moments of inertia of molecule	β_{ij}	$\square_{\alpha+3}$
Coefficients for coupling between internal and overall rotation	γ_{mi}	$\Delta_{\alpha+3}\gamma_\alpha\Omega^{-1}$ $^+$
Hindering potential	$\theta_m=V_m(8\pi^2A_m\Omega_m/h^2\nu_m^2)$	$\eta=V_1(8\pi^2/A\nu^2h^2)=(4/\nu^4)\beta^2$
Mathieu energy levels	$w_{mr}=(a_{mr}+2\theta_m)(h^2\nu_m^2/32\pi^2F_m)$ $=(a_{mr}+2\theta_m)(V_m/4\theta_m)$	$w_r^{(0)}=(a_r^{(0)}+2\eta)(h^2\nu^2A/32\pi^2)$ $=(a_r^{(0)}+2\eta)(V_1/4\eta)$
Characteristic constants of Mathieu equation	$a_{mr}=(4\theta_1/V_m)w_{mr}-2\theta_m$ $q_m=V_m/2RT$ (V_m for mole)	$a_r^{(0)}=(4\eta/V_1)w_r^{(0)}-2\eta$ $\mu=V_1/2kT$ (V_1 for molecule)

Appendix II

Relationship between the quantum numbers.

The quantum number r has positive integral values only, and is used to label the actual energy levels. The letters m and t are used to label, respectively, the rotational and vibrational levels; m is a positive or negative integer, t is a positive integer.

$$\begin{aligned} r&=\nu t+n & n&=0, 1\cdots(\nu-1).\\ &=2|m|-k & k&=0, 1.\end{aligned}$$

Analysis of the Near Ultraviolet Absorption Spectrum of Monochlorobenzene

H. SPONER AND S. H. WOLLMAN*
Department of Physics, Duke University, Durham, North Carolina

(Received August 18, 1941)

The absorption spectrum of C_6H_5Cl at 2750–2400A has been studied in the first order of a 3 m grating spectrograph. The band system corresponds to an electronic transition $A_1 \rightarrow B_1$ (monochlorobenzene has the symmetry C_{2v}) with the transition moment lying in the molecular plane perpendicular to the C−Cl bond. In agreement with this assignment to an allowed transition the 0,0 band appears strongly. Several progressions have been found involving various totally symmetrical vibrations. Besides this "allowed" part of the spectrum there appear "forbidden" bands which are due to the excitation of a non-totally symmetrical vibration of suitable symmetry. This vibration corresponds to the one (ϵ_g+ 606 cm^{-1}) whose excitation is responsible for the appearance of the benzene spectrum. The analysis is supported by comparison with the absorption of solid monochlorobenzene at −259°C.

INTRODUCTION

AFTER the near ultraviolet electronic transition in benzene had been recognized as a forbidden transition[1] and its vibrational structure was found to be in agreement with this assumption,[2] it seemed of interest to analyze the corresponding spectra of monosubstituted benzenes. These spectra should have the characteristics of allowed transitions because the sixfold symmetry of the carbon ring, which is responsible for the forbidden character of the transition in benzene, is destroyed by the substitution. The simplest kind of substitution is the one in which one hydrogen of benzene is replaced by one other atom. This is the case in the monohalogenated benzenes. Monochlorobenzene has been investigated in the vapor phase by Henri and collaborators,[3] but the data published are very incomplete. A recent investigation by Asagoe and Ikemoto[4] came to our attention only during the writing of this paper. We shall refer to their results in connection with ours. The spectra of C_6H_5Cl in solutions have been studied by Wolf and Herold and Conrad-Billroth,[5] and the spectrum of solid C_6H_5Cl was studied at very low temperatures by Kronenberger.[6] We present here the spectrum of monochlorobenzene in the gaseous state and its interpretation.[7] It will be seen that the spectrum shows indeed the characteristics of an allowed transition but that it also exhibits features which are prominent in the forbidden transition of benzene.

EXPERIMENTAL

The spectrum of monochlorobenzene which lies in the region of 2750–2400A was photographed in the first order of a 3 m grating spectrograph (Eagle mounting) with a hydrogen discharge lamp of the conventional type as light source. The monochlorobenzene, which was extremely pure,[8] was carefully introduced into quartz absorption tubes of 15 and 75 cm length by vacuum distillation. While the absorption spectra were taken, the substance was kept in a side arm at temperatures varying from −40°C to +130°C, covering pressures from 0.1 to 720 mm. In runs above room temperature a gradual fogging of the quartz windows was observed due to a slow photodecomposition of the vapor. Tests of the absorption of the fogged windows showed only a continuous absorption with no band structure in the studied region. With type I 0 and II 0 Eastman spectroscopic plates exposure times

* Present address: Naval Ordnance Laboratory, Washington, D. C.

[1] A. L. Sklar, J. Chem. Phys. **5**, 66 (1937).

[2] H. Sponer, G. Nordheim, A. L. Sklar, and E. Teller, J. Chem. Phys. **7**, 207 (1939).

[3] V. Henri, Comptes rendus **176**, 1298 (1923); *Structure des Molécules* (J. Hermann, Paris, 1925), p. 75, 112 and spectrograms.

[4] K. Asagoe and Y. Ikemoto, Proc. Phys. Math. Soc. Japan **22**, 677 (1940).

[5] K. L. Wolf and W. Herold, Zeits. f. physik. Chemie **B13**, 201 (1931); H. Conrad-Billroth, Zeits. f. physik. Chemie **B19**, 76 (1932).

[6] A. Kronenberger, Zeits. f. Physik **63**, 494 (1930).

[7] Preliminary report H. Sponer and S. H. Wollman, Phys. Rev. **57**, 1078A (1940).

[8] We are indebted to Dr. Eunice Moore of the Chemistry Department for the courtesy of providing us with the monochlorobenzene.

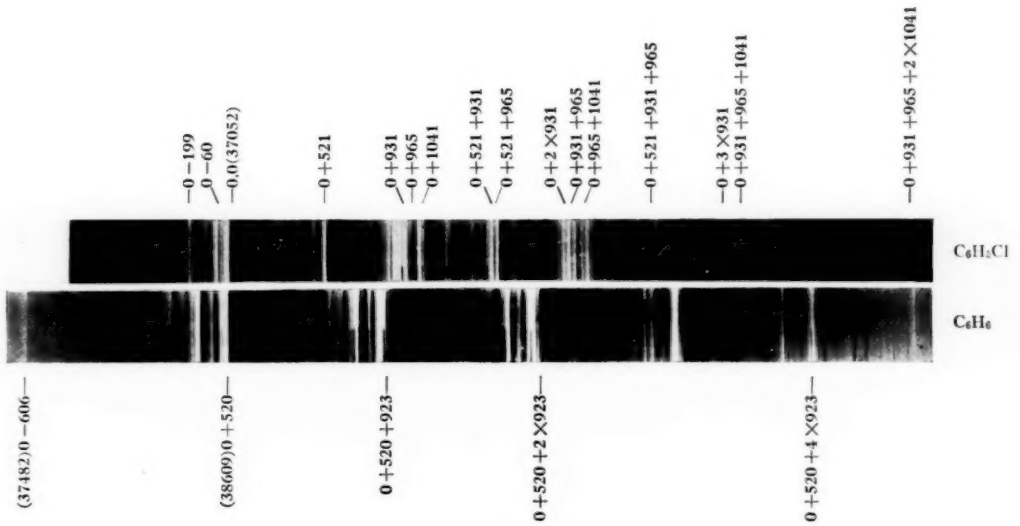

FIG. 1. Absorption spectra of monochlorobenzene and benzene.

varied between 1 and 5 hours. Most spectra were taken with II 0 plates. An iron arc furnished the comparison spectrum. The edges of the sharper bands could be measured to 0.2–0.4 cm^{-1}. The more diffuse bands could be measured only with an accuracy of several wave numbers.

RESULTS

Figure 1 represents the main part of the absorption spectrum of C_6H_5Cl taken at $-7°C$, which corresponds to a pressure of 1.7 mm. For comparison the benzene spectrum is reproduced below it as it appears at 25 mm pressure. Both spectra have been photographed with the same instrument using the 75 cm tube and are enlarged equally. The 0,0 band of monochlorobenzene and the $0\rightarrow 1$ band in benzene of the ϵ_g^+ vibration which makes the forbidden transition in C_6H_6 allowed have been arranged above one another for a more convenient discussion of the spectra.

At higher pressures of C_6H_5Cl there appear bands on the red side of the spectrum. They originate from vibrational levels in the ground state. Figure 2 shows this part of the spectrum. It was obtained with the side arm at 73°C corresponding to about 100 mm Hg while the main tube was at 96°C.

Wave-lengths and wave numbers of all measured bands are collected in Table I. The bands are degraded to the red. The intensities represent visual rough estimates from the plates and enlargements. The letters in the column "Intensity" mean *ew* = extremely weak, *vw* = very weak, *w* = weak, *m–w* = medium to weak, *m* = medium, *st* = strong, *vst* = very strong, *d* = diffuse. This classification could not very well be applied to the whole spectrum appearing at a single pressure because bands from higher vibrational levels in the ground state may not be present at all, and on the other hand, when they begin to come into appearance, the absorption in the short wave-length part is so strong that practically all bands have overlapped each other. Therefore a particular intensity classification refers to the particular experimental conditions which are stated in the last column under "Remarks." The column "Assignment" will be discussed in the next section, but it may be

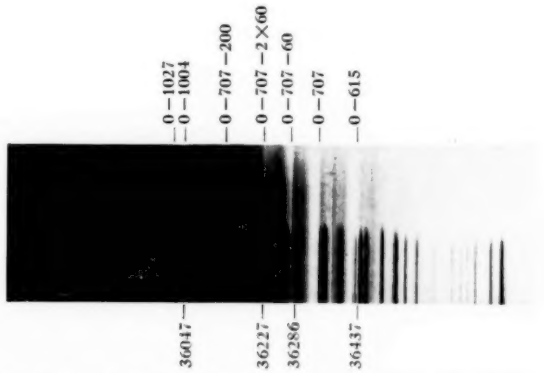

FIG. 2. Bands of C_6H_5Cl originating from vibrational levels in the ground state.

TABLE I. *Bands of* C_6H_5Cl.

Wave-Lengths	Wave Numbers	Intensity	Assignment	Remarks
2833.3	35,284	*vw d*		Intensities were estimated from plate taken with reservoir at +85°C and vapor at 110°C with 15 cm absorption path.
2827.9	35,351	*w d*		
2821.46	35,432.2	*m*	0−615−1004	
2795.7	35,759	*w d*		
2793.65	35,785.0	*w d*	0−1004−*60*−*200*	
2791.8	35,808	*w d*		
2789.47	35,838.6	*w*		
2788.8	35,847	*w*	0−1004−*200*	
2787.7	35,861	*w d*	0−1004−3×*60*?, 0−1191	
2785.5	35,890	*w d*		
2784.86	35,897.9	*m*		
2782.6	35,927	*m*	0−1004−2×*60*	
2780.9	35,949	*m*	0−707−2×*200*	
2780.1	35,959	*w*		Intensities were estimated from plate taken with reservoir at 29°C and 75 cm absorption path.
2777.93	35,987.4	*w*	0−1004−*60*	
2776.25	36,009 2	*vw*		
2775.0	36,025	*w d*	0−1027	
2774.0	36,038	*w d*		
2773.30	36,047.5	*w*	0−1004	
2770.53	36,083.5	*vw*		
2769.54	36,096.5	*vw*		
2765.77	36,145.7	*w*	0−707−*200*	
2763.6	36,174	*vw d*	0−615−*200*−*60*	
2762.5	36,189	*vw d*		
2761.7	36,199	*vw d*	0−615−4×*60*?	
2759.5	36,227	*w d*	0−707−2×*60*	
2758.92	36,235.3	*w*	0−615−*200*	
2758.19	36,245.0	*vw*		
2757.34	36,256.2	*vw d*	0−615−3×*60*	
2755.9	36,275	*w d*		
2755.08	36,286.0	*m*	0−707−*60*	
2753.3	36,309	*w d*	0−707−*38*?	
2752.67	36,317.7	*w*	0−615−2×*60*	
2751.16	36,337.8	*w*		
2750.57	36,345.4	*st*	0−706.6	
2749.4	36,361	*vw d*		
2748.7	36,370	*w d*		
2748.16	36,377.2	*m*	0−615−*60*	
2747.1	36,391	*w d*		
2746.6	36,398	*w d*	0−615−*38*	
2744.26	36,428.9	*st*	?	
2743.66	36,436.9	*st*	0−615; (0−418−*200*)	
2742.15	36,456.9	*w d*		
2741.6	36,464	*w d*		
2738.15	36,510.2	*m−w*	0−418−2×*60*	
2733.56	36,571.5	*m*	0−418−*60*	
2732.0	36,592	*w d*	0−2×*200*−*60*	
2729.6	36,624	*vw d*		
2728.93	36,633.6	*st*	0−418	
2727.50	36,652.8	*vw*	0−2×*200*	Intensities of all bands with larger wave numbers than 36,652.8 were estimated from plate taken with reservoir at −7°C with 75 cm absorption path. Bands from 36,652.8 till 37,054.9 belong to first strong group.
2726.42	36,667.3	*vw*		
2725.1	36,685	*vw*		
2721.89	36,728.3	*vw d*	0−*200*−2×*60*	
2719.60	36,759.2	*w d*	0−293	
2717.33	36,790.0	*w*	0−*200*−*60*	
2716.22	36,805.0	*vw*		
2715.6	36,813	*vw d*		
2714.01	36,835.0	*vw*		
2713.31	36,844.5	*m−w*	?	
2712.82	36,851.1	*w*		
2712.59	36,854.3	*m*	0−*200*	
2711.8	36,865	*vw d*		
2711.2	36,873	*vw*	0−3×*60*	
2709.48	36,896.6	*vw*		
2708.84	36,905.3	*w*		
2707.67	36,921.2	*w*		
2706.80	36,933.1	*m−w*	0−2×*60*	
2705.7	36,948	*vw*		
2703.7	36,975	*w*		
2703.14	36,983.1	*w*	?	
2702.44	36,992.8	*st*	0−*60*	
2702.32	36,994.1	*w*		
2700.91	37,013.6	*m−w*	0−*38*	
2699.24	37,036.5	*w*		
2698.68	37,044.2	*st*	?	
2698.11	37,052.0	*vst*	0,0	
2697.90	37,054.9	*m*		
2689.7	37,168	*vw d*		Bands from 37,168 till 37,576.8 constitute second strong group.
2689.0	37,178	*vw d*		
2687.9	37,192	*ew d*	0+140	
2686.18	37,216.6	*ew*	0+521−295−*60*	
2684.55	37,239.1	*vw*		
2683.58	37,252.6	*ew*	0+521−2×*60*−*200*; 0+201	
2682.33	37,270.0	*vw*		
2681.77	37,277.7	*w*	0+521−295; 0+931−707	
2680.24	37,299.0	*w*		
2679.47	37,309.7	*w*	0+521−*60*−*200*; 0+966−707	
2679.13	37,314.6	*w*		
2678.64	37,321.3	*w*		
2678.4	37,325	*w*		
2677.9	37,332	*m−w*		
2677.36	37,339.2	*m−w*	?	
2676.79	37,347.1	*m−w*	0+295	
2675.06	37,371.3	*m−w*	0+521−*200*	
2674.62	37,377.4	*w*		
2674.10	37,384.7	*vw d*		
2673.2	37,397	*ew d*	0+521−3×*60*	
2671.9	37,415	*ew d*		
2671.27	37,424.2	*m*	0+372	
2670.80	37,430.9	*m−w*		
2669.4	37,451	*vw d*	0+521−2×*60*	
2668.95	37,456.8	*w*		
2665.35	37,507.4	*m−w*	?	
2665.07	37,511.3	*m−w*	0+521−*60*	
2664.70	37,516.5	*m−w*		
2663.17	37,538.1	*vw d*	0+521−*38*	
2661.01	37,568.6	*m*	?	
2660.73	37,572.5	*st*	0+520.5	
2660.43	37,576.8	*m*	0+524.8	
2658.78	37,600.1	*ew d*	0+670−2×*60*	Bands from 37,600 till 38,117.9 constitute third strong group.
2657.59	37,616.9	*ew d*		
2656.5	37,632	*ew d*		
2654.5	37,661	*ew d*	0+670−*60*	
2652.32	37,691.6	*w*	0+931−295	
2650.16	37,722.3	*w*	0+670; 0+966−295; 0+931−*60*−*200*	
2649.42	37,732.9	*vw*		
2648.55	37,745.3	*vw*		
2647.90	37,754.5	*vw*	0+966−*60*−*200*	
2646.42	37,775.5	*vw*		
2645.86	37,783.6	*w*	0+931−*200*; 0+732	
2644.36	37,805.0	*w*	0+931−3×*60*; 0+1043−295	
2643.56	37,816.5	*m−w*	0+966−*200*	
2642.85	37,826.7	*vw*	0+1066−295	
2642.21	37,835.9	*vw*	0+966−3×*60*; 0+1043−*60*−*200*	
2640.00	37,867.5	*m−w*	0+521+295; 0+931−2×*60*	
2637.98	37,896.5	*w*	0+966−2×*60*; 0+1043−*200*	
2636.65	37,915.8	*w*	0+1066−*200*	
2636.05	37,924.3	*m*	0+931−*60*	
2634.57	37,945.6	*m*	?	
2633.83	37,956.3	*st*	0+372+521; 0+966−*60*	
2632.59	37,974.1	*w*	?	
2631.94	37,983.5	*vst*	0+931.5	
2630.20	38,008.6	*m−w*	?	
2629.55	38,018.0	*vst*	0+966	
2628.53	38,032.8	*w*	0+1043−*60*	
2627.42	38,048.8	*vw*		
2624.23	38,095.1	*st*	0+1043; 0+2×521	
2622.73	38,117.9	*m*	0+1066	
2619.55	38,163.1	*w*		Group character becomes less pronounced beyond 38,118. One may consider bands from 38,163 till 38,640 as belonging to a fourth strong group.
2618.1	38,184	*w*	0+931+200?	
2617.5	38,193	*w*		
2616.9	38,201	*w*		
2613.91	38,245.5	*m*	0+1190; 0+521+670	
2613.4	38,253	*w*		
2612.8	38,261	*m−w*		
2612.2	38,271	*w*		
2611.6	38,279	*w*	0+295+931	
2610.0	38,303	*w*	0+372+931−*60*; 0+521+931−*200*; 0+295+966?	
2607.8	38,335	*w*	38,395−*60*; 0+521+966−*200*	
2606.0	38,361	*w*	0+372+931	
2604.2	38,388	*m*	0+295+1043; 0+521+931−2×*60*	
2603.7	38,395	*w*	0+372+966; 0+2×670	
2603.21	38,402.7	*w*		
2602.39	38,414.8	*w*	0+295+1066; 0+372+1043−*60*	
2600.13	38,448.2	*w*	0+521+931−*60*	
2598.31	38,475.1	*w*	0+372+1043; 0+521+966−*60*	
2596.8	38,497	*m−w*	0+372+1066	
2596.37	38,503.8	*st*	0+521+931	
2596.1	38,508	*w*		
2594.27	38,535.0	*st*	0+521+966	
2593.93	38,540.1	*w*		
2589.20	38,610.4	*w*	0+521+1043	
2587.8	38,631	*w*	?	
2587.55	38,635.0	*m−w*	0+521+1066	
2587.27	38,639.3	*w*		

TABLE I—*Continued.*

Wave-Lengths	Wave Numbers	Intensity	Assignment	Remarks
2585.5	38,666	*vw*		Bands from 38,666 till 39,080 may be considered as a fifth strong group.
2584.3	38,684	*vw d*	0+670+966	
2580.1	38,747	*w d*	0+931+966−*200*	
2575.0	38,823	*vw d*	0+931+1043−*200*; 0+931+966−2×*60*	
2573.0	38,854	*w d*	0+2×931−*60*	
2570.8	38,887	*w*	0+931+966−*60*	
2569.1	38,913	*m*	0+2×931	
2566.7	38,948	*st*	0+931+966	
2564.6	38,981	*m*	0+2×966	
2561.8	39,024	*m–w*	0+931+1043	
2560.3	39,046	*m*	0+931+1066	
2559.59	39,057.0	*m*	0+966+1043; 0+3×670?	
2558.09	39,079.9	*m–w*	0+966+1066	
2555.9	39,114	*vw*	0+1190+931−*60*	No group distinctions will be made beyond 39,080.
2555.1	39,125	*vw*	0+2×1066−*60*	
2553.1	39,156	*vw*	0+1043+1066	
2552.5	39,165	*w*		
2551.9	39,174	*m–w*	0+1190+931	
2551.3	39,184	*m–w*	0+2×1066	
2550.7	39,193	*w d*		
2550.0	39,204	*w d*		
(2549.5)	(39,210)	*w d*	0+295+2×931; 0+1190+966	Bands in parentheses are present but are too diffuse to measure.
2648.84	39,221.8	*m–w d*		
2547.5	39,242	*w d*	0+295+931+966	
2546.5	39,258	*vw d*		
(2545.8)	(39,268)	*w d*	0+295+2×966; 0+521+931+966−*200*	
2544.3	39,292	*w d*	0+372+2×931	
2542.4	39,321	*vw d*	0+295+931+1043	
(2541.2)	(39,340)	*w d*	0+295+931+1066; 0+295+966+1043	
2539.6	39,364	*vw d*	0+295+966+1066	
2535.2	39,433	*w*	0+521+2×931; 0+2×1190	
2533.6	39,458	*w*		
2533.04	39,466.4	*m*	0+372+966+1066; 0+521+931+966	
2531.1	39,497	*m–w d*	0+521+2×966	
2528.67	39,534.6	*m–w*	0+521+931+1043?	
2526.5	39,568	*w d*	0+521+931+1066	
2524.5	39,600	*w d*	0+521+966+1043	
2522.9	39,625	*vw d*		
(2521.1)	(39,653)	*vw d*	0+521+2×1043	
2519.6	39,677	*ew d*	0+521+1043+1066; 0+2×931+966−*200*	
2516.5	39,725	*ew d*	0+4×670?	
2509.5	39,836	*ew d*	0+3×931	
2507.0	39,876	*m–w d*	0+2×931+966	
2504.9	39,910	*m–w d*	0+931+2×966	
2502.7	39,945	*vw d*	0+3×966	
2500.1	39,987	*m–w d*	0+931+966+1043	
2498.5	40,012	*vw d*	0+931+966+1066	
2498.0	40,020	*m–w d*	0+2×966+1043	
2491.3	40,127	*m d*	0+521+2562; 0+966+1043+1066	
2490.8	40,135	*m*		
2487.5	40,190	*vw d*	0+521+2×931+966−*200*; 0+3×1066−*60*	
2483.8	40,248	*vw d*	0+3×1066	
2478.8	40,330	*vw d*		
2477.0	40,359	*vw d*	0+521+3×931	
2475.0	40,392	*w d*	0+521+2×931+966	
2473.0	40,425	*w d*	0+521+931+2×966	
2471.1	40,455	*w*	0+521+3×966	
2468.8	40,494	*vw d*	0+521+2×931+1066	
2466.9	40,525	*w d*	0+521+931+966+1043	
2465.0	40,555	*ew d*		
2450.2	40,801	*w d*	0+3×931+966	
2434.5	41,063	*w d*	0+2×966+2×1043	
2432.5	41,098	*vw d*		
2426.7	41,196	*ew d*		
2416.1	41,376	*ew d*		

mentioned here that all numbers in italics represent differences between vibrational frequencies in the upper and lower states to distinguish them from the frequency values.

Discussion and Analysis of the Spectrum

If we substitute a Cl atom for an H atom in benzene the symmetry D_{6h} is reduced to C_{2v}. The symmetry elements of the C_{2v} group are a twofold axis C_2^z in the molecular plane passing through the chlorine atom, a plane of reflection through this axis and perpendicular to the molecular plane (perpendicular to the y axis), and the molecular plane σ_h. Only four different kinds of electronic levels (and also of vibrations) are possible for group C_{2v}. The lower state of the discussed absorption spectrum is, as in benzene, totally symmetrical, i.e., A_1 in the usual notation. The upper state of the respective benzene system is a B_{2u}, which for the D_{6h} symmetry is antisymmetrical to a twofold axis corresponding to the above defined z axis. It is furthermore antisymmetrical to a plane of reflection which corresponds to the above plane through the z axis, but symmetrical to the molecular plane. Electronic states in the C_{2v} group antisymmetrical to the twofold axis and symmetrical to the molecular plane are denoted by B_1 (Table II). Hence, from analogy to the spectrum of benzene, the spectrum under discussion represents a transition $A_1 \rightarrow B_1$. It is allowed in group C_{2v} and the transition moment lies in the molecular plane in a direction (y axis) perpendicular to the C−Cl bond. (The transition moment has the transformation properties of a translation, denoted as T in Table II.)

The components of the electric moment M in the two other directions z and x do not occur in this transition unless they are made allowed by the excitation of a proper vibration. In Table II, which refers to electronic and vibrational levels as well, the essential symmetry elements are given. The + and − signs indicate symmetrical and antisymmetrical behavior when symmetry operations with respect to these elements are performed. It can readily be seen from this table that the product $A_1B_1M_z = A_1B_1A_1$ contains B_1 and that the product $A_1B_1M_x = A_1B_1B_2$ contains A_2. Hence excitation of vibrations of type[9] β_1 and

[9] If the symbol indicates the symmetry character of a vibrational rather than an electronic level, Greek letters will be used.

TABLE II. *Essential symmetry elements in group C_{2v}.*

SYMMETRY	C_2^z	σ_h	
A_1	+	+	T_z
A_2	+	−	
B_1	−	+	T_y
B_2	−	−	T_x

α_2 may give rise to weak bands otherwise not included in the allowed transition $A_1 \rightarrow B_1$. We shall therefore expect a spectrum with the characteristics of an allowed transition and possibly much weaker bands resulting from the forbidden transition of the z and x components of the electric moment, made allowed by vibrations of type β_1 and α_2.

The group C_{2v} has no degenerate representations, therefore all degenerate benzene vibrations will split. Most of them furnish one totally and one nontotally symmetrical vibration each. The total number of totally symmetrical vibrations becomes eleven as compared with two in benzene. While in benzene (Fig. 1) progressions of the one totally symmetric carbon vibration (923 cm^{-1} in the upper state) give the spectrum its striking group character, we shall expect in the spectrum of C_6H_5Cl progressions of several totally symmetrical vibrations. Moreover, the structure should become more complicated towards the ultraviolet because of the increasing number of possible combinations of totally symmetrical vibrations, so that the group character will become less distinct towards shorter wave-lengths. From polarization measurements[10] in the Raman effect of monochlorobenzene one finds four totally symmetrical vibrations in the 1000 cm^{-1} region. In all of them motions of the carbon atoms are involved. If one takes degrees of freedom of the carbon atoms alone three vibrations are expected in this region, to which the wave numbers 1001, 1024 and 1084 may be attributed. The fourth one of 1134 cm^{-1} probably contains more contributions from the hydrogen atoms.

If we now look at the ultraviolet spectrum of C_6H_5Cl (Fig. 1) with the preceding remarks in mind we see immediately that the strongest band at 37,052 cm^{-1} must be the 0,0 band in agreement with the assumption of an allowed transition. The bands at 37,984, 38,018, 38,095 and 38,118 cm^{-1} can be interpreted as transitions to vibrations in the upper state which correspond to the just mentioned vibrations in the lower state. The vibrational wave numbers in the upper level are 931, 966, 1043 and 1066. The bands concerning the last two values will be discussed later again in some other connection. The strong violet edges have been used throughout for the evaluation of frequencies. As expected all possible combinations of the mentioned totally symmetrical vibrations occur, some of which are indicated in Fig. 1 and others are found in Table I under "Assignment." Evidence for the occurrence of two of these vibrations in the ground state was found on plates taken at the highest pressures. It is the bands 36,047 and 36,025 which yield the vibrational frequencies 1004 and 1027 cm^{-1} (Fig. 2). The values 1001 and 1024 cm^{-1} have been found in the Raman effect of the gas.[11]

A band at 38,245 cm^{-1} of medium intensity may also belong to a totally symmetrical vibration in the upper state. Its value would be 1190 cm^{-1}. It may represent a carbon vibration, but another possibility will be mentioned later. The band occurs strongly in the solid. Superimposed on the 1190 appears the 931 vibration. The superposition of other totally symmetric vibrations in the 1000 region leads to transitions which fall on top of other bands.

Although the spectrum of monochlorobenzene belongs to an allowed transition its total absorption strength is not much larger than that of the corresponding benzene absorption. From measurements in solution[5] an intensification of about two has been obtained,[12] while Asagoe and Ikemoto[4] estimate about nine for this ratio. From our measurements we would also estimate the absorption strength of C_6H_5Cl to be at least twice as much as that of benzene. This small factor is not surprising since the substitution means a very slight perturbation of the ring. Therefore one may expect that the mechanism which brought the benzene spectrum into appearance will remain relatively important. The ϵ_g + 606 cm^{-1} vibration in benzene which was mainly responsible for making that transition allowed, splits in monochlorobenzene into an α_1 and a β_1 vibration.

[10] L. Simons, Soc. Sci. Fennica, Com. Phys.-Math. **6**, No. 13 (1932).

[11] H. Sponer and J. S. Kirby-Smith, J. Chem. Phys. **9**, 667 (1941).

[12] A. L. Sklar, J. Chem. Phys. **7**, 984 (1939).

Excitation of the latter can produce the otherwise forbidden transition in the z direction, i.e., parallel to the C−Cl bond and corresponds to the forbidden transition in benzene. Consequently we should expect 0→1 and 1→0 transitions of this vibration. From polarization measurements in the Raman effect[10] one finds a totally symmetrical vibration at 416 cm^{-1} and a nontotally symmetrical vibration at 608 cm^{-1} which are reasonably assigned to this ϵ_g^+ vibration.[13] Now a striking feature of the monochlorobenzene spectrum is the appearance of the second group whose strongest band on the violet side lies 520.5 to 524.8 cm^{-1} apart from the 0,0 band. The two figures correspond to the violet edges of the two main components of the band, the violet component being the much stronger of the two. The components represent very likely band heads. From the band heads toward the red extends a narrow fine structure which is not present in the other bands discussed so far. It is suggestive to interpret the 521 band as the 0→1 transition of the just mentioned 608 vibration. This interpretation is confirmed by the appearance of a band displaced by 615 cm^{-1} to the red from the 0,0 band.[14] Superimposed on these 0→1 and 1→0 transitions appear, of course, progressions of the already mentioned totally symmetrical vibrations of the 1000 cm^{-1} region.

It is noteworthy that 1043 is within the limits of accuracy equal to 2×521 and, of course, 521+1043 is numerically very nearly 3×521. The twofold excitation of the non-totally symmetrical vibration of 521 could occur because this yields a totally symmetrical eigenfunction. But the band should be very weak on account of the Franck-Condon principle since non-totally symmetrical vibrations have their minima above one another.[15] Actually the 1043 is a strong band. It is considerably weaker than the 0+931 and the 0+966, it is also weaker than the 0+521 but it seems definitely too strong for a 0+2×521. If, however, there would be an accidental degeneracy between 2×521 and the frequency giving the band 0+1066, then a gain in intensity of the weak 0→2 transition would be possible. But this would require that the frequency is really not 521 but a little higher. Now if we use the weaker violet head we obtain in fact 525, and in a band shifted from this one by 60 cm^{-1} to the red, the violet head is actually a little stronger, but the bands at 38,504 (0,0+521+931) and at 38,535 (0,0+521+966) show very distinctly the same intensity relation as the 0+521 band. The explanation of the 1043 and 1066 bands by accidental degeneracy has the advantage that the 931, 966, 1043 and 1066 bands would involve only three carbon vibrations which can be considered as upper state values of the Raman frequencies of 1001, 1024 and 1084 in the ground state. One can favor this explanation[16] but, of course, a definite conclusion cannot be drawn. In the following we will use, for the sake of consistency, the value of 521 resulting from the stronger violet head of the 37,572 band and leave open the final decision about its interpretation.

Asagoe and Ikemoto have come to the same conclusions as we have regarding the bands 0+931 and 0+966 and the totally symmetrical progressions superimposed on them. But they have interpreted the 521/525 vibration as being totally symmetric (they used 525 for the frequency) and hence concluded that the 1043 is 2×525 and the band 525+1043 is 3×525. They correlate the 525 with the Raman frequency of 611. But from polarization measurements[10] one can conclude that this frequency belongs to a nontotally symmetrical vibration, so that their interpretation cannot be correct.

The other vibration related to the mode giving the frequency 606 cm^{-1} in benzene is the totally symmetrical 416 cm^{-1} vibration. It gives rise to a 1→0 transition (band at 36,634 cm^{-1}) which appears with very low intensity in Fig. 1. None of the totally symmetrical vibrations in the 1000 cm^{-1} region was found superimposed on it in the ground state. The respective 0→1 transition leading to a corresponding vibration in the upper state does not stand out clearly enough for an

[13] K. W. F. Kohlrausch, Physik. Zeits. **37**, 58 (1936).

[14] The value of 615 cm^{-1} agrees better with the Raman frequency of 611 found in the liquid than with the 608 found in the gas. We are unable to account for the discrepancy.

[15] The corresponding band seems to be present very weakly in monobrombenzene. One of us (H. Sponer) acknowledges private communication from Dr. I. Walerstein, Purdue University, of results obtained with C_6H_5Br.

[16] The spectrum of C_6H_5Br does not indicate an accidental degeneracy (results by Dr. I. Walerstein, and K. Asagoe and Y. Ikemoto, Proc. Phys. Math. Soc. Japan **22**, 685 (1940)) and clearly shows only three totally symmetrical carbon vibrations occurring in the corresponding region; this is in favor of the above interpretation.

unambiguous identification. One of the relatively strong bands at 37,347 (0,0+295) and 37,424/31 (0,0+372) for which no other obvious explanation can be offered, may be assigned to this transition. Superimposed on both bands appear totally symmetrical vibrations of the 1000 region. No bands corresponding to the twofold excitations 2×295 and 2×372 have been found. Bands due to transitions to 295+521 and 372+521 in the upper state fall, if present, very closely on top of other bands of greater intensity.

The behavior of another totally symmetrical vibration, the C−Cl vibration, is even more peculiar. Its 1→0 transition, 706.6 cm^{-1} apart from the 0,0 band, appears with an intensity comparable to that of the nontotally symmetrical 615 vibration, while the 0→1 transition appears at best rather faintly if one interprets the band at 37,722 as this transition. It yields 670 cm^{-1} in the upper state for the chlorine vibration. The same assignment was proposed by Asagoe and Ikemoto. It is not quite impossible that the band at 37,784 cm^{-1} corresponds to this vibration, although it seems that another interpretation (to be discussed later) is more probable. There is no other stronger band in this spectral region which can be taken into consideration. In order to find an explanation for the described unusual behavior of the C−Cl (and also of the 416) vibration we remember that there are two possible reasons for the appearance of these totally symmetrical vibrations:[17] First if the equilibrium positions in the lower and upper states are a little different for these vibrations then both the 0→1 and 1→0 transitions will occur according to the Franck-Condon principle; second the electronic transition moment may depend upon the normal coordinate of this vibration. The electronic matrix element of the dipole moment $\mathfrak{M}$ is namely independent of the nuclear positions only in first approximation. For small displacements it can be represented by a power series in the displacements

$$\mathfrak{M}=\mathfrak{M}_0+\sum_i\mathfrak{M}_i\xi_i+\sum_{ik}\mathfrak{M}_{ik}\xi_i\xi_k+\cdots,$$

where the ξ_i stand for normal coordinates giving the magnitude of the displacements in the ith normal vibration and where $\mathfrak{M}_0$, $\mathfrak{M}_i$, $\cdots$ are coefficients. We designate now the wave functions of the four vibrational states concerned (0→1 and 1→0 transition) with ψ'_0, ψ''_0, ψ'_1, ψ''_1, where the primes distinguish the electronic states in the usual way and the subscripts 0 and 1 indicate the quantum numbers of the C−Cl vibration. Using the first two terms in the expansion we obtain for the 1→0 transition the contributions $\int\psi'_0\psi''_1\mathfrak{M}_0d\xi+\int\psi'_0\psi''_1\mathfrak{M}_1\xi d\xi$ to the transition matrix and for the 0→1 transition the contributions $\int\psi''_0\psi'_1\mathfrak{M}_0d\xi+\int\psi''_0\psi'_1\mathfrak{M}_1\xi d\xi$. The magnitude of the first integral in each of the last two expressions is given by the shift in equilibrium position during the transition (Franck-Condon principle) while the second integral represents the change $\mathfrak{M}_1\xi$ of the transition moment. If we assume that the two effects reinforce each other in the 1→0 transition and work against each other in the 0→1 transition, then the relatively high intensity of the first and low intensity of the second can be understood. As can be seen from Fig. 3 the integrals $\int\psi'_0\psi''_1d\xi$ and $\int\psi''_0\psi'_1d\xi$ have opposite signs because the integrand $\psi'_0\psi''_1$ takes its maximal value in a region where ψ''_1 is negative while $\psi''_0\psi'_1$ reaches a maximum where ψ'_1 is positive. The integrals $\int\psi'_0\psi''_1\xi d\xi$ and $\int\psi''_0\psi'_1\xi d\xi$, on the other hand, have probably both negative signs as can be found from Fig. 3 in a similar way. They would be negative for equal equilibrium positions in both states. This discussion shows that it is conceivable that there is an adding effect of the matrix elements for a 1→0 transition and a canceling effect for a 0→1 transition. The described argumentation might also hold for the

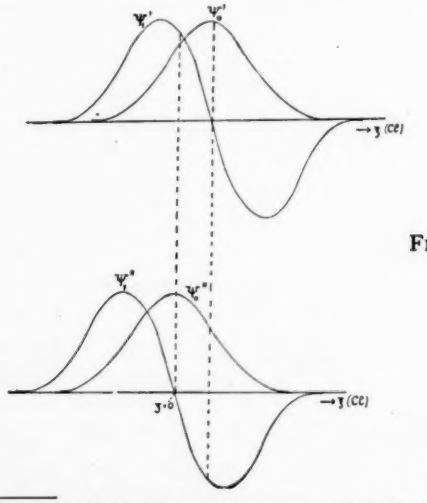

FIG. 3.

[17] See for this discussion H. Sponer and E. Teller, Rev. Mod. Phys. **13**, 97 and 119 (1941).

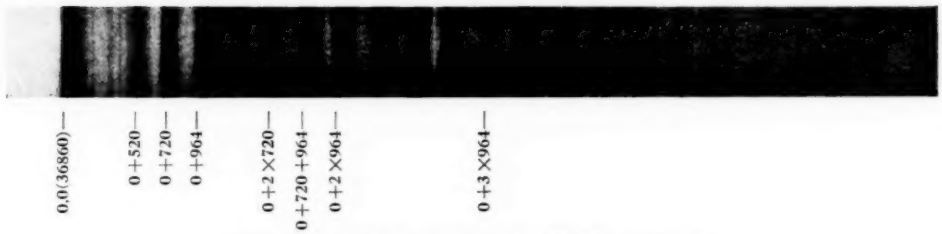

FIG. 4. Absorption spectrum of C_6H_5Cl at $-259°C$
(Taken from A. Kronenberger, Zeits. f. Physik **63**, 512 (1930).)

416 cm^{-1} vibration although the two vibrations show only a qualitative resemblance.

It is interesting to discuss in this connection the spectrum of solid monochlorobenzene[6] taken at $-259°C$. It is represented in Fig. 4 which has been rephotographed from Kronenberger's paper with the addition of part of the analysis. It shows a very strong 0,0 band which is shifted by 192 cm^{-1} to the red as compared to the spectrum of the vapor. Contrary to the latter the C−Cl vibration appears strongly with a value of 720 cm^{-1} in the upper state. This is higher than the ground state frequency and much higher than the value of 670 cm^{-1} reported here. If, however, the band at 37,784 cm^{-1} should be taken instead of 37,722, then the chlorine frequency in the excited state would have the still larger value of 732 cm^{-1}. But we believe the value of 670 cm^{-1} to be more probable. If that is so, the larger value in the solid may be due to forces from neighbors which may also cause a different shift in the equilibrium distance of the C−Cl vibration in the solid so that the cancellation of matrix elements may not take place in the outlined way. Another difference between the spectra in the two phases is that the C−Cl vibration in the solid forms evidently a long fairly strong progression, seven members of which (some are overlapped) can be followed whereas in the gas, if there is a weak 670 progression at all, all members except a possible fourth, fall on top of other bands.

It should be mentioned here that the band 0+1190 (at 38,245 cm^{-1}) which, as we discussed before, may be due to the single excitation of a totally symmetrical vibration, can also be explained as a superposition of the chlorine vibration of 670 on the 521 vibration. This interpretation was chosen by Asagoe and Ikemoto. Although the numerical fit is excellent it seems surprising that the band 0+521+670 should be many times stronger than the 0+670+966, and the 0+670+931 could not be identified with certainty at all. Moreover, the strong 0+1200 band in the solid cannot be explained in the same way as 0+720+520. Therefore, the previous interpretation of the 38,245 band seems more probable but we hesitate to consider it as conclusive enough.

The totally symmetrical vibrations in the 1000 region show well up in the spectrum of the solid, but they have different values from the gas, probably caused by crystal forces. Frequencies of 960, 1030 and 1200 have been identified. All main progressions involve the 960 cm^{-1} frequency which forms a strong progression with six members and appears in progressions on top of the 520, 720, 1030 and 1200 frequencies. There are also the other totally symmetrical progressions and combinations between the different totally symmetrical vibrations. All this causes considerable overlapping. Consequently for some bands two or three interpretations may be given. Besides this there is probably, as in benzene, a splitting of the bands present due to superposition of crystal frequencies.[2] No definite interpretations can be given for the weaker bands but it is clear that they cannot originate from vibrational levels at such a low temperature as $-259°C$. In agreement with this the 0,0 band is the first band of the spectrum and is not accompanied by weaker bands on the red side as is the case in the spectrum of the vapor.

Turning back to the spectrum of the gas we notice a fairly strong band at 40,127/35 towards the violet end of the spectrum. It seems to have the characteristic structure of a 521 band and hence must be a transition superimposed on this vibration. The intensity suggests that this transition involves a single excitation, which leads to a frequency value of 2562 cm^{-1}. This reminds one

immediately of the identical frequency in the benzene spectrum which was attributed there to the totally symmetric hydrogen vibration. We would like to make the same suggestion for monochlorobenzene. From a group theoretical point of view the hydrogen vibration could also occur superimposed directly on the 0,0 transition but apparently it does not, at least not with measurable intensity. Considering that the electronic transition involves electrons from the carbons only, it is not too surprising that pure hydrogen vibrations are not excited with noticeable intensity without simultaneous excitation of carbon vibrations.

We shall now discuss bands which accompany the main bands on the red side. There is first a band of high intensity 58–62 cm^{-1} to the red apart from all stronger bands. We use here 60 cm^{-1} as an average value. These bands must be interpreted as 1→1 transitions of a low frequency. The lowest frequency observed in the Raman spectrum of monochlorobenzene is 200 cm^{-1} for the gas[11] and 196 for the liquid.[18] It represents a medium strong line. The next higher frequencies belong to the much weaker lines 270 and 295 cm^{-1}, both observed in the liquid. Although no actual proof can be given it seems preferable to correlate the drop of 60 cm^{-1} with the lowest frequency. This would make it understandable that bands have also been found displaced by 2×60 and 3×60 to the red from the main bands, even though they start in some cases from vibrational levels. The measurements of the temperature dependence of the 60 cm^{-1} bands by Asagoe and Ikemoto[4] are also in agreement with the proposed interpretation. If it is correct the 200 frequency would drop to 140 in the upper state. Now it is possible that this vibration is a β_1 which by its excitation could bring out the z component of the transition moment. Hence weak bands may be expected with a single excitation of this vibration. There is in fact a very weak band at 37,192 cm^{-1} which is numerically 0+140. But no corresponding bands are found superimposed on the other very strong bands 0+931 and 0+966. It is true that a relatively strong band occurs shifted by 198 cm^{-1} to the red from the 0,0 but it cannot be interpreted as a 1→0 transition because of discrepancies with the spectra of monobromobenzene[15,16] and monofluorobenzene.[19] It seems though, that in these latter spectra the 1→0 transitions of the corresponding lowest vibration appear faintly (it would be overlapped in C_6H_5Cl), but using the above interpretation no sign of the expected 0→1 transitions could be found. The same explanation which was used for the peculiar behavior of the C—Cl vibration cannot be applied here because the first term in the expansion vanishes for the here discussed nontotally symmetrical vibration.

No better results have been obtained by correlating the difference of 60 cm^{-1} with the next higher frequencies. We must therefore leave open the question of the definite assignment of the 60 difference until more experimental material of other monosubstituted benzenes is available. At present the high intensity of the transition 0–60 and the temperature dependence measurements point to a very low and quite likely to the lowest frequency.

It seems also not possible at the moment to give an unambiguous interpretation of the band at 36,854 cm^{-1} which is 199 cm^{-1} displaced to the red from the 0,0 band. It has just been mentioned that it cannot be a 1→0 transition because the corresponding bands in the other monohalogenated benzenes do not confirm this assumption. Therefore it must also be a 1→1 transition. Because of the relatively strong appearance of the band a fairly low vibration must be involved in the transition. This is also suggested by the occurrence of bands with distances 2×200 from the main bands, or of bands originating from various vibrational levels besides the one involved in the 200 difference (for example the band at 37,784 mentioned before in connection with the chlorine vibration can be represented by 0+931−200). It agrees also with the study of the temperature dependence of the 200 cm^{-1} bands.[4] A drop of 200 cm^{-1} is unusually large for a small vibration but we remember that in benzene a drop of 160 cm^{-1} was observed for the ϵ_u^+ carbon vibration of 400 cm^{-1} and it was pointed out[2] that for this particular vibration, whose restoring force is due to the π electrons, a large drop is really expected.

[18] A. Dadieu, A. Pongratz, and K. W. F. Kohlrausch, Monat. f. Chem. **61**, 426 (1932); J. W. Swaine and J. W. Murray, J. Chem. Phys. **1**, 512 (1933); R. Ananthakrishnan, Proc. Indian Acad. Sci. **3A**, 52 (1936).

[19] S. H. Wollman, unpublished results; H. Sponer and S. H. Wollman, Phys. Rev. **59**, 924A (1941).

Now the ϵ_u^+ in benzene splits into an α_2 and a β_2 vibration one of which (α_2) will remain numerically very little changed, whereas the β_2 will decrease in value.[20] It is plausible though not certain, that the 160 cm^{-1} difference in benzene corresponds to the 200 cm^{-1} in monochlorobenzene. Taking this for the moment to be the case, and assuming $\alpha_2''=400$, this would lead to $\alpha_2'=200$ cm^{-1}. The excitation of α_2 could make appear the forbidden x component of the transition moment. Now there is a very weak band 200 cm^{-1} toward the violet from the 0,0 band, but it fits already another interpretation. (See Table I). The same is true for the $1\rightarrow 0$ transition (36,653). A weak band at 38,184 can be represented by $0+931+200$; but no corresponding bands could be detected in combination with the other totally symmetrical vibrations in that region, so that the proposed interpretation cannot be supported in this way. On the other hand, it does not seem likely that the drop of 200 is associated with the 416 frequency which has been discussed before, because this interpretation is not borne out in the bromine compound.[15,16] It is unlikely from the intensities of the involved bands that it contains a vibration of much higher frequency than 400. Therefore, the correspondence with the 160 difference seems at present more plausible than other possibilities.

Another difference of 38 cm^{-1} may also be explained by a $1\rightarrow 1$ transition but because of too many possibilities no attempt at an interpretation will be given. Just to mention one possibility: it fits numerically well with $0+966-1004$, only the intensity seems too high for that.

It should be mentioned that a very weak band at 36,759 cm^{-1} is displaced by 293 cm^{-1} to the red from the 0,0 band. It may be that this corresponds to the Raman frequency of 295 cm^{-1}, the symmetry character of which is not known, but it is probably nontotally symmetric. In case the correlation is correct, the vibration must be a β_1 or an α_2, as follows from the theoretical introduction of this section. The difference of 295 occurs also in the 500 and 1000 groups.

Finally, a few words should be said about the structure of the individual bands. Since the band system consists of an "allowed" and a "forbidden" part, one should expect to find two kinds of bands which are distinguished by a different rotational structure. This seems indeed to be the case. All bands in which the 521 frequency is involved show a narrow peculiar fine structure, while most of the other bands look double-headed like the benzene bands. Some have perhaps a third head. In the bands with the narrow structure the transition moment lies parallel to the C—Cl bond and in the others it is perpendicular to it, but also in the molecular plane. The double heads may be interpreted, as in benzene, as R and Q branches. The structure looks a little different in different progressions. This may come from a coupling between vibration and rotation. In the 0,0 band the second head is the strongest with a difference of 3 cm^{-1} between the two. In this case there occurs an apparently third head 8 cm^{-1} to the red from the second which is of fairly strong intensity. The bands $0+931$ and $0+966$ have very much the same structure, only the first weak heads could not be measured. The structure is also repeated in the -60 and -200 progressions. There may be some doubt whether the third head 8 cm^{-1} apart from the main head belongs really to the rotational structure. It is conceivable that it represents a separate band which would then have to be interpreted as a $1\rightarrow 1$ transition, probably of a low vibration. The Raman frequencies 270 and 295 cm^{-1} could serve for this purpose. Because of the uncertainty of the correlation a question mark has been put after the corresponding bands under the brackets.

The narrow fine structure of the bands with the 521 frequency might also be expected in other parallel bands made allowed by the interaction of other β_1 vibrations, but no such bands could be identified with certainty from the appearance of the structure. It seems that only the "forbidden" transition of benzene is of importance in producing forbidden bands in monochlorobenzene.

Some vibrations seem to have interesting effects of anharmonicity. The effects are small, however, and a discussion is better postponed until more has been found out about the rotational structure.

It is a pleasure to acknowledge valuable and helpful discussions with Dr. E. Teller.

[20] This relationship was found for the deuterobenzenes, see A. Langseth and R. C. Lord, Det Kgl. Danske Videnskab. Selskab. Math.-fys. Meddelelser **16**, No. 6 (1938); the same is assumed here for analogy reasons.

Letters to the Editor

THIS section will accept reports of new work, provided these are terse and contain few figures, and especially few halftone cuts. The Editorial Board will not hold itself responsible for opinions expressed by the correspondents. Contributions to this section should not exceed 600 words in length and must reach the office of the Managing Editor not later than the 15th of the month preceding that of the issue in which the letter is to appear. No proof will be sent to the authors. The usual publication charge ($3.00 per page) will not be made and no reprints will be furnished free.

Molecular Configurations in Rotational Isomerism

SAN-ICHIRO MIZUSHIMA, YONEZO MORINO, AND MASATAMI TAKEDA
Chemical Institute, Faculty of Science, Tokyo Imperial University, Tokyo, Japan
July 24, 1941

EDGELL and Glockler[1] reported in this journal that the coexistence of the *trans* and the gauche (C_2) forms (see Fig. 1) can reasonably account for the number of depolarized lines observed for these substances. The view for the *trans* and the gauche forms of the rotational isomers was already suggested by us[2,3] based on our studies on the Raman spectra and dipole moments of molecules having axes of internal rotation. Recently we included *n*-pentane, *n*-hexane, *n*-heptane, and 2,2-dimethylbutane in this series of researches and observed their Raman spectra in the solid state (at liquid air temperature) as well as in the liquid state (at room temperature). For all the normal paraffins mentioned above the disappearance of many Raman lines was observed on solidification as in the case of *n*-butane[3] and ethylene dihalides[4] reported in our previous papers, while the spectrum of 2,2-dimethylbutane in the liquid state was found to be practically the same as that in the solid state. We have so far observed such spectral changes on solidification for the substances for which the rotational isomers of different spatial configuration exist, since owing to the crystal force one isomer or more become unstable in the solid state. (We could show definitely that only the *trans* isomer is stable for butane[3] and ethylene halides[4] in the solid state.) Hence it can be considered that for 2,2-dimethylbutane only one molecular form is realized in the liquid state as well as in the solid state. Furthermore, the spectrum of this substance can be explained as the normal frequencies of only one molecular form in contrast to the spectra of *n*-butane and ethylene dihalides in the liquid state which have too many lines to be accounted for from one spatial configuration. These results can be explained quite naturally from our view of the *trans* and the gauche forms but not from that of the *trans* and the *cis* forms (see Fig. 1) suggested by some investigators.[5] Figure 2 shows that the three stable configurations of 2,2-dimethylbutane conceivable from our view are equivalent to one another.

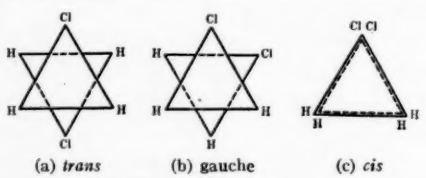

FIG. 1. The configurations of ClH_2C-CH_2Cl as viewed along the C−C axis.

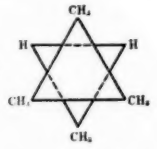

FIG. 2. 2,2-dimethylbutane.

[1] W. F. Edgell and G. Glockler, J. Chem. Phys. **9**, 375 (1941).
[2] Mizushima, Morino, and Kubo, Physik. Zeits. **38**, 459 (1937).
[3] Mizushima, Morino, and Nakamura, Sci. Pap. I.P.C.R. (Tokyo), **37**, 205 (1940).
[4] Mizushima, Morino, and co-workers, Sci. Pap. I.P.C.R. (Tokyo), **29**, 63 (1936); Proc. Ind. Acad. Sci. **8**, 315 (1938), (Raman jubilee volume).
[5] See for example the summary given by K. W. F. Kohlrausch, Ber. d. D. Chem. Ges. **71**, 171 (1938).

The Unsensitized Slow Combination of Hydrogen and Oxygen Between the Second and Third Explosion Limits in the Temperature Range 500–560°C

F. S. DAINTON
Laboratory of Physical Chemistry, Cambridge University, Cambridge, England
September 2, 1941

RECENT detailed measurements by Oldenberg and Sommers[1] of the rate of slow reaction of 2 : 1 mixtures of hydrogen and oxygen at total pressures greater than the second explosion limit and less than the third, have established that in a variety of vessels (Pyrex and quartz, either clean or coated with a visible layer of KCl) and over the temperature range 500° to 560°C, the Arrhenius law is obeyed. From this result the authors conclude that the reaction chains in this pressure-temperature region are unbranched. Three serious objections to this conclusion may be raised:

Firstly, the pressure *vs.* time curves which are obtained in this reaction show quite definitely that in the first stages the branching of the chains *is* occurring, and in fact is occurring more frequently than their termination. Thus for the typical experiment of which Fig. 1 of Oldenberg and Sommers[1] paper is a record, photographic enlargement has permitted the evaluation of $\log \Delta p$ and the rate, (expressed as $\delta(\Delta p)/\delta t$), at any instant. It is then found, that over the first four minutes of this reaction, not only the rate, but also the first derivative $(\delta^2(\Delta p)/\delta t^2)$ is increasing and that the plot of $\log \Delta p$ against time is linear. From these two facts alone, the conclusion that the net branching factor[2] ϕ is initially positive, is inescapable.[3]

Secondly, Semenoff's criterion that for a non-branched chain reaction the value of E in the expression

$$\text{rate} = R_0 \cdot e^{-E/RT}$$

is independent of T, whereas for a branched chain reaction the experimentally determined value of E shows an in-

crease with T, has been incorrectly applied and the authors' conclusions thereby invalidated. In all chain reactions the dilution of the reactants by the products as the reaction proceeds causes the net branching factor ϕ to vary continuously, and for a chain reaction in which ϕ is initially positive the maximum rate occurs when that combination of parameters is attained for which ϕ is zero, i.e., when the branching of the chains is just counterbalanced by their termination. In this region the chains are of constant finite length and the temperature coefficient of the rate is the product of the temperature coefficients of the initiation (θ) and the propagation processes. This would be expected to be constant and thus constancy of E found by the authors is accounted for. Their argument that this constancy of E indicates non-branched chains would only have been valid if it could have been shown that the initial value of ϕ was negative ($\delta^2(\Delta p)/\delta t^2$ being a decreasing function of time even at the beginning of the reaction) and hence that the steady rate had a value approximating to Semenoff's expression[4] that $w = N_0/(\beta - \delta)$, where $\beta \gg \delta$.

Thirdly, it is universally conceded, and Kowalski[5] has shown directly, that the reaction chains are branched in the ignition region enclosed by the first and second explosion limits. It is unlikely that the sharp change of mechanism from a branched chain to a completely non-branched chain which must be assumed if Oldenberg and Sommers' conclusion is accepted, will occur as the slight increase in reactant pressure is made in order to traverse the boundary from ignition to slow reaction. If this sharp change in mechanism did exist it would have been anticipated that corresponding discontinuities in the experimental observables would have been detected at the boundary. Actually in the recent, more refined, experimental analysis made by von Elbe and Lewis,[6] the change of reaction rate with pressure near the second limit has been shown to be quite smooth, whilst earlier measurements by Kowalski[5] have shown that in the same region the induction period is also a continuous function of the pressure.

[1] O. Oldenberg and H. S. Sommers, J. Chem. Phys. **9**, 432 (1941).
[2] The net branching factor ϕ has been defined as the difference between the coefficient of linear branching f (which is zero in unbranched reactions) and the coefficient of termination of the chains singly. The coefficient of termination is composite, embracing both wall and gas phase processes. ϕ has been widely used in this sense by Norrish *et al.*, see for instance S. G. Foord and R. G. W. Norrish, Proc. Roy. Soc. **152A**, 196 (1935).
[3] See N. Semenoff, *Chemical Kinetics and Chain Reactions* (Oxford, 1935), paragraphs 15 and 16, p. 57.
[4] N. Semenoff, reference 3, p. 49, Eq. (7).
[5] Kowalski, Physik. Zeits. d. Sowjetunion, **1**, 595 (1932); **4**, 723 (1933).
[6] G. von Elbe and B. Lewis, J. Chem. Phys. **9**, 194 (1941).

A Modified Theory of the Electrical Double Layer

ROBERT B. WHITNEY AND DAVID C. GRAHAME
Department of Chemistry, Amherst College, Amherst, Massachusetts
October 3, 1941

WE have succeeded in devising a method for checking the Stern equation[1] for the electrical double layer in a manner which does not require the evaluation of constants of uncertain magnitude. This is done by applying the equation to a system composed of mercury in contact with an aqueous solution containing capillary-active anions, at the potential for which the interfacial tension is a maximum. From purely thermodynamic considerations,[2] which have also been checked experimentally,[3] it is known that there is no charge on the mercury surface at the electrocapillary maximum, and that there is accordingly no difference of potential between the metallic phase and the first layer of ions at the interface. As a result, the potential of the first layer may be definitely ascertained, and the electrical and geometrical properties of the region between the metallic surface and the first layer of ions do not need to be known.

TABLE I.

Electrolyte	Conc. Moles/Liter	Γ_{max} Moles/sq. cm. $\times 10^{10}$	Potential Observed Volts	Potential Calculated Volts
KI	1.0	1.57	0.30	0.037
	0.1	0.94	0.20	0.068
	0.01	0.50	0.14	0.097
	0.001	0.14	0.07	0.098
KBr	1.0	1.10	0.13	0.029
NaCNS	1.0	1.45	0.20	0.035
	0.1	0.65	0.10	0.056

The adsorption of the electrolyte, Γ_{max}, may be calculated thermodynamically[2] from the interfacial tension of mercury in contact with solutions of the salts under consideration. Typical results of such calculations are shown in Table I. (Original data by Gouy.[4])

Column 4 gives the value of the potential of the first layer of ions relative to that of the interior of the solution, obtained by subtracting the potential observed at the electrocapillary maximum with a dilute solution of capillary-inactive electrolyte, from that observed with the salt in question. Column 5 is calculated from the Stern equation. The seriousness of the disagreement is especially evident when one considers that the charge is an exponential function of the potential.

The disagreement is fundamental to the qualitative picture upon which the Stern theory is based. In that theory a compact layer of positive and negative ions is assumed to lie adjacent to the metallic surface, and it is implicitly assumed that positive and negative ions are at the same electrical potential. The results presented above are incompatible with that concept. They prove, instead, that the layer of specifically adsorbed negative ions lies slightly closer to the mercury surface than the first layer of positive ions. Our picture of the double layer at a metal-solution interface will therefore be as follows: (1) Adjacent to the metallic surface there will usually be a partially filled layer of specifically adsorbed negative ions. These ions are not separated from the surface by water molecules. (2) A diffuse layer of positive and negative ions will extend from the metallic surface into the interior of the solution. This layer resembles that postulated by Gouy[5] and Chapman,[6] excepting that the maximum electrical potential of the layer will be that of the region of closest approach to the metallic surface of the type of ion predominating in the diffuse layer. (3) Because a hydrated cation is in most cases larger than an unhydrated anion, the latter will be

able to approach the surface more closely than the former. As a consequence the electrical potential of a layer of specifically adsorbed negative ions will generally be different from the potential of those hydrated positive ions lying closest to the metallic surface. There is evidence that no large part of the cations is dehydrated as a result of the forces acting upon them in the double layer.

This picture of the double layer can be put into quantitative form by the application of methods analogous to those used by Stern. The results of that treatment, together with a discussion of the application and limitations of the method, will be presented shortly in a full report.

[1] O. Stern, Zeits. f. Elektrochemie **30**, 508 (1924).
[2] F. O. Koenig, J. Phys. Chem. **38**, 111, 339 (1934); D. C. Grahame and R. B. Whitney, (in preparation).
[3] D. C. Grahame, J. Am. Chem. Soc. **63**, 1207 (1941). See also I. M. Kolthoff and J. J. Lingane, *Polarography* (Interscience Publishers, Inc., 1941), p. 106.
[4] G. Gouy, Ann. Chim. Phys. [7] **29**, 145 (1903).
[5] G. Gouy, J. de physique [4] **9**, 457 (1910).
[6] D. L. Chapman, Phil. Mag. [6] **25**, 475 (1913).